Industrial lab on a chip: design, applications and scale up for drug discovery and delivery

Goran T. Vladisavljević[a], Nauman Khalid[b,c], Marcos A. Neves[b,d], Takashi Kuroiwa[b,e], Mitsutoshi Nakajima[b,d], Kunihiko Uemura[b], Sosaku Ichikawa[d,*], and Isao Kobayashi[b,*]

[a]*Chemical Engineering Department, Loughborough University, Loughborough, Leicestershire LE11 3TU, UK.*

[b]*Food Engineering Division, National Food Research Institute, NARO, 2-1-12 Kannondai, Tsukuba, Ibaraki 305-8642, Japan.*

[c]*Graduate School of Agricultural and Life Science, The University of Tokyo, 1-1-1 Yayoi, Bunkyo-ku, Tokyo 113-8257, Japan.*

[d]*Faculty of Life and Environmental Sciences, University of Tsukuba, 1-1-1 Tennoudai, Tsukuba, Ibaraki 305-8572, Japan.*

[e]*Faculty of Engineering, Tokyo City University, 1-28-1 Tamazutsumi, Setagaya-ku, Tokyo 158-8557, Japan.*

* Corresponding authors.

E-mail addresses: isaok@affrc.go.jp (I. Kobayashi), ichikawa.sosaku.fn@u.tsukuba.ac.jp (S. Ichikawa)

Abstract

Microfluidics is an emerging and promising interdisciplinary technology which offers powerful platforms for precise production of novel functional materials (e.g., emulsion droplets, microcapsules, and nanoparticles as drug delivery vehicles- and drug molecules) as well as high-throughput analyses (e.g., bioassays, detection, and diagnostics). In particular, multiphase microfluidics is a rapidly growing technology and has beneficial applications in various fields including biomedicals, chemicals, and foods. In this review, we first describe the fundamentals and latest developments in multiphase microfluidics for producing biocompatible materials that are precisely controlled in size, shape, internal morphology and composition. We next describe some microfluidic applications that synthesize drug molecules, handle biological substances and biological units, and imitate biological organs. We also highlight and discuss design, applications and scale up of droplet- and flow-based microfluidic devices used for drug discovery and delivery.

Keywords: Microfluidics, Device fabrication, Unit operation, Scale-up, Monodisperse droplets, Parallel flow, Functional materials, Biological processing

Contents

1. Introduction

Microfluidics is the science and technology of manipulating and processing fluids in microchannels (MCs) that have at least one dimension (e.g. channel depth, width or diameter) smaller than 1 mm [1]. The early applications of current microfluidic technology include blood rheology [2, 3] and chemical analysis [4], which were prompted by the capability of microfluidic devices to use very small volumes of samples and reagents, to carry out analysis in short time due to short diffusion distances and to achieve high levels of compactness due to process integration. The rapid progress in silicon microfabrication technology, which started in the 1980s, enabled the development of these silicon-based microfluidic devices. A number of recent microfluidic devices have been fabricated using transparent polydimethylsiloxane (PDMS) elastomer [1]. Microfluidic device (also referred to as lab-on-a-chip device) allows for single unit operation (e.g., mixing, separation, droplet generation, particle manipulation, heating, and detection) or incorporates multiple unit operations [5-8]. Microfluidic technology is a rapidly growing interdisciplinary field and has received a great deal of attention in a broad spectrum of fields from fluid physics to biomedicine within the past two decades. Promising applications of microfluidic devices also include drug discovery, drug development, and drug synthesis [9-11].

In microfluidic technology, continuous and multiphase fluidic systems are usually used for various applications including biomedicals, chemicals, and foods. Multiphase fluid flows in microfluidic devices can be classified into droplet-based flows and parallel (coaxial) flows. Droplet-based microfluidic devices have at least one droplet generation unit (e.g., T-, X-, and Y-junctions, flow focusing, co-flow, and comb geometry) and have droplet splitting/merging unit for some applications [11-14]. At a droplet generation unit, a dispersed phase fluid is compartmentalized into numerous droplets that are surrounded by a continuous phase fluid in a channel. The growth of microfluidic drop generation processes in the past decade was driven by a rising number of applications that can take advantage of precision generation and manipulation of droplets on a microscale [15]. For instance, the generated monodisperse droplets are useful templates for producing monodisperse microcapsules and microparticles for delivering drugs and functional nutrients as well as for encapsulating living cells [11, 13]. Moreover, monodisperse droplets that range in volume from picoliter to nanoliter can function as numerous individual

microvessels for fast mixing and reaction [11, 13]. Wetting of a dispersed phase fluid and droplets to the channel wall is usually prevented by a thin wetting layer of a continuous phase, which is required for successful droplet generation/manipulation. It is also noteworthy that surfactant must be appropriately selected for successfully generating droplets [14, 16].

The scale-up of droplet-based microfluidic devices is a challenging field. A single microfluidic device usually produces emulsions at a droplet throughput of tens to hundreds of microliters per minute, while much greater throughputs are needed, even for very expensive pharmaceutical and biomedical applications [17, 18]. Several research groups have increased the throughput capacity of droplet-based microfluidic devices by parallelizing droplet generation units and/or such devices [17, 19-23]. Kobayashi et al. [23] recently achieved the production of monodisperse emulsions at a droplet throughput higher than 1 L h^{-1} by MC emulsification using asymmetric straight-through MC arrays. Spontaneous-transformation-based droplet generation for MC emulsification [24] is basically insensitive to the flow rates of two phases, making the scale-up and parallelization of MC emulsification device easier. Although the robust scale-up of the other droplet-based microfluidic devices is still quite challenging, these devices are promising for producing compound droplets with precisely controlled inner structure and morphology [20, 25].

Continuous and parallel multiphase flows in a microfluidic device are formed downstream Y-, T-, and Ψ-junctions [5, 9, 26]. Flows in a straight MC are laminar due to low Reynolds number; e.g., pure water that flows in a 10-μm diameter MC at its flow velocity of 10^{-3} m s^{-1} has a Reynolds number of ~10^{-3}. Since it is difficult to stabilize immiscible multiphase flows in an MC with homogenous hydrophilic/hydrophobic surface, several selective surface modification methods have been proposed to realize stable parallel multiphase flows consisting of immiscible fluids [5]. Continuous and parallel-flow-based microfluidic devices can be applied to unit operations, such as mixing, reaction, extraction, and separation. These devices have also been used for forming self-assembled nanoparticles as drug delivery vehicles and for fabricating drug-loaded microfibers [8, 27]. Integrated microfluidic devices have been used in research labs for almost two decades.

The scale-up of these microfluidic devices through integration techniques increases their popularity in diagnostic and medical sciences [28]. The integration of nanoparticle and microreaction technologies also offers enormous opportunities for the further development of smart drug delivery systems and microreactors for drug development and other biochemical synthesis [29]. Microfluidic integration technology, referred to the development of microfluidic devices with thousands of integrated micromechanical valves, enables hundreds of assays to be performed in parallel with multiple reagents in an automated manner [30]. This technology has been used for protein crystallization [6], cell chemotaxis and morphogenesis [31], genetic and amino acid assays [32, 33], high-throughput screening [25], neurobiology [34], bioreactors [35], chemical and material processing and synthesis [36], three-dimensional (3D) cell cultures [37] and single cell analysis [38]. Integrated microfluidic systems can be readily extended to solar-fuel generators, fuel-cell devices [27], organ-on-a-chip, human-on-a-chip, and point-of-care (POC) devices [39]. The commercialization of these scaled-up devices would revolutionize the world.

This review primarily focuses on multiphase microfluidics for producing biocompatible materials that are precisely controlled in size, shape, internal morphology and composition. The applications of continuous and multiphase microfluidics for bioassays, screening, detection systems, and diagnostics are in detail discussed in other review articles [10, 40-42], whereas their scale-up strategies have not yet been comprehensively evaluated. In the following sections, we first provide an overview of materials and fabrication techniques for existing microfluidic (lab-on-a-chip) devices, as well as of on-chip unit operations (droplet generation, droplet splitting/merging/loading, and formation of parallel multiphase flows). We then describe recent applications of microfluidic devices for producing functional biocompatible materials including drugs as well as drug delivery vehicles, bioassays, diagnostics, screening and detection techniques. We further discuss the scale-up strategies of microfluidic devices together with large scale microfluidic integration techniques that aim at materials processing at industrial scales.

2. Chip materials and fabrication

The most common materials used for fabrication of microfluidic devices along with fabrication methods are listed in Table 1.

2.1 Fabrication of single-crystal silicon chips

Single-crystal silicon MCs can be fabricated in the form of microgrooves [2], straight-through holes [44] or micronozzles [63]. Single crystal silicon is hydrophobic, but after anisotropic wet etching and subsequent thermal oxidation, the surface of silicon wafer becomes hydrophilic [64]. The hydrophobic surface can be obtained by the treatment with a silane coupling agent, such as *n*-octyltriethoxysilane [65] and octadecyltriethoxysilane [66].

Microgrooves. Microgrooves are usually fabricated by photolithography and anisotropic wet etching, as shown in Figure 2.1.1a. Photolithography includes masking of substrate with SiO_2 and photoresist, UV exposure, and photoresist developing. A channel structure that will be etched into the substrate is first generated by computer and then drawn onto a transparent plate (mask). A positive photoresist is then applied to the substrate in a thin layer, usually by a spin-coating process, and exposed to UV light through the mask. The illuminated areas of photoresist are then dissolved in a developer, exposing SiO_2 and the silicon substrate below to the etchant. Wet etching includes: (i) etching the SiO_2 layer by hydrofluoric acid at locations unprotected by photoresist; (ii) removing the remaining photoresist, usually by a mixture of sulfuric acid and hydrogen peroxide, and (iii) etching the silicon substrate. Anisotropic etching occurs when etchant (typically a KOH solution) etches silicon at different rates depending upon which crystal face is exposed. KOH etches silicon 1–2 orders of magnitude faster than SiO_2, so the SiO_2 layer remains intact. Anisotropic etching is greatly preferred in fabrication of microfluidic devices, because it produces channels with sharp, well defined edges. A typical isotropic etchant is a mixture of hydrofluoric acid and nitric acid. Isotropic etching is undesirable, because it results in undercutting of mask features.

Straight-through microchannels. Deep vertical MCs that completely penetrate silicon substrate can be fabricated by deep reactive ion etching (DRIE) [44]. DRIE requires aluminium mask to protect the underlying substrate against etching (Figure 2.1.1b). DRIE is a three-step process, patented by Robert Bosch GmbH, that involves: (i) etching a shallow trench into silicon substrate using sulfur hexafluoride (SF_6) plasma; (ii) passivating that newly formed cavity with

fluorocarbon polymer ($-(CF_2)_x-$) similar to teflon, created with the addition of octafluorocyclobutane (C_4F_8) plasma, and (iii) etching a subsequent and deeper trench with SF_6 plasma. Passivation with polymer prevents lateral etching of the sidewalls, while the hole becomes deeper. The reactive species (neutral radicals and ions) are formed by the collision of SF_6 molecules with a cloud of energetic electrons excited by an electric field [67]: $SF_6 + e^- \rightarrow SF_n + (6-n)F^* + e^-$ and $SF_6 \rightarrow SF_n^+ + (6-n)F^-$ with n = 0, 1, 2, 3, 4, or 5. The reactive species (F^* and SF_n^+) react with silicon forming SiF_4 (e.g. $Si + 4F^* \rightarrow SiF_4$), a gaseous substance that can be removed by a vacuum pump.

Micronozzles (MNs). Micronozzles can be fabricated by two-step DRIE process, as described in Figure 2.1.1c. The purpose of the first DRIE process is to form a rectangular of cylindrical pillar on the surface of silicon wafer. The role of the second DRIE process is to create a straight-through channel inside that pillar. MNs can be used for cross-flow droplet generation [68] or drop generation by flow focusing [63]. The main advantage of MNs over conventional straight-through channels is in higher cross-flow velocity at the channel exit, which is useful when the viscosity of the dispersed phase is high [68].

2.2 Fabrication of PDMS chips

Poly(dimethylsiloxane) (PDMS) chips are usually fabricated by soft lithography [1, 69]. Soft lithography shown in Figure 2.2.1a begins with a creation of reusable master with positive relief features, which can be used to fabricate more than one hundred PDMS replicas [69]. Fabrication of the master usually consists in spin-coating negative photoresist (e.g. SU-8) onto a substrate (usually a silicon or glass wafer), exposing it to UV light through the mask and dissolving the non cross-linked photoresist. After master fabrication, a mixture of PDMS pre-polymer, a catalyst and curing agent is poured over the master, degassed, cured at elevated temperature, and peeled off the master. Channels fabricated using planar soft lithography are rectangular and open. To enclose the channels, the PDMS mold is sealed to the flat surface of a glass slide or another PDMS block either covalently by plasma oxidation or non-covalently by applying pressure. Cylindrical channels can be fabricated by bonding two PDMS blocks with semi-circular channels face-to-face [70] or introducing compressed air inside a rectangular PDMS channel pre-filled with PDMS pre-polymer [71]. As shown in Figure 2.2.1b, semi-circular PDMS channels can be fabricated by combining mechanical micromilling, polymer molding and soft lithography [70].

First, high-precision micromilling is used to create a brass or aluminium alloy master with semi-circular channels. This master is then employed to create a poly(vinyl siloxane) (PVS) [70] or poly(methyl methacrylate) (PMMA) [72] mold with positive features that is used in the final fabrication step to cast channel structures into the PDMS substrate. This technique can be used to fabricate semi-circular channels of different patterns and shapes, such as T-shaped and S-shaped channels [70], and there is no limitation on substrate size or channel length that can be generated.

In planar PDMS devices, an emerging droplet typically contacts the channel walls during the process of drop generation, which can be exploited in fabrication of non-spherical particles [73], but it may lead to damage of the newly formed fragile solid/liquid interface or wetting problems [74]. Three-dimensional PDMS devices in which the dispersed phase is completely surrounded by the continuous phase during droplet formation process can be produced by embedding a microfiber in PDMS mold before curing [74], as shown in Fig. 2.2.1c. In this technique, insulated optical fibre is employed as a master for circular channel. A section of the insulation is removed using a scalpel to expose the bare fibre in the central region. The fibre is molded in PDMS, and after curing, the fibre is removed from the PDMS block, leaving the circular channel with a narrow section in the middle suitable for flow focusing. An inlet for the dispersed phase and an outlet for the droplets can be formed by inserting glass capillaries into both sides of the orifice. Topographical features can be created in PDMS channels using laminar flows of etching solutions [75], whereas a complex non-branching interwoven network of channels can be fabricated by pouring and curing PDMS pre-polymer between two masters fabricated by two-level photolithography [76]. PDMS is hydrophobic material, but the surface can be rendered hydrophilic by plasma oxidation of PDMS surface [77], coating with inorganic materials such as silica and titania *via* sol–gel chemistry [78], layer-by-layer deposition of polyelectrolytes [79], and ultraviolet graft polymerization of acrylic acid [80]. The surface modification in multistream microfluidic devices includes plasma oxidation, ultraviolet (UV) irradiation, chemical vapor deposition and sputter coating of metal compounds. All of these techniques are regarded as gas-phase methods. Wet chemical methods like layer-by-layer deposition, sol-gel coatings, silanization, dynamic modification with surfactants and protein adsorption are also very important as sometime used in combination with gas-phase methods [81]. Scaled-up versions of PDMS microfluidic devices are discussed in Section 5.2.

2.3 Fabrication of glass/metal/PMMA chips

PDMS channels swell in strong organic solvents and siloxane-based compounds and tend to deform with applied pressure due to their high elasticity. On the other hand, glass is more chemically robust than PDMS, does not swell, has excellent optical properties, low electrical conductivity, smooth surface, and can easily be functionalized to control surface properties (zeta potential and contact angle). A treatment with octadecyltrimethoxysilane (OTMS) will make the glass surface hydrophobic, whereas a treatment with 2-[methoxy(polyethyleneoxy)propyl]trimethoxysilane will enhance the hydrophilicity of the glass surface [82]. A glass surface is normally negatively charged due to dissociation of silanol groups, but positive charges can be introduced by the treatment with amino trialkoxysilanes, such as (3-aminopropyl)-trimethoxysilane (APTMS) and (3-aminopropyl)-triethoxysilane (APTES).

A wide range of glass micromachining processes is available [83] including wet etching using hydrofluoric acid based etchants and Cr/Au and/or acid resistant photoresist masks [47], deep reactive ion etching (DRIE) using SF_6 plasma [84], powder blasting using fine abrasive particles injected by compressed air [85], laser drilling using CO_2, Nd:YAG and excimer lasers [86], ultrasonic drilling using high frequency vibration of a microstructured tool [87], hot press imprinting [88], mechanical sawing [46], and pulling and microforging [82, 89]. Glass capillary microfluidic devices are coaxial assemblies of tapered borosilicate glass capillaries glued onto the surface of a microscope slide [82, 89, 90]. Shaping the tip of a glass capillary using a micropipette puller and microforge is a labour intensive, manual microfabrication process not suitable for large scale production. However, glass capillary microfluidic devices are very useful for small-scale production of complex multiphase droplets and particles (see Section 3.2), due to a wide range of possible multiphase flow configurations that can be achieved in these devices.

In addition to the above mentioned methods, photo etchable glasses have been used to fabricate high aspect ratio structures such as inkjet printer heads [91], microlens arrays [92], and hollow microneedle arrays for transdermal drug delivery [93]. As shown in Fig. 2.3.1a [92], the fabrication of microstructures in lithium silicate photo etchable glasses consist of Cr mask patterning on the glass wafer, UV exposure, heat treatment and glass etching. As a result of the

adsorption of UV light in the areas of photosensitive glass unprotected by the chromium, Ce^{3+} is combined with Ag^{+} to form silver nanoparticles ($Ce^{3+} + Ag^{+} \rightarrow Ce^{4+} + Ag^{0}$). During heat treatment at 550–590 °C, heterogeneous crystallization occurs around silver nuclei resulting in the formation of lithium metasilicate (Li_2SiO_3) crystals. The crystallized parts, when etched with a solution of hydrofluoric acid have an etching rate up to 20 times higher than that of the vitreous region.

Shallow horizontal MCs can be fabricated in poly(methyl methacrylate) (PMMA) by hot embossing [56], laser drilling [59], injection molding [57, 94], and mechanical micromilling [95]. Micromilling is a fast and low-cost microfabrication technique, which can be used to produce channel features down to 50 μm, including semi-circular and 3D structures that are difficult to create with optical lithography techniques [96]. The ability of mechanical micromilling to produce semi-circular channels in PMMA was exploited to fabricate complex artificial microvascular networks with circular channels by bonding face-to-face two milled PMMA sheets [97]. These artificial microvascular networks that closely mimic key geometrical features of real human vasculature can find applications in a wide range of biophysical, biochemical and clinical investigations in areas such as hemodynamics, cell mechanics, cell mechanotrasduction, and intravenous carrier-mediated drug delivery [97]. Despite the advantages over other microfabrication techniques, the surface roughness obtained by micromilling is generally poor (hundreds of nanometers) and very far from optical grade, i.e. <15 nm [96]. To improve the surface quality of micromilled PMMA channels, a number of post-processing methods have been developed, including thermal cycling, coating with different materials, and exposure to a solvent vapour [96]. A treatment with solvent vapour can be used not just to reduce the surface roughness of PMMA channels, but also to irreversibly bond microfluidic chips [96].

Hot embossing shown in Figure 2.3.1b is a three-step process, which can be used to fabricate PMMA microfluidic devices with optical grade (less than 15 nm surface roughness) channel walls. The silicon mold and PMMA plate are brought into contact and heated up above the glass transition temperature of PMMA. The mold is then pressed into a softened polymer to force it to flow into the cavities of the mold. Once the polymer has conformed to the shape of the stamp, it is cooled to a temperature below the glass transition temperature so that it is sufficiently

hard to be separated from the mold. Finally, a transparent cover plate must be bonded to the PMMA substrate. Deep vertical MCs can be fabricated in PMMA by X-ray lithography using synchrotron radiation and subsequent etching [98]. PMMA straight-through MCs were used for the production of W/O emulsions without any surface modification of the channels [98]. Monolithic PMMA microfluidic devices can be fabricated by stereolithography [60]. The main advantage of stereolithography is that peripheral units such as inlet and outlet ports can be incorporated within the device without bonding.

In addition to glass and plastic microfluidic devices, metallic chips are increasingly being used in microfluidics, due to their superior mechanical and thermal properties, especially for undertaking high-temperature chemical conversions in microreactors [99, 100], but also as a master mold in soft lithography and hot embossing lithography, as explained in Figures 2.2.1b and 2.3.1b. Stainless steel is among the most common materials for manufacture and handling of food and pharmaceutical products. Stainless steel chips with grooved MC arrays have been fabricated using an end mill [101] and dicing saw [62]. Stainless steel chips with asymmetric straight-through channels have been fabricated by end-milling and used for generation of millimeter-sized droplets [102]. Microengineered nickel membranes with regular hexagonal array of cylindrical or slotted pores can be fabricated using UV-LIGA process [103].

3. Microfluidic unit operations

3.1 Generation of simple droplets and bubbles

The most common microfluidic strategies for generation of liquid-liquid or gas-liquid dispersions (droplets and bubbles) are shown in Fig. 3.1.1.

T-junction. T-junction is the simplest microfluidic structure for producing droplets and bubbles [55, 104-107]. In standard geometry (Fig. 3.1.1a), the main channel carries the continuous phase and the dispersed phase is injected through the orthogonal (inlet) channel. The shear stress generated by the continuous phase and evolution of the pressure upstream of the emerging droplet causes the tip of the dispersed phase to distort in the downstream direction until the neck of the dispersed phase breaks up into a droplet [11, 108, 109]. Several modifications of the

standard T-junction geometry have been implemented, including injection of the dispersed phase through the main channel into the continuous phase supplied from the orthogonal channel (Fig. 3.1.1b) [95], head-on geometry (Fig. 3.1.1c) [110], capillary-embedded T-junction [95, 111], and double-pore T-junction [112]. In head-on geometry, the two fluids are injected from two opposite sides of the main channel and the droplets are collected from the orthogonal channel [110, 113].

The dispersed phase should not wet the walls at the junction, e.g. hydrophilic channel walls are required to produce O/W or W/O/W emulsions. The wetting properties of microfluidic channels can be altered by surface modification [114] or changing the concentration of surfactant dissolved in the continuous phase [115]. It has been found that both monodisperse O/W and W/O emulsions can be prepared in the same T-junction device, solely by the appropriate choice of surfactants added to the oil or aqueous phase [115].

Three distinct regimes of droplet formation in T-junction are squeezing, dripping, and jetting [116]. In squeezing regime, the tip of the dispersed phase stream occupies almost the entire cross section of the main channel because the shear stresses exerted by the continuous phase are small compared to interfacial stresses. As a result, the continuous phase is confined to thin films between the droplet (or bubble) and the channel walls, which leads to a build-up of pressure in the continuous phase upstream of the droplet [109, 116, 117]. It causes the continuous phase to squeeze the neck of the stream until breakup occurs. Within squeezing regime, the droplet size is a function of the ratio of the flow rates of the two fluids and does not depend significantly on the interfacial tension or the viscosities of the two liquids [116]. In dripping regime, the size of the droplet (or bubble) is determined by a balance between the drag force that the continuous phase exerts on the emerging droplet and the interfacial force that opposes the elongation of the neck [116]. The capillary number of the continuous phase, Ca_c (= $\mu_c u_c/\gamma$, where μ_c and u_c are the viscosity and mean velocity of the continuous phase and γ is the interfacial tension), can be used to predict a dominant mechanism of droplet formation: $Ca_c < 0.002$ within squeezing regime and $0.01 < Ca_c < 0.3$ within dripping regime [118]. As Ca_c is further increased, the breakup point moves progressively downstream, which leads to a transition from the stable dripping regime to a jetting regime.

The size of droplets produced in T-junctions can be controlled passively, through the control of the fluid flow rates, and actively, through external actuation. The active control of the droplet size can be achieved using controllable moving wall structures [11], integrated microheaters [119] (Fig. 3.1.1d), and pneumatically [120, 121] or magnetically [122] actuated microvalves. When generating droplets by opening and closing valves, the resulting droplet volume and breakup frequency can be controlled independently from each other by varying the opening time (t_{open}) and cycle time ($t_{close} + t_{open}$) of the valve, respectively [120].

X- and Y-junction. In a cross-junction (Fig. 3.1.1e), droplets are generated using a microfluidic modification of Rayleigh's approach [123], with two streams of the continuous phase fluid flanking a stream of the dispersed phase [45, 124, 125]. The flow conditions in cross-junction can be described by the Weber number of the dispersed phase, We_d ($= \rho_d u_d^2 l/\gamma$, where ρ_d and u_d are the density and velocity of the dispersed phase, respectively, and l is the diameter of the channel) and Ca_c. For We_d, $Ca_c > 1$, the dispersed phase does not break into droplets, whereas for We_d, $Ca_c < 1$, a dripping instability occurs, breaking the dispersed phase into droplets [126]. In a Y-junction, the dispersed and continuous phases are injected through two separate inlet channels and the emulsion is removed using a common outlet channel (Fig. 3.1.1f). The size of the droplets formed in Y-junction is independent on the flow rate and viscosity of the dispersed phase [127], which is a behaviour different to that in a T-junction. At low Reynolds numbers, two fluids (miscible of immiscible) introduced into a Y-junction from two different inlets will form two parallel laminar streams in a downstream channel. Mixing of the two streams can occur by diffusion only, and is restricted to an interfacial width at the centre of the channel. Utilization of this phenomenon in microfluidic systems has resulted in a number of applications such as membraneless microfluidic fuel cells [128, 129], blood diagnostics [130], generation of anisotropic (Janus) particles [45, 131, 132] and continuous crystal lines, metal wires and polymer strings that are less than 5 μm wide [133, 134].

Co-flow. A co-flow microfluidic device consists of two coaxially aligned tubes; the inner one is usually a glass capillary tube with a tapered tip made by microforging [135]. At low flow rates of

both fluids, droplets grow spherically from the tip of the inner tube until they reach a size where the viscous drag exerted by the co-flowing continuous phase exceeds the interfacial tension (the dripping regime). At faster flows, the dispersed phase forms a thin stream that breaks into droplets further downstream due to Rayleigh-Plateau instability (the jetting regime). Two distinct classes of transitions from dripping to jetting have been identified [136]. The first is driven by the flow rate of the continuous phase; as it is increased, droplets formed at the tip decrease in size until a long narrowing jet is formed and drop breakup occurs at the end of this jet. The second class of dripping to jetting transition is driven by the flow rate of the dispersed phase; as it is increased, the emerging drop is pushed downstream and is ultimately pinched off at the end of the jet forming large droplets. In the first jetting regime, the shear stress exerted on the droplet by the continuous phase is large compared to interfacial tension. In the second jetting regime, the inertial forces of the dispersed phase are large compared to interfacial tension [14, 136, 137]. At very high flow rate ratios, viscous stress exerted by the continuous phase becomes so large that the growing drop takes a conical shape ("Taylor cone") and a very thin fluid jet can evolve from its sharp tip, which subsequently breaks into tiny droplets (the tip-streaming regime) [138].

Microfluidic flow focusing. When droplets are generated in co-flowing streams or at a cross-junction, the combined two-phase flow is often forced through a small orifice which is known as hydrodynamic flow focusing [117, 139, 140]. Planar microfluidic flow focusing device (MFFD) developed by Anna et al. [141] is depicted in Fig. 3.1.1h and scaled-up versions of these devices are shown in Figure 5.2.3 and 5.2.5. The dispersed phase (focused fluid) flows through the middle channel and the continuous phase (focusing fluid) is supplied through the two outside channels. Both fluids are forced to flow through a small orifice located downstream of the three channels. The continuous phase exerts pressure and shear stress that force the dispersed phase into a narrow thread, which breaks inside or downstream of the orifice. The principle may be extended to two or more coaxial fluids [54] and depending of the geometry of the feed channels and orifice, the flow pattern may be planar or cylindrical (axisymmetric) [117, 142]. In Fig. 3.1.1h, the liquid in the middle channel does not wet the walls of the orifice and thus, hydrophilic and hydrophobic walls are needed to produce O/W and W/O emulsions, respectively. If the liquid in the middle channel wets the orifice walls, droplets of the liquid flowing through the outside channels will be formed downstream of the orifice (Fig. 3.1.1i). The size of the droplets

formed in flow focusing devices can be reduced by using an electric field [143], active pneumatic choppers [144], and controllable moving wall structures [145]. An alternative flow pattern in flow focusing devices is a counter-current flow shown in Fig. 3.1.1j. In contrast to co-flow design, the two fluids are supplied from the two ends of the same channel in opposite directions and droplets are collected from another, coaxially aligned, channel. A major advantage of MFFDs compared to co-flow devices is that they can be used to produce droplets with the sizes smaller than that of the orifice at the entrance of the collection channel. This feature is useful because for any given droplet size, a channel with a larger orifice size can be used compared to that in the co-flow design, which minimizes the probability of clogging the orifice by the suspended particles or any entrapped debris.

Four distinct regimes of drop generation in MFFDs are squeezing, dripping, jetting and tip-streaming [146]. The squeezing or "geometry-controlled" regime is characterised by droplet sizes that are roughly equal to the orifice size and independent on Ca_c [146]. The mechanism of droplet breakup is similar to that observed in T-junction geometry at low Ca_c values [147]. The dispersed phase liquid occupies a significant portion of the cross-sectional area of the orifice, forcing the continuous phase to flow through a narrow gap between the interface and the orifice wall. To maintain the applied flow rate, a higher upstream pressure is needed in the continuous phase stream, which leads to pinching of the interface. In the dripping regime, the dispersed phase jet narrows due to viscous stresses from the continuous phase, and the resulting droplet sizes are within one order of magnitude smaller than the orifice size. In the jetting regime, the dispersed phase forms a long jet that extends downstream of the orifice resulting in less controlled droplet breakup. The droplet size is larger than in the dripping regime and can be larger than the orifice size [146]. In both dripping and jetting regimes, droplet breakup occurs because of the combined effects of capillary instability and viscous drag [148]. Tip-streaming regime occurs in the presence of surfactants and at very high flow rate ratios of outer to inner phase of 300 and above [146]. Here, a very thin and long thread is formed, which breaks up into small droplets with a diameter of 1/20 of the orifice size and smaller. The tip streaming is an alternative route to the generation of submicron emulsions and particles without using nanofluidic channels [149].

Cross flow. In a cross-flow microfluidic device, the dispersed phase is injected through a porous substrate (membrane) containing a single pore [150, 151] or an array of pores [152] into a continuous phase flowing tangentially over the membrane surface. The main difference between microfluidic cross-flow (Fig. 3.1.1k) and T-junction (Fig. 3.1.1a) geometry is that in a cross-flow device, the dimensions of the cross-flow channel are large compared to the width or depth of the inlet channel (pore), so that the droplet generation process is unaffected by the geometry of the cross-flow channel. The droplet size mainly depends on the pore size, the flow rate of the dispersed phase, the shear stress at the surface of the membrane, and physical properties of the dispersed and continuous phase [14, 153]. Apart from simple cross flow, a shear stress at the surface of the membrane required for drop detachment can be produced by pulsed cross-flow [154] or rotating [155-157] or vibrating [158, 159] the membrane within otherwise static continuous phase.

Spontaneous drop generation. Monodisperse droplets can be formed in the absence of any bulk flow of the continuous phase which is known as "spontaneous drop generation" [160]. In order to create driving force for spontaneous drop generation, the dispersed phase emerging from a vertical or horizontal channel is squeezed in a confined geometry and thus forced to take a disc-like shape which is characterized by a higher interfacial area per unit volume than a spherical shape, resulting in hydrodynamic instability (Fig. 3.1.1i) [24]. The discoid shape may be a result of expansion of the dispersed phase on a horizontal terrace [161] or in a vertical slit [162]. Three main regimes of spontaneous drop generation are size-stable, size-expanding and continuous outflow [163]. In the size-stable regime, the drop generation is dominated by the interfacial tension; the droplet size is independent on the fluid flow rates and proportional to the channel size. In the size-expanding regime, the interfacial stress is still dominant force acting on the droplet, but the inertial forces cannot be completely ignored and the droplet size slightly increases with increasing the dispersed phase flow rate. In the continuous outflow regime, the dispersed phase flows out continuously from the channel, forming a very large droplet that eventually pinches-off. Recently, a new method of spontaneous droplet generation was developed based on generation of multiple droplets at the edge of a shallow, but rather wide and long microfluidic plateau (typically 1–3 μm deep, 200 μm long and 500–10,000 μm wide) [21].

3.2 Generation of compound (multiphase) droplets

The ability to create compound droplets with versatile inner structure and morphology is one of the major advantages of microfluidic technology. Typical microfluidic strategies for producing core/shell droplets are shown in Fig. 3.2.1. These strategies are based on a single-step break-up of co-axial fluid thread composed of two immiscible fluids or two sequential drop break-up events in drop makers with alternating wettability. In a planar MFFD, core/shell droplets can be formed using either of the two strategies mentioned above. In Fig. 3.2.1a, a coaxial jet composed of two immiscible fluids (inner and middle phase) breaks up and forms core/shell droplets in the outer phase [54]. In Fig. 3.2.1b, core/shell droplets are formed using two consecutive flow focusing generators with alternating wettability [166]. If the middle phase is a mixture of monomer and initiator, these core/shell droplets can be used as templates in the production of hollow polymeric particles [54].

In axisymmetric devices, core/shell droplets can be generated by combining co-flow and counter-current flow (Figs. 3.2.1c and 3.2.1e) [74, 89] or employing stepwise emulsification of co-flowing streams (Fig. 3.2.1d) [167]. In axisymmetric glass capillary devices, the shell thickness can range from several microns to several tens of microns and can be controlled by adjusting the ratio of the middle phase flow rate to the inner phase flow rate [103]. To obtain shells in the nanometer region (100 nm or even less), a modified design was used with a biphasic flow in the injection capillary [168]. A similar design was used to produce core/shell structures with gas core and oil shell [169]. The shell material can be polymerised or cross-linked to produce polymer or ceramic shells around the inner phase [169-173] or a chemical reaction can take place within the core material which allows controlled addition of reactants through the shell [174]. Alternatively, a shell may contain dissolved amphiphilic molecules or particles which can undergo self-assembly upon solvent evaporation, leading to the generation of giant vesicles such as liposomes [175], polymersomes [176, 177] and colloidosomes [178].

Two co-flow (Fig. 3.2.1d) or T-junction (Fig. 3.2.1f) drop makers with alternating surface wettability were used to produce multiple emulsions containing a controlled number of inner phase droplets within each middle phase drop [48, 131, 167]. The number of inner droplets can be controlled by adjusting the fluid flow rates to satisfy the following equation: $f_1/f_2 = N$, where f_1 and f_2 is the frequency of drop generation at the upstream and downstream drop maker,

respectively and N is a positive integer (1, 2, ...). Core/shell droplet morphology will be obtained when $N = 1$. These emulsions can be used as templates for synthesis of non-spherical particles [179]. Higher-order multiple emulsions containing four or more immiscible liquid phases can be made by adding more sequential stages [167, 180]. Chu et al. [167] made triple emulsions by adding a third co-flow stage and both the diameter and the number of the individual droplets was controlled at every level. Using this approach, triple emulsions have been formed containing between one and seven innermost droplets and between one and three middle droplets in each outer drop. The integration of a large number of triple emulsion drop generation units on a single chip is shown in Figure 5.2.7a.

Core/shell droplets were also produced using two serial planar cross-junctions with alternating wettability (hydrophilic and hydrophobic) [79, 126] or non-planar cross-junction with the same hydrophobic properties [181] (Figs. 3.2.1g and 3.2.1h). An extension of this principle to three or more cross-junctions in series can lead to the production of higher-order multiple emulsions, such as triple (Fig. 3.2.2c), quadruple, and quintuple emulsions [182, 183]. Two sequential hydrophobic cross-junctions with different depth of the main channel can produce core/shell droplets with an ultra-thin (<1 μm) oil shell surrounding a water core [184, 185]. When forming core/shell droplets using two cross-junctions in series, dripping instabilities are normally present in both junctions. This produces core/shell droplets in a two-step process, as shown in Figs. 3.2.1b and 3.2.1g: the inner drop is formed in the first T-junction and encapsulated in the outer drop in the second. Core/shell droplets can also be formed in a one-step process by removing the first dripping instability, by increasing the flow rates in the first T-junction [126]. This produces a jet of the inner phase that extends into the second junction, where it is surrounded by a layer of middle phase, producing a coaxial jet, as illustrated in Fig. 3.2.1g. If the flow rates in the second junction are set to induce a dripping instability, the coaxial jet is pinched into core/shell droplets, as illustrated in Fig. 3.2.1b. One-step mode is preferred in microfluidic generation of core/shell droplets, since it avoids the difficulty of matching the frequencies of different drop-maker junctions, which improves drop uniformity. A large-scale integration of core/shell drop generation units operating in one-step mode is shown in Figure 5.2.9.

When two different liquids are injected from two opposite T inlets, cross-junction can produce an array of droplets of alternating composition, e.g. an array of alternately coloured droplets [48, 186, 187]. Multiple emulsion droplets with two distinct inner phases can be generated by combining an upstream cross-junction and a downstream T-junction (Fig. 3.2.2a) [48] or using a glass capillary device with two separate internal channels in the injection tubes (Fig. 3.2.2b) [188]. Gas-in-water-in-oil emulsions with a controlled number of gas bubbles encapsulated within each water droplet can be generated by combining an upstream flow focusing drop generator and a downstream T-junction [189].

3.3 Droplet splitting

To split a droplet into two or more daughter droplets, a droplet is flowed into a bifurcating T or Y-junction or past isolated obstacles of different shapes. At a bifurcation, the droplet is split either symmetrically or asymmetrically depending on the downstream flow resistance [190]. The ratio of volumes of the two daughter droplets V_1/V_2 is inversely proportional to the ratio of hydrodynamic resistances of the two side arms, R_1/R_2 [190]. Provided the hydrodynamic resistances of the two arms are equal and the flow rate is sufficiently high, the drop will be bisected into two equal portions [182], as illustrated in Figure 3.3.1a. An extension of this strategy to microfluidic tree network consisting of four consecutive Y junctions is shown in Figure 5.2.6a. For optimal splitting, the capillary number of the continuous phase, Ca_c, should have an optimum value. If it is too low, droplets may not split and if it is too high, it leads to production of satellite droplets [182].

Droplets can also be split into two portions by flowing past isolated obstacles. When a single stream of droplets, with size comparable to the channel, flows past a square obstruction placed symmetrically in the channel, each drop breaks into two identical daughter droplets, as shown in Fig. 3.3.1c [190]. If the obstruction is off-centered, daughter droplets of two different sizes will be formed, as shown in Fig. 3.3.1d. The ratio of droplet sizes produced by the obstacle corresponds to the ratio of gap widths at each side of the obstacle. When two coexisting streams of droplets encounter an obstacle placed off centre, under certain flow conditions only droplets in one of the streams break, resulting in a regular sequence of three different sizes of droplets, as illustrated in Fig. 3.3.1e [190]. Similar results can be achieved with other patterns, such as three

coexisting streams where every third droplet breaks. Droplet splitting can also be achieved using a flow focusing junction (Fig. 3.3.1f) [191]. In contrast to splitting with bifurcation or obstacles, here the droplet is divided along its length in the flow direction. The number and size of the daughter droplets can be tuned by changing the flow rate of the splitting liquid supplied through two T inlets.

3.4 Droplet merging

Microfluidic strategies for droplet merging can be divided into passive and active. Passive (flow-induced) methods utilize microchannel geometry to bring into contact two droplets in a MC. The pairwise merging of two adjacent droplets can be initiated by temporary trapping or slowing down one droplet inside a channel until a subsequent droplet arrives and merges with the trapped droplet [192]. Three different types of traps can be used: an obstruction placed in the channel (Fig. 3.4.1a) [192], a circular expansion chamber (Fig. 3.4.1b) [192, 193] and a locally deformed cross section of the channel [192]. The expansion chamber enables fusion by draining the continuous phase that separates two adjacent droplets in a channel. Upon entering the expansion chamber, the continuous phase spreads around the droplets to occupy the increased volume, causing the droplets to come into contact with each other in the center of the chamber (Fig. 3.4.1b). The removal of spacing between the droplets induces their fusion owing to minute disturbances in surface tension [194].

Alternatively, droplets can be merged at Y-, Ψ- or T-junctions [192, 195, 196]. The pairwise droplet coalescence occurs spontaneously when droplet production in two upstream generators is synchronized. In Fig. 3.4.1c, the droplets of two different liquids (DP1 and DP2), generated synchronically at two upstream T-junctions, are transported to the downstream T-junction, where they collide and flow together into a common outlet channel. No collision occurs when there is a timing difference between the arrivals of the two droplets at the junction [196]. The precision of pairing of alternating droplets can be improved by implementing various passive microfluidic components into the device [197] or using electric field [198]. Hung et al. [199] have developed a tapered chamber with diverging walls to generate velocity gradient and allow droplets to approach each other (Fig. 3.4.1d). The spacing between alternately generated

droplets gradually decreases as they travel along the diverging section, which leads eventually to droplet coalescence.

Flow-induced droplet merging has also been achieved using a trifurcating junction ("flow rectifying design") to aid film drainage (Fig. 3.4.1e) [192, 200, 201]. In the trifurcating junction, the continuous phase is removed via the upper and lower channels at equal flow rates, so that the droplets trapped at the junction do not experience any net force along the vertical axis and stay aligned with incoming droplets until coalescence occurs. Alternatively, the continuous phase can bypass the trapped droplets using microfluidic pillar arrays [202]. As shown in Fig. 3.4.1f, the merging chamber is divided into three branches by two sets of pillars. A droplet entering the merging channel is stopped in the middle branch and merged with the subsequent droplet, whilst the continuous phase is allowed to flow between the pillars and through two side branches.

Active droplet coalescence methods employ an externally generated energy to achieve droplet coalescence. The examples of active droplet merging strategies are electro-coalescence [198, 203-205], use of pneumatically driven membrane valves [120], optical tweezers [105], and thermo-coalescence [206, 207]. The pneumatically driven membrane valve consists of a flat elastic membrane sandwiched between the control and flow channel. Whenever a sufficient pressure is applied to the upper control channel, the membrane deflects downward and blocks the lower flow channel, which leads to the accumulation of droplets in the space between the valve and the last pair of the bypassing branches (Fig. 3.4.1g). Eventually, the entrapped droplets would fuse together after which, the membrane valve is opened to allow the combined droplet to leave the waiting zone. Temperature-induced droplet coalescence can be achieved by incorporating heater directly in a merging chamber (Fig. 3.4.1h) [206, 207] or in a bypass line (Fig. 3.4.1i) [192]. In the latter case, a bypass line allows passage of the lower viscosity continuous phase when the heater is activated. The drainage of the continuous phase via bypass line forces the adjacent droplets to approach each other and merge. When the heating is turned off, the continuous phase flows only through the main channel, which has a larger cross-sectional area than the bypass line. Optical tweezers [105] and electric panel devices [208] have also been used for active droplet merging. Electric panel devices consist of a thin polyester substrate containing electrode arrays or electrode dots on its surface coated by an insulating film. Droplets

on an electrode panel can be moved toward each other by a travelling electric field, which arises on applying a sequential voltage to the electrodes [208].

3.5 Formation of parallel multiphase flows

Microstructured devices with multiphase flow can find numerous chemical and biological applications in fine chemicals synthesis [210], nano-materials preparation [211], drug development [212], microfluidic fuel cells [129] and highly efficient separations [213]. The main advantage of a multiphase microstructured chemical device is the small cross-sectional area of MCs, which provides much shorter mixing distance and much larger interfacial area in comparison with common chemical engineering processes [214, 215]. Besides this effect of reagent mixing and mass/heat transport processes, the stable flow patterns in MCs are also important features for process control [15]. Due to these special characteristics, the microstructured chemical device has become a new tool to increase process yield [216], to control product structure and morphology [90], and to develop new chemical and biochemical engineering processes [217].

Two phase microflows (gas-liquid and liquid-liquid phases) in bubbles and droplets (squeezing, dripping, jetting, etc.) in the T-junction, flow focusing, coaxial and some other modified MC devices have been extensively discussed in section 3.1 to 3.4, and have numerous applications in drug delivery, drug formulation, food science, oil and dairy industries. Besides two phase microflows, three-phase systems such as gas-liquid-liquid are also important for industrial chemical and biochemical engineering processes. These multiphase systems commonly exist in the organic synthesis reaction and extractive distillation process, and together they play a significant role in drug formulation and delivery [218]. Multiphase parallel microflows are used in microfluidic devices such as microreactors [219], micro heat exchangers [220] and lab-on-a-chip modules [221] and are characterized by rectangular channels with cross-sectional dimensions on the order of tens or hundreds of microns. Multiphase parallel microflows have potential scale-up applications in the generation of monodisperse emulsions, high-throughput catalyst screening and combinatorial material science. In the life sciences, applications range from pharmaceutical research to diagnostic testing and DNA manipulation [222]. The concept of parallel multiphase microflows can also be applied on low cost microfluidic fuel cells, also

called laminar flow-based fuel cells or membraneless fuel cells [129, 223]. Microfluidic fuel cells uses laminar flow to operate without a solid membrane separating fuel and oxidant, making possible to produce efficient alkaline fuel cells that could provide cheap and effective power for small electronic devices [223]. These cells can be an alternative towards miniaturized power supplies, and easily be scaled up in parallel arrays to produce more power for industrial applications.

3.5.1 Types of flows

Parallel multiphase microfluidic flows are readily manipulated by using many kinds of external fields (pressure, electric, magnetic, and so on) (Fig. 3.5.1) [224]. Depending on the type of driving force, the most important flows in microfluidic channels are pressure differential, electro-osmotic, capillary, and free-surface. In pressure differential flow, fluid is transported by means of applied pressure difference [225]. In electro-osmotic (electrokinetic) flow [226, 227], transport is initiated by application of a high electric field. The third type involves the capillary driving forces driven by surface tension, wetting of surfaces by the fluid, and pressure gradients in various liquids [228]. Free-surface (Marangoni) flows are caused by gradients in interfacial tension and can be manipulated using the dependence of surface tension on temperature or chemical concentration [229, 230].

The basic channel configurations used to generate parallel multiphase flows (liquid-liquid and gas-liquid) are T-, Y- or cross-junctions (see Section 3.1) [231-233]. They have the ability to generate high specific interfacial area (interface-area-to-volume ratio [m^2 m^{-3}]) and consequently high interfacial forces [176]. Typical types of parallel multiphase flows in a MC are shown in Fig. 3.5.2. Aota et al. [5] reviewed separated (or parallel) multiphase microflows with focus on fundamental physics, methods for stabilization of the interface, and applications for liquid–liquid extraction. An advantage of parallel flow over segmented flow is that it permits counter-current flow of the phases which is of interest in non-equilibrium mass-transfer applications. An essential requirement for parallel multiphase microflows is to stabilize the interface under varying flow rates. Parallel multiphase flows with integrated microfluidic systems are powerful tools for high-throughput analysis and synthesis of novel compounds. These novel microfluidic systems were developed by integrating microfluidic unit operations and are available for

continuous flow chemical and biochemical processing [5] (Fig. 3.5.3). Viscous forces and interfacial tension dominates over gravity in parallel multiphase microflows, hence stabilization of their interface is important in microfluidic chemical and biochemical synthesis.

3.5.2 Selective surface modifications

Detailed information regarding the fabrication of microfluidic devices have been presented in Section 2.3. As mentioned before, PDMS has got popularity as the material of choice for microfluidic devices due to its low cost, easeness of fabrication, oxygen permeability and optical transparency [81]. There are some drawbacks in this material as PDMS's hydrophobicity and fast hydrophobic recovery after surface hydrophilization, attributed to its low glass transition temperature of less than 120°C, negatively impacts on the performance of PDMS-based microfluidic devices [234].

Utilizing these various techniques Kitamori and coworkers have developed microfluidic unit operations for various purposes, such as mixing and reactions, phase confluence and separation, solvent extraction, reaction on surfaces, heating, cell culture, and ultrasensitive detection based upon thermal lens microscope [5]. Recently Kim et al. [235] developed a neuro-optical microfluidic device for studying injury and subsequent regeneration of individual mammalian axons that was not possible with conventional cell culture platform and tools.

4. Applications of lab-on-a-chip devices for materials processing

4.1.1 Fabrication of microparticles and nanoparticles

Numerous chemical and physicochemical processes have been used to microengineer particles including ionotropic gelation [68], cold-set gelation [236], polymerisation [20], self-assembly [175] and nanoprecipitation. These processes can be triggered by rapid mixing (Figure 4.1.1a), solvent evaporation (Figure 4.1.1b), UV irradiation (Figure 4.1.1d, e, and f), and temperature gradient (Figure 4.1.1h). Non-spherical particles (discoid, cylindrical, rod-like, and square prisms) can be generated using microfluidic channels with confined geometries (Figure 4.1.1c), photolithography (Figure 4.1.1d), and micromolding (Figure 4.1.1e). Typical biocompatible particles synthesised in lab-on-a-chip devices are microgels, biodegradable polymeric particles, solid lipid particles, and vesicles. Liposomes have been the most successful candidates for drug

carriers in clinical applications [237]. Liposome-encapsulated anti-cancer drugs (liposomal anthracyclines e.g., doxorubicin for breast, ovarian and other solid tumors) has been studied extensively and has shown to exhibit improved efficacies over non-encapsulated conventional drugs [237-239]. Furthermore, "stealth" liposomes have been developed by the addition of poly(ethylene glycol) (PEG) to the exterior surface as a flexible hydrophilic polymer to serve as a shield [240]. Biodegradable polymers and block copolymers, such as poly (lactic acid) (PLA), poly(glycol acid) (PGA) and poly (lactide-co-glycolide) (PLGA) acid are widely used as carriers in drug delivery systems because of their biodegradability, biocompatibility and ease of processing [241]. Microgels derived from biodegradable polymers such as alginate [242], gelatin [243], chitosan [244], pectin [245], agarose [246], κ-carrageenan [247] and carboxymethylcellulose [247] have been extensively used in drug delivery [243], biosensing [248] and tissue engineering [249-251]. Solid lipid particles [252], as well as gelatin [243] and agarose [246] beads were produced in microfluidic channels by temperature-controlled emulsification followed by cooling below the phase transition temperature, T_0 (T_0 is the melting point or helix-to-coil transition temperature), as shown in Figure 4.1.1h. The lab-on-a-chip strategies used to fabricate microgels by in-situ ionotropic gelation were external gelation [247], internal gelation [253, 254], droplet merging [193] and rapid mixing [255]. The examples of drugs encapsulated within micro-engineered microgels are 5-fluorouracil [256], vitamin C [243], lidocaine [257] and bupivacaine [257]. Emulsification/solvent evaporation is a common microfluidic strategy for production of synthetic biodegradable polymeric particles [103], 3D colloidal assemblies [104] and giant vesicles ($d > 1$ μm) [175, 177].

4.1.2 Loading of droplets with discrete objects or macromolecules

Droplets generated in microfluidic channels can be loaded with cells or enzymes for the purpose of high-throughput screening (Figure 4.1.1i): typically, encapsulation efficiencies of 100% can be achieved, whereas, by contrast, bulk methods often achieve less than 50% of the actives encapsulated. Although drop formation in microfluidic channels is highly controlled and periodic, the process of loading discrete objects, such as cells or particles, into droplets is normally random, and the distribution is dictated by Poisson statistics. The probability of a drop containing k cells is: $\lambda^k \exp(-k)/(k!)$, where λ is the average number of cells per drop. This means that only 15.6% of all droplets will contain one cell if no more than one in ten of the occupied droplets can

be allowed to hold two or more cells. This intrinsic inefficiency led to the development of new cell and particle manipulation methods prior to droplet loading that provide more efficient single cell/particle encapsulation, such as laser guidance of particles [105], inertial self-ordering of particles as they travel within a high aspect-ratio MC [263], ordering of deformable particles into closely packed arrays [264], and cell-triggered jet breakup in a flow focusing geometry [265]. Microfluidic methods have also been developed for separation of cell-loaded droplets from empty droplets based on externally induced forces such as dielectric, magnetic, acoustic and optical [266] or passive hydrodynamic effects [267]. The encapsulation of biomolecules into drops is achieved exclusively using limiting dilution because molecules are too small to passively organize with inertial or packing methods and to trigger the breakup of a jet [268].

Formulated nanoparticles and droplets from these devices were used to delivery small drugs [29, 269, 270], plasmid DNA [271] and peptides and proteins [272, 273].

4.1.3 Parallel-flow based microfluidic devices

The laminar property of microflows is useful for structuring streams and the combination of microgeometries and fluid injections allows for manipulating complex sequences of events. Continuous-flow-based methods for micro-manipulating droplets include geometrically induced breakup at T-junctions [190, 274, 275] and breakup with focusing sections [276, 277]. For drug discovery, they can be used for testing multiple drugs doses simultaneously or for lead optimization [278]. Cells can be stimulated in order to study the effects of drug concentration on chemotaxis [279] and gradients can be applied to cell behavioral studies on stem cell differentiation [280, 281].

Nano-sized lipid vesicles (d < 200 nm) can be fabricated by mixing of miscible liquids under laminar flow [261], as shown in Figure 4.1.1g. This method uses hydrodynamic focusing to squeeze an isopropanol-lipid mixture into a very narrow central stream between two aqueous streams. The narrow width of the focused stream and laminar flow in the channel enables rapid mixing through molecular diffusion at the liquid-liquid interface where the lipids self-assemble into vesicles. A similar microfluidic strategy of single-step nanoprecipitation was used to fabricate poloxamer 407 micelles for co-delivery of dexamethasone and ascorbyl-palmitate [282], lipid nanoparticles for in vivo delivery of siRNA [283], poly(lactic-*co*-glycolic acid)-*b*-

poly(ethylene glycol) micelles [284], doxorubicin-loaded PLGA nanoparticles [285], and chitosan nanoparticles [286]. Hood et al. [287] developed a microfluidic hydrodynamic flow focusing technique for the continuous-flow synthesis of PEG-modified and PEG-folate-functionalized liposomes for targeted drug delivery. The hydrophilic nature of chitosan makes it appropriate for carrying hydrophilic drugs [288], but most anticancer drugs are hydrophobic in nature [288]. Hydrophobically-modified chitosan polymers are being used in an increasing number of biological applications. Majedi et al. [289] fabricated chitosan based nanoparticles to encapsulate hydrophobic anticancer drugs and achieve a sustained controlled release of the drugs. The nanoparticles were synthesized in a flow focusing microfluidic device via self-assembly at physiological pH.

4.2 Continuous microflow in microreaction technology

Parallel-flow-based microfluidic devices are considered as the base of microreaction technology. There are two ways to perform synthesis in parallel microflow based devices either by using microflow reactors in parallel or sequential modes. For synthesis of compounds in parallel mode, the number of reaction MCs needed is the same as the number of final products. For a library of n compounds when coupled with a library of m compounds, $n \times m$ reaction MCs are prepared by connecting $n + m$ with branched pipes (Fig. 4.2.1). The sequential mode of material synthesis is preferred over the parallel reaction mode [290]. In the sequential mode, reagent segments are sequentially injected into a single reaction MC. When flow segments of reagents in the starting material libraries are sequentially introduced to a MC in all possible combinations, segments of the combinatorial products library can be obtained [290, 291].

Benefits of this technology pose a vital influence on chemical industry, biotechnology, the pharmaceutical industry and medicine, life science, clinical and environmental diagnostic [292]. These devices perform sampling, sample preparation, detection and data processing in integrated model [292]. Cell sorting [293], cell lysis [294], single cell analysis [295] and non-destructive single cell experiments were also performed with real time microscopic image processing [296]. High throughput screenings combine chemistry, genetics and protein analysis together with the help of microchip/microdevices with the capillary electrophoresis [292]. They could be used for fast DNA replication [32], microbial suspensions [297], biological agents and

diseases diagnostics including infectious diseases like the human immunodeficiency virus (HIV) [298], the human papillomavirus (HPV) [299], the hepatitis virus and other [32]. To increase the high throughput capacity different evolving technologies like microlithography, MEMS technology, microfluidics and nanotechnology are being developed in parallel [32]. In drug discovery, vitamin D_3 was recently obtained by using a photo-micro reactor in a highly efficient, two-stage, flow synthesis from provitamin D_3 [300]. By adopting the similar strategy, NicOX has developed Naproxcinod in 2009, which is the first compound in the cyclooxygenase-inhibiting nitric oxide-donating (CINOD) class of anti-inflammatory agents to treat patients with osteoarthritis [301]. Several microfluidic platforms have been developed for the rapid determination of enzymatic activity. Recently, immobilized microfluidic enzyme reactors (IMERs) are getting more importance, as the enzyme is typically immobilized on a solid substrate and supplied with a continuous flow of reagents. The major function of IMERs includes enzyme immobilization, molecular weight quantification and determining enzyme kinetics in heterogeneous protein samples [302, 303]. Kundu et al. [304] developed a microreactor for solid supported enzyme-catalyzed polymerization in continuous flow conditions. They polymerized ε-caprolactone by using immobilized *Candida Antarctica* Lipase B (CALB) in the form of commercial Novozyme 435 (N435) beads (diameter 400 ± 50 μm) packed within a microfluidic channel [304, 305].

4.3 Micromixing in microfluidic devices

Mixing is the most commonly practiced unit operation in chemical and biochemical industrial processes and is also important for different analytical processes [306, 307]. Micromixers can be integrated in a microfluidic system or work as stand-alone devices [308]. Furthermore, the investigation of micromixers is fundamental for understanding transport phenomena on the microscale [308]. These micromixers are used for micro-encapsulation for drug delivery [309], organic synthesis with unstable intermediates [310], high-throughput kinetic screening of chiral homogeneous catalysts in multi-phases [310], powder production [311], and analytical techniques such as time-resolved NMR and time-resolved Fourier transform infrared spectroscopy (FTIR) [306]. The fabrication of micromixers was based on technologies of MEMS like silicon, PDMS or glass. Depending on the mixing principle, micromixers are categorized into active and passive [312]. In drug formulation systems passive micromixers plays important

role and can be further classified into parallel lamination, serial lamination, injection, chaotic advection and droplet. The flow behavior in these micromixers is either electrohydrodynamic, dielectrophoretic, electrokinetic, magnetohydrodynamics or acoustic [308].

4.4 Continuous microfluidics in Point-of-Care devices

Point-of-care (POC) diagnostic devices have useful applications in quick screening and disease testing in sport science, military tactics and space applications [314]. Polymer- and paper-based microfluidic systems with lateral microflow are used for production of POC devices. Despite of popularity the commercialization of these devices is still a challenging job because of operational complexity [315]. POC devices are used for pregnancy testing [316], the diagnosis of infectious diseases (such as *Streptococcus*, influenza, and HIV) [317], screening for drug abuse [315], and blood glucose biosensing [318]. Recent advances in the development of microfluidic systems includes PDMS−glass platform for rapid measurement of blood plasma proteins. The chip separated plasma from whole blood, and the plasma flowed across channels patterned with a barcode-like array of DNA-linked antibodies to detect multiple proteins [319].

4.5 Multiphase parallel microflow devices for cell biology and single cell analysis

Specific applications of microfluidic systems in cell biology [320] and single-cell analysis [295] have been reviewed previously. PDMS is the primary microfluidic device material used for cell culture [321, 322] but other materials like Cyclic-olefin Copolymer (COC), poly(ethylene terephthalate glycol) and combination of these are also used [321]. Microfabricated and microfluidic devices have demonstrated their suitability for single-cell manipulation and analysis of thousands of cells at automatic conditions [1, 323, 324]. Furthermore, these experimental designed devices present a high level of integration for massive parallelization [325], and as well as implementation of complex processes [326]. An efficient integrated microdevice for the analysis of gene expression in single cells was developed by Toriello et al. [327]. The system captures a single cell, transcribes and amplifies the mRNA, and quantitatively analyzes the products of interest. The key components of this microdevice include integrated nanoliter metering pumps and affinity capture matrix for the purification and concentration of products that is coupled to a microfabricated capillary electrophoresis separation channel for product analysis [327]. Van den Brink et al. [328] reported a cell entrapment microfluidic device called

PaSCAl (Fig. 4.5a). In this platform cells are trapped individually in an array of 16–32 lateral pockets using a simple, reproducible, efficient and automated protocol for single cell analysis. The multiphase parallel microfluidic devices are also employed to study the brain functions and functionality of neurons in the body [329]. Recently, Dinh et al. [330] studied the mechanism behind Alzheimer and Parkinson diseases by using Compartmentalized Neuron Arraying (CNA) microfluidic circuits for the preparation of neuronal networks using minimal cellular inputs (10–100-fold less than existing systems). The approach combines the benefits of microfluidics for precision single cell handling with biomaterial patterning for the long term maintenance of neuronal arrangements [330]. The same group also utilized the same microfluidic technique for rapid, reproducible and sensitive neurotoxicity testing platform that combines the benefits of neurite outgrowth analysis with cell patterning [331]. Kim et al. [332] logarithmically scaled continuous perfusion culture of 3T3 fibroblasts for 3 days on microfluidic device by modifying the flow rates through four separate cell-culture chambers using syringe-driven flow and a network of fluidic resistances. Genomic applications often require nanoliters of sample to process and to get high quality results. Marcy et al. [333] developed a two-layer valve-based microfluidic chip for genomic amplification of single cells and used this device to sequence the genomes of uncultivated bacteria found in the human oral cavity (Figure 4.5b). They showed that multiple displacement amplification benefits from the 60-nl reaction chambers, which both increase the effective concentration of genetic material from a single bacterial cell, and reduces amplification bias [334].

4.6 Continuous microfluidics in nucleic acid assays

PDMS, glass and COC are the primary material for integration nucleic acid assays [335, 336]. Synthetic Microfluidic systems for DNA synthesis require less reagents for more cost-effective synthesis and can create more complex genes. Lee et al. [337] parallelized the synthesis of genes on a chip using a multilayer microfluidic device. They used conventional solid-phase chemistry to synthesize a gene fragment of *Bacillus cereus* in a design that encompassed valves, purge lines, reagent controllers, a herringbone binary tree for proper mixing of reagents and an array of 16 nl reaction columns (Fig. 4.6a). The multiple reaction chambers allowed to obtain homogeneous samples, as opposed to the mixtures obtained from common microarray technologies. A PDMS−glass microfluidic device with integrated PCR, enzymatic ssDNA generation, and

electrochemical detection was developed for determination of genomic DNA from Salmonella. The system showed improved detection limits over other microchip-based PCR electrochemical methods [338]. Recently, a compact disk microfluidic device was developed for generating the reciprocating flow of DNA samples within the MCs for rapid DNA hybridization assay with nanoliter-volume samples. The system was tested with a Dengue virus gene sequence and showed better performance than flow-through hybridization under the same conditions [339].

4.7 Microfluidics in proteomics and metabolomics

Zhou et al. [341] have reviewed important aspects of proteomics in microfluidic devices. PMMA, COC and PDMS-glass materials are used for production of proteomics devices. In proteomics applications, the most important features of microfluidic devices are related to delivery of fluid reagents, immobilization of proteins, mixing and reactions, and geometric microarrays [342]. In proteomics microfluidic devices electroosmotic (or electrokinetic) flow and centrifugal pressure flow are used to move analytes through a chip. The proteomics devices are used for enzymatic assays, immunoassays and peptide mass fingerprinting [342]. The enzymatic assays in microfluidics involves the enzyme-protein interaction studies in MCs [342]. This approach was used for the identification of protein drug targets, or for the evaluation of compound libraries in drug discovery. Puckett et al. [343] developed a centrifugal microfluidic device in which homogeneous protein ligand binding assays were performed to detect and characterize the binding interaction between phenothiazine antidepressants and calmodulin, a calcium-binding protein known to interact with this class of drugs.

Metabolomics is the study of metabolite intermediates and byproducts that provides information regarding cellular functions and health. It can be used in diagnostics to identify disease states in individuals [319]. Metabolomic analysis utilizes a high resolution separation technique to aid in the identification or measurement of complex mixtures of metabolites. Separations on the microfluidic format are typically performed by electrophoretic means, such as microchip capillary electrophoresis, or through pressure driven flow. Microchip-capillary electrophoretic (microchip-CE) devices with electrochemical detection have been used in several targeted metabolic profiling studies. Holcomb et al. [344] introduced a microchip-CE device with an electrode array detector for monitoring small molecule metabolites and xenobiotics.

Recently, Shintu et al. [345] made an organ-on-a-chip device that was probed via proton nuclear magnetic resonance for metabolomic analysis of liver and kidney cell cultures exposed to several toxic compounds.

4.8 Human on-a-chip microfluidic systems

The concept of integrated microfluidics has gone beyond tissue or organ level engineering. Investigators are developing integrated 'human-on-a-chip' models that consist of interconnected compartments, each containing a cell type representing a different organ, linked through a microfluidic circulatory system (Fig. 4.8). Esch et al. [346] developed a pharmacokinetics models having microfabricated bioreactor that contained 2D cultures of liver and lung cells in different microchambers interconnected by microfluidic channels. Under different physiological conditions, this system analyses liquid-to-cell ratios, hydrodynamic shear stresses and liquid residence times in living whole-organ systems [347]. The present system also evaluates toxicity levels in the body [347]. This microfluidic system was later modified from 2D to 3D culture system for adipocytes, cancer cells and bone marrow stem cells. The main aim of this conversion was to study drug accumulation, distribution, metabolism and toxicity [37].

5. Scale-up strategies of lab-on-a-chip devices for materials processing

5.1 Microchannel array devices

Although the frequency of droplet generation in flow focusing devices can reach 1,000 Hz for oil-in-water droplets and 12,000 Hz for water-in-oil droplets [348], the volume flow rate of dispersed phase is very low, because there is typically only one droplet generation unit (DGU). Note that when 10 μm diameter droplets are produced at 12,000 Hz frequency, the flow rate of dispersed phase flow is just 0.02 mL h^{-1}. In microchannel (MC) array devices, droplets are formed simultaneously from hundreds or even hundreds of thousands of parallel MCs, which enables much higher total droplet throughputs [162]. E.g., when 10 μm diameter droplets are produced at a frequency of 400 Hz using an array of 100,000 MCs, the overall dispersed phase flow rate is 75 mL h^{-1}. Table 2 compares frequencies of droplet generation and dispersed phase flow rates for microfluidic devices with single DGU and MC array devices. It should be noted

that the maximum frequency of droplet generation increases with decreasing the dispersed phase viscosity. The maximum frequency of drop generation in MC array devices is typically around 10 Hz for edible oil-in-water emulsions, but several hundred Hz for tetradecane-in-water emulsions [349].

Grooved-type MC array devices. The first microfluidic device consisting of grooved-type MC array was developed by Kikuchi et al. [2] using photolithography and anisotropic wet etching in (100) single-crystal silicon (Figure 2.1.1a). This device with a trade name MicroChannel array Flow ANalyzer (MC-FAN) was commercialised by Hitachi Haramachi Electronics Ltd and used for the measurement of blood flow rate (fluidity). The MC-FAN system was first tested for droplet generation by Nakajima group at the National Food Research Institute in Tsukuba, but polydispersed droplets were obtained (Fig. 5.1.1a), due to insufficient channel spacing. In the subsequent studies, MC arrays purposely designed for drop generation have been used and droplets with a CV below 5% have been routinely produced (Fig. 5.1.1c). In addition to single crystal silicon and stainless steel, grooved MC arrays have also been also fabricated by injection molding in PMMA [57]. PMMA channels are inherently hydrophobic and suitable for generation of W/O emulsions [57].

Modules with microgrooves can be either dead-end or cross-flow. In a typical dead-end module shown in Figure 5.1.2a, MCs are fabricated on a terrace line and there are four terrace lines arranged on all four sides of a square silicon plate. Each MC is typically 6–12 μm wide, 4–7 μm deep and 25–140 μm long and the size of MC plate typically ranges from 15×15 mm to 40×40 mm [43, 351]. During operation, MC plate is tightly sealed with a transparent cover plate. The dispersed phase is supplied through the central hole and flows out through MCs on all four sides forming droplets in the surrounding continuous phase. Different designs of grooved MC arrays have been developed including MCs without terrace [352] (Fig. 5.1.1b) and MCs with partition walls on the terrace [353, 354] (Fig. 5.1.1d).

Dead-end modules with grooved MC arrays cannot provide a dispersed phase flow rate above 0.1 mL h^{-1} for vegetable oils, due to limited number of MCs that can be accommodated on the plate (100–1,500). Cross-flow modules with grooved MC arrays are more convenient for the higher droplet throughputs, because many parallel cross-flow channels can be incorporated on a

single MC plate [355]. A simplest cross-flow module shown in Fig. 5.1.2b consists of only one cross-flow channel and two holes at its both ends for introduction and withdrawal of the continuous phase. MCs are arranged at both longitudinal sides of the cross-flow channel [161, 356, 357]. The role of cross-flow is to collect droplets from the module and not to control the droplet size. In the dripping regime, the droplet size is independent on the flow rate of the dispersed or continuous phase. In contrast, in flow focusing devices and T-junctions, the flow rate of all fluid streams has a strong effect on the droplet size. Cross-flow modules with multiple cross-flow channels are available with a maximum size of the MC plate of 60×60 mm. This plate, shown in Figure 5.1.3, consists of 7 cross-flow channels and 11,900 microgrooves arranged in 14 parallel arrays (two arrays per each cross-flow channel) and can provide a dispersed phase flow rate of 1.5 mL h^{-1}, when used in production of soybean oil-in-water emulsions [355].

Straight-through microchannel array devices. A disadvantage of grooved-type MC modules is a limited droplet throughput, due to poor utilization of MC plate surface, because MCs are arranged on the plate surface in longitudinal direction and the feed channels for handling the dispersed and continuous phase must be provided on the plate surface. A vertical array of straight-through MCs allows much better utilisation of the plate surface resulting in significantly higher throughputs. For example, 60×60 mm grooved-type plate with 12,000 MCs can accommodate only 3.3 MCs per 1 mm^2 and provides a maximum soybean oil flow rate of 1.5 mL h^{-1}. On the other hand, 40×40 mm straight-through MC plate has 211,248 MCs, i.e. 132 MCs per 1 mm^2 and a soybean oil flow rate can exceed 30 mL h^{-1} [350].

Straight-through MCs can have either symmetric (Fig. 5.1.4a) or asymmetric (Fig. 5.1.4b) structure. Symmetric MCs are of the same size and shape (e.g., circular or rectangular) over the whole cross section of the plate. Rectangular MCs provide better performance in microchannel emulsification, compared to circular MCs and a slot aspect ratio of at least 3–3.5 is required to ensure production of uniform droplets [66, 358, 359]. Asymmetric MC plate typically consists of circular channels on the upstream (bottom) side and slots on the downstream (top) side. This asymmetric geometry is particularly useful for generation of uniform droplets when the dispersed phase viscosity is less than 1 mPa s, e.g. when the dispersed phase is a volatile (C6-C10) hydrocarbon, such as decane [350]. Asymmetric straight-through MCs have also been used

successfully for production of W/O emulsions [360], polyunsaturated fatty acids (PUFA)-loaded O/W emulsions [361] and n-tetradecane emulsions [349, 362]. The size of droplets produced using asymmetric silicon MCs can range from just several microns [363] to several hundred microns [66]. The droplet size can reach several millimeters using asymmetric MCs with a diameter in the range of 300−500 μm micromachined in stainless steel plates, [102]. For an asymmetric MC plate, the maximum theoretical drop generation frequency (in Hz) that can be achieved in generation of soybean oil-in-water emulsions is given by Kobayashi et al. [364]:

$$f_{\max} = 2.1\times10^{2} d_{MC}^{-1}$$

where d_{MC} is the MC diameter (in μm) and d_{MC} < 100 μm. For example, for a MC plate consisting of 211,248 MCs with d_{MC} = 6.6 μm [350], the maximum drop generation frequency per channel is up to 32 Hz and the maximum overall drop generation rate is up to 6,7 million droplets per second. It should be noted that the maximum drop generation frequency increases with decreasing the viscosity of the dispersed phase. For example, the maximum drop generation frequency of n-tetradecane droplets for an asymmetric MC with d_{MC} = 10 μm was found to be over 400 Hz. A maximum throughput of n-tetradecane droplets in an asymmetric MC plate with a size of 24×24 mm was about 270 mL h^{-1} [349]. Kobayashi et al. [23] have achieved a throughput of n-tetradecane droplets of 1,400 mL h^{-1} using a large 40×40 mm asymmetric MC plate. It was found by CFD simulation that a maximum droplet throughput per unit area of an asymmetric MC plate is independent of the MC diameter [364].

Straight-through micronozzle array includes a plurality of micronozzles having outlets extending above the plate surface (Figure 5.1.4c). They can be used to increase the velocity of the continuous phase at the channel outlet, which could be useful if the viscosity of the dispersed phase is relatively high [68].

5.2 Scaled-up versions of flow focusing devices and microfluidic junctions

5.2.1 Scaled-up devices with a common outlet channel

Microfluidic devices with a common outlet channel allow formation of dispersions that contain droplets or bubbles of two or more distinct fluids (“composite emulsions”) or droplets or bubbles

of a single fluid with bimodal, trimodal or polymodal distribution [365]. Although each of the generators forms distinct families of bubbles or droplets, they influence each other, especially if the dispersed phase is gas [366]. Droplets or bubbles produced from different generators can self-assemble in a common outlet channel to form a wide variety of highly organised dynamic lattices, whose morphology can be controlled by fluid flow rates. In a coupled device, every two adjacent flow focusing droplet generators (FFDGs) share one of the inlets of the continuous phase (Fig. 5.2.1a). In the device shown in Fig. 5.2.1b, two separate inlets of the continuous phase are implemented in each droplet generator. Simultaneous generation of droplets with different sizes was achieved by integrating in a single chip multiple FFDGs with distinct geometries [19]. Simultaneous generation of droplets with nearly identical sizes but different compositions was achieved by integrating in a single chip interconnected bifurcated inlet channels with micromixers and multiple parallel FFDGs [367].

5.2.2 High-throughput microfluidic junction and flow focusing devices

A single microfluidic junction or flow focusing orifice can produce up to 1 g h^{-1} of drops, depending on the drop size and dispersed phase viscosity. The productivity increases with increasing drop size and decreasing dispersed phase viscosity. In a continuous operation, the running time is about 8000 hours per year and therefore, the productivity of a continuous microfluidic device with a single drop generation unit (DGU) is less than 8 kg per year. The productivity requirements of a typical industrial emulsification process are about 10^3 tonnes per year [18] which means that more than 125,000 DGUs are necessary to meet this level of production.

Increasing throughput of microfluidic devices merely by using multiple devices with a single DGU is not feasible, because each device needs a separate set of pumps or pressurized tanks to supply fluids [25]. 125,000 such devices would require 250,000 pumps and therefore, the only viable option for increasing production is to integrate many DGUs in a single chip, and drive the assembly with a single set of pumps. However, a single chip with large number of DGUs is impractical, because if only one DGU does not work properly, e.g. due to channel clogging, the whole device would require decommissioning for cleaning or complete

reconstruction. Secondly, a production plant with a monolithic chip cannot easily meet different productivity requirements, because the total number of DGUs is fixed. Finally, the fabrication of chips with smaller number of parallelized DGUs is easier. Therefore, scaling up microfluidic drop generators to industrial level requires a hierarchical approach with at least two levels of structural integration of drop makers: (i) integration of multiple parallel DGUs in a single chip and (ii) integration of multiple chips, each containing hundreds of paralellized DGUs, into a production plant. In the next section, we will review scale-up strategies used to achieve both levels of structural integration.

Simple droplets. Parallelized microfluidic junction devices for producing larger quantities of simple emulsions have been demonstrated by several groups [20, 368, 369]. The two most common layouts of microfluidic channels used to distribute fluids from a single manifold into multiple parallel drop generation units are tree-type and ladder-type (Fig. 5.2.2). The tree-type network has one inlet for each phase at the zeroth branching level and 2^m inlet channels for each phase at the m^{th} branching level. Therefore, the number of inlet channels increases by a factor of 2 between two consecutive branching levels [370]. The ladder-type structure has two main feed channels (stiles), one for the dispersed phase and one for the continuous phase, and smaller channels branching off them (the rungs of a ladder). The ladder-type structure offer three advantages over tree layout: (i) More compact design; a chip with the ladder-type architecture consisting of 8 droplet generation units occupies around 7 cm^2, as compared to 84 cm^2 for the tree structure; (b) The performance of ladder-type microfluidic network is less affected by small random variations in the channel size (±0.4 μm), caused by the limitations of the fabrication process; (c) In the tree-type network, a defect (e.g. clogging) in one arm will break the symmetry of the system and affect the whole branch from the very first bifurcation [369]. However, the tree layout is the more energy efficient means of feeding droplet generation units in parallel. Tetradis-Meris et al. [369] integrated 180 drop generation units (cross-junctions), each consisting of 20 × 20 μm channels, to produce W/O emulsions with a droplet diameter of 21 μm and the droplet diameter variations of less than 5%. The cross junctions were arranged in 9 parallel lines, each line having 20 cross junctions, and connected using the ladder-type architecture. A strategy used for interconnection of these cross-junctions is shown in Figure 5.2.3. The device was assembled using three layers of channels fabricated in PMMA and stacked on top of each other.

The bottom layer was a secondary distribution layer containing long vertical manifolds, the middle layer was a primary distribution layer with horizontal manifolds and the top layer was a drop generation layer containing cross junctions and short inlet and outlet channels. Long vertical channels on the right-hand side of the chip are drainage manifolds; they were open during startup and cleaning procedures but closed during drop generation.

Nisisako and Torii [20] integrated 128 cross junctions consisting of 256 drop generation units (2 per each cross junction) on a 42 × 42 mm chip to produce droplets of photopolymerizable acrylate monomer at a throughput of 320 mL h^{-1}. The chip was composed of 128 inlet holes for the dispersed phase and 64 inlet holes for the continuous phase, all circularly arranged around a large outlet hole (Fig. 5.2.4a). In this design, both the dispersed and continuous phase stream was split into two streams before reaching a drop generation unit (Fig. 5.2.4b), which enabled to reduce the number of inlet holes and the chip size.

Kawai et al. [368] produced gel particles with a variation of particle diameter of 12% in a microfluidic device consisting of three piled-up glass discs, each having 100 radially arranged Y junctions (300 in total). They also demonstrated a simultaneous operation of five separate modules (1500 Y-junctions in total) to produce O/W emulsions with a similar coefficient of variation of droplet diameters [368]. Li et al. [371] produced 50 g h^{-1} of poly(N-isopropylacrylamide) (PNIPAAm) particles with an average diameter of 141 μm and a variation of diameters of less than 5% using a PDMS microfluidic device comprising 8 individual modules, each consisting of 16 flow focusing DGUs and 16 wavy channels where the droplets are exposed to UV-irradiation to trigger photo-initiated polymerization of NIPAAm (Fig. 5.2.5). Each module was fabricated by sealing the planar bottom layer, the intermediate 'reactor' layer and a top 'adapter' layer containing a bifurcated manifold for the injection of the dispersed phase. In Figure 5.2.5, the reactor and adapter layers occupy gray and blue areas, respectively. 'Crosstalk' (coupling) between parallel DGUs within the module was prevented by elongating a hydrodynamic path of the dispersed phase prior to its entrance to the orifice, thereby increasing the hydrodynamic resistance between adjacent DGUs. It was done by introducing a 40 mm-long wavy channel for the dispersed phase upstream of the orifice, as shown in Fig. 5.2.5.

Another strategy of increasing droplet throughput in microfluidic devices is to use a splitting array consisting of a series of channels that divide into two channels several times [182, 190]. In the device shown in Fig. 5.2.6a, droplets produced in the upstream cross junction are split into 16 equal daughter droplets, each having a diameter $2^{4/3}$ times smaller than the initial droplet diameter, and the diameter of droplets decreases by a factor of $2^{1/3}$ between two consecutive branching levels. In Fig. 5.2.6b, water droplets with a diameter of 88 μm were split into daughter droplets with a diameter of 35 μm at the dispersed phase flow rate of 7 mL h^{-1}. To produce 35 μm droplets directly, the maximum production rate would be 0.6 mL h^{-1}, which means that the splitting device operates more than 10 times faster. For optimal splitting, the flow velocity should be neither too low nor too high. If too low, droplets may not split and if too high, satellite droplets may produce. In order to keep a constant flow velocity in all channels, the total cross-sectional area of the channels was kept constant at all branching levels and thus, the channel diameter decreased by a factor of $2^{1/2}$ at each bifurcation.

Compound (multiphase) droplets and bubbles. Microfluidic devices have become increasingly popular for making droplets and bubbles with complex morphologies, since appropriate alternative technologies are lacking. Faster microfluidic production of multiple emulsions was demonstrated by several groups [20, 25, 50, 182]. Abate and Weitz [182] used a splitting array shown in Figs. 5.2.6c and 5.2.6d to split core/shell droplets three times, into 8 equal daughter droplets. In this way, the throughput was increased by a factor of 5 compared to that in a direct emulsification.

Nisisako et al. [50] and Nisisako and Torii [20] used radial array of droplet generation units to produce compound droplets of different internal structure. The channels shown in Fig. 5.2.7a were manufactured in fused silica glass by dry reactive ion etching. The chip incorporates 32 sets of triple emulsion droplet generators, each consisting of three consecutive ψ junctions. To avoid problems associated with partial hydrophobisation of the channels, the chip was used to produce oil-in-oil-in-oil-in-water (O/O/O/W) droplets (all dispersed phases were organic liquids). The maximum flow rates of innermost, inner, middle, and continuous phases in this device were respectively 5.0 mL h^{-1}, 6.0 mL h^{-1}, 20.0 mL h^{-1}, and 90.0 mL h^{-1} [50]. Fig. 5.2.7b shows a chip consisting of 128 sets of droplet generation units for production of bifacial (Janus) droplets. Two distinct dispersed phases (1 and 2) were introduced from the alternately arranged outer inlets and

each stream was split into two streams in bifurcated inlet channels to form a combined two-phase stream that was eventually broken up into Janus droplets.

Romanowsky et al. [25] developed three-dimensional (3D) arrays of double emulsion droplet generators, interconnected by a 3D network of distribution and collection channels. Each droplet generator comprised two consecutive junctions operating in one-step double emulsification mode shown in Fig. 3.2.1g. By making the distribution channels with much lower flow resistance than the droplet generator, the input fluids were evenly distributed to all droplet generators, so all of them produced droplets of the same size. In the first stage of parallelization, several droplet generators were arranged in a line, and connected to a single set of inlets and outlets using a primary distribution layer placed above the droplet generation layer (Fig. 5.2.8). In the second stage of parallelization, several lines of drop generators were arranged in a planar (xy) array, each line having its own primary distribution layer (Fig. 5.2.9a). The channels in all primary distribution layers were then connected to yet larger distribution and collection channels using a secondary distribution layer (Fig. 5.2.9b) placed above the primary ones. In the final stage of parallelization, a series of planar arrays of drop generators were stacked together, each planar array having its own primary and secondary distribution layers, and the channels in all secondary distribution layers were connected with vertical, tertiary distribution channels. The locations of these vertical channels are shown by arrows in Fig. 5.2.9c. By integrating 15 double emulsion droplet generators in a planar (3×5) array, core/shell droplets were produced at the flow rates of the core aqueous phase, shell octanol phase and continuous aqueous phase of 24, 30, and 215 mL h^{-1}, respectively, and both inner and outer diameter variation was below 6% [25]. By integrating hundreds of double emulsion drop generators, it would be possible to fabricate a device occupying one litre of space that produces uniform core/shell droplets at more than one litre per hour, or nearly nine tons per year [25].

Kendall et al. [372] developed a radial array of flow focusing droplet generators (FFDGs) capable of generating dual layer microbubbles for combined ultrasound imaging and drug delivery. They constructed a 33-mm diameter module assembled from 3 stacked PDMS layers to generate microbubbles ~ 20 μm in diameter with a coefficient variation of about 5% at rates exceeding 10^5 Hz. The core gas enters a single inlet on the top PDMS layer and bifurcates into 8

serpentine channels, serving as resistors, before entering each orifice. Oil and lipid solution are infused through inlets in bottom layer and bifurcate in the middle and bottom layers respectively, to reach vertical distribution channels, which connect to the top layer. The top layer consisting of 8 FFDGs is shown in Figure 5.2.10. Given a larger chip area, this design can be expanded into any 2N number of FFDGs to further increase the throughput.

5.3 Scaled-up versions of flow-based microreaction devices

Microfluidic reaction devices utilize single-phase flow and/or multi-phase flow in microchannel(s). Microfluidic reaction devices can be used to generate products in higher yield, purity and selectivity when compared to batch reactors, while a disadvantage of the microfluidic reaction technology is the fact that only small quantities of product can be prepared [373]. The major advantage of microfluidic reaction devices deals with decreasing linear dimensions, which significantly increases the surface-to-volume ratio in this technology. For the channel diameter from tens to hundreds of micrometers, the surface-to-volume ratio in the range of 10000 to 50000 m^2 m^{-3} is achieved [374]. Consequently, significant intensification of mass and heat transfer can be achieved, resulting in considerable reduction in operation times [375]. Additionally, microfluidic reaction devices can be operated at high pressures (up to 600 bar in stainless steel microreactors), therefore opening a path to novel process windows [376] where a significant intensification of the reaction rate canbe achieved by operating at high pressures and temperatures [377] or in explosive regimes [378].

Scale-up of the microfluidic reaction devices is an ongoing challenge, as two approaches exist: (a) Parallelization, whereby large numbers of identical microchannels are employed and (b) Internal scale-up, whereby a combination of microstructured reactor design and conventional dimension scale-up is applied. Parallelization was demonstrated as an efficient method in the case of single phase or gas-solid reaction systems. An on-chip system has preferably a minimum number of inlets, one for each reactant and/or fluid catalyst, and one outlet. To achieve parallelization, flow splitters are required, to split the inlet flows into n number of flows, where n is the number of parallel reactors. In microchannels small deflections and imperfections always exist, easily varying the hydraulic resistance over parallel channels in the range of a few percent, resulting in flow variations. In highly exothermic reactions flow splitter balancing

becomes very important, due to the relation between temperature, viscosity and flow resistance. The second important parameter in designing parallel microreactors is avoiding bubbles blocking channels. At encapsulated bubbles two forces are applied: capillary forces that tend to keep the bubble in position and pressure drops across the bubbles that try to push the bubble out of position. Currently, flow splitter reactor chips with 8 parallel reactors are being fabricated by LioniX BV [379]. Velocys Inc. has been one of the pioneers of microfluidic reactor parallelization concept for gas-to-liquid (GTL) applications [380]. Internal scale-up is highly promising but not widely employed approach, with most application reports coming from Lonza Ltd. [381]. Last, the small sizes of microfluidic reaction devices, excellent safety profile coupled with their high performance have been touted as one of the future tools of modular chemical production. To operate the microfluidic devices, microfluidic fuel cells could be the alternative that can be scaled up in parallel arrays to meet the industrial demands, recently Fuerth and Bazylak [382] presented a up-scaled microfluidic cell architecture that provides higher available surface area compared to conventional microfluidic fuel cells, providing the potential for higher overall power outputs and this newly designed cell has nine times more active electrode surface area in comparison to previously designed microfluidic cell by Kjeang et al. [223, 383].

5.4 Scale-up versions of biochemical and biological microfluidic devices

Highly integrated microfluidic devices show great promise for basic biomedical and pharmaceutical research, and robust and portable point-of-care devices could be used in clinical settings and revolutionize the whole world [384]. The concept of microfluidic large scale integration was firstly developed by Thorsen et al. [385]. They developed high-density integrated microfluidic chips contain plumbing networks with thousands of micromechanical valves and hundreds of individually addressable chambers. The system was regarded as fluidic multiplexor, which exponentially increases the processing power of a network and resembled as random-access memory. The integrated microchip has 2056 microvalves, with 256 subnanoliter reaction chambers. This device was primarily created to test for the expression of a particular enzyme (cytochrome c peroxidase) in *E.coli* [385]. Hong et al. [386] developed microfluidic chips for automated nucleic acid purification from small numbers of bacterial or mammalian cells in a single parallel integrated microchip that utilized nanoliter fluid for processing. They concluded that parallelization of complex sequential bioprocesses comprising cell isolation, cell lysis, DNA

affinity purification and the recovery of the purified DNA could be possible from this integrated chip and this process can be applied to many different biological procedures [386].

Recently, Gomez-Sjoberg et al. [387] developed a general platform for integrated microfluidic cell culture. The system contained 96 independent cell culture chambers to which customized media and reagents could be delivered at pre-set conditions (Fig. 5.4a). Tay et al. used this platform to monitor NF-κB signaling dynamics in single cells responding to TNF-α [388]. With active fluidic control, temporal TNF-α stimulation could be delivered to cell chambers as digital response signals independently. Similarly, whole organism investigation is becoming a growing trend in microfluidic applications, the typical examples include microfluidic devices for manipulating, sorting, and screening *Caenorhabditi elegans* [389-392]. Crane et al. scale up these devices to screen up to 40, 000 animals and identify novel phenotypic variants, previously undetected by manual classification [28, 393]. Microfluidic systems level integration has also got popularity in single cell genome sequencing studies. Recently an amplified version of the single cell isolation and genomic amplification device developed by Marcy et al. have been used in a variety of single human cell sequencing applications. Similar modified version of Marcy et al. developed by Fan et al. [394] sorted individual human metaphase cells to perform whole genome personal haplotyping. Wang et al. [395] used a similar device to isolate the genetic material from single human sperm cells for whole-genome sequencing in order to measure genomic variation caused by recombination and de novo mutation during gametogenesis (Fig. 5.4b).

Cellular microarrays are useful for screening large-scale libraries of materials for drug discovery and toxicity testing [396-398] at high throughput, while reducing the time and cost required for the assays and increasing their portability. Applications of high-content screening are circumscribed by several practical aspects, including low sample throughput and absence of sorting capability. Moreover, high-resolution two-dimensional (2D) images consume limited detector bandwidth, introduce a data-acquisition delay that is a barrier for real-time decisions needed for sorting and introduce noise via inaccuracies in image segmentation. McKenna et al. [399] developed one dimensional flow cytometer by using parallel microfluidic cytometer (PMCMC) with 384 parallel flow channels that use a high-speed scanning photomultiplier-based detector to combine low-pixel-count. This newly device investigate protein localization in a

yeast model for human protein misfolding diseases. Multiplexed analysis based upon multiphase parallel flows has been used for the simultaneous quantification of different targets within a single sample. Adopting this concept Chapin et al. [400] developed a microfluidic system for the rapid alignment of multifunctional hydrogel microparticles designed to bear one or several biomolecule probe regions, and graphical code to identify the embedded probes. This system performs multiple functions such as high particle throughput, ensures proper particle alignment for decoding and target quantification, and reliably operated continuously without clogging. Huang et al. [401] developed a 3D microfluidic vascular network that operates on electrostatic discharge phenomena. This process generates highly branched tree-like microchannel architectures that bear remarkable similarity to naturally occurring vasculature. This method can be applied to a variety of polymers, and may help to produce organ-sized tissue scaffolds containing embedded vasculature.

Protein crystallization by conventional methods often results in low yield of protein purification. The problem can be solved by using microfluidic devices that uses microgram of sample and results in higher yield. In an early application of microfluidic large scale integration, Hansen et al. used a microfluidic platform for high throughput screening of crystallization reagents [402, 403]. They used two devices; one was a microfluidic formulation device (Figure 5.4c) based on a ring-shaped mixing chamber to purify the protein against combinations of various precipitants and buffers, while the second device (Figure 5.4d) incorporated a passive diffusion-based mixing scheme and was used to screen high potential conditions identified in the formulation device [403]. With less than three microliters of protein this chip could perform crystal screens on 244 conditions demonstrating a screening efficiency of over 100-fold better than commercial screens [403].

6. Conclusions and outlook

Microfluidic technology offers an unprecedented level of control over size, shape, morphology, and composition of emulsion droplets, enabling production and manipulation (sorting, splitting, merging, single cell encapsulation, incubation, etc.) of highly uniform single and compound droplets with a typical variation of droplet diameters of less than 5%. Microfluidic devices can only be industrialized if they meet the following two requirements: scalability and versatility. High throughput analysis is required for optimizing drug delivery systems, and efforts have been

made to scale-up microfluidic throughput devices capable of analysing and generating particles or droplets with high productivity [20, 22].

Microfluidic devices that consist of a single unit for droplet generation have very low throughput (typically < 1 mL h^{-1}), indicating that their scale-up is essential to perform industrial-scale production. Microfluidic systems can be scaled-up by two-dimensional and three-dimensional integration of numerous drop generation units in a large device and/or by numbering-up of devices. To date, several research groups have demonstrated the integration of droplet generation units into planar (orthogonal or radial) or 3D arrays (Weitz's group [25], Kumacheva's group [371], Torii's group [50], and Unilever's group [369]]. To date, the maximum droplet throughput achieved in scaled-up microfluidic systems was above 300 mL h^{-1}, which means that the productivity was improved by 2–4 orders of magnitudes, depending on the number of drop generation units. Droplet throughput in microfluidic systems can be additionally improved by splitting each generated droplet multiple times into even number of equal daughter droplets.

Apart from integration of planar microfluidic drop generation units, large efforts have been made to increase throughput of microchannel array devices with 3D architecture that exploit a mechanism of spontaneous droplet generation through Laplace pressure differences. The maximum throughput of microchannel array devices, on a litre per hour scale, has been achieved using asymmetric straight-through microchannel plates [23]. Membrane emulsification, especially in premix mode [155] is another microfluidic process suitable for large scale production of size controlled emulsion droplets on a scale of hundreds of tonnes per m^2 of membrane area, although it should be admitted that a coefficient of variation of droplet diameters in this method is well above 10 %.

The scale-up of integrated microfluidic devices that utilize continuous and parallel flows have been received much attention to medical science, as those integrated with optical techniques (optofluidics) can increase the screening, detection and imaging capacity of microfluidic devices and as well as increase the scope of their applications like generation of energy. Parallel combination is preferred to scale up integrated microfluidic devices, as demonstrated by Erickson's group [404], Yanik's group [405], Bhatia's Group [406] and Burns' group [407]. A recent approach that uses a photomultiplier to combine one-dimensional imaging with microfluidic flow cytometry demonstrated its usefulness in high content and throughput

screening with a speed of several thousand cells per second [399], providing a good example of integrated scale-up microfluidics. On-going efforts to scale up microfluidics devices for single cell analysis (e.g., valve-based microfluidic qPCR system) would provide a low-volume (nanoliter) and high-throughput (thousands of PCR reactions per device) [408].

From an industrial point of view, it is highly desirable that microfluidic systems operate with a minimum number of pumps (or pressure tanks) and distribution channels. Another key point for industrial-scale applications of microfluidic technology is to achieve successful continuous long-term operation and to minimise the crosstalk between parallel droplet generators sharing supply manifolds. Additional challenges of operating an industrial microfluidic emulsification plant include the start-up procedure, the filtration of fluids to remove particles that would clog the channels, and the exchange of deteriorated devices while operating the others. Finally, it must be bear in mind that consumers will not pay more for a product just because it is made by microfluidics [18]. The implementation of large scale microfluidic processes will critically depend on the ability to create a ‘killer application’ - an application of microfluidics to make an innovative, powerful product with a sustainable need in the market that cannot be made with any other technology.

References

[1] G.M. Whitesides, The origins and the future of microfluidics, Nature. 442 (2006) 368-373.

[2] Y. Kikuchi, H. Ohki, T. Kaneko, K. Sato, Microchannels made on silicon wafer for measurement of flow properties of blood cells, Biorheol. 26 (1989) 1055.

[3] Y. Kikuchi, K. Sato, H. Ohki, T. Kaneko, Optically accessible microchannels formed in a single-crystal silicon substrate for studies of blood rheology, Microvascular Res. 44 (1992) 226-240.

[4] A. Manz, D.J. Harrison, E.M.J. Verpoorte, J.C. Fettinger, A. Paulus, H. Lüdi, H.M. Widmer, Planar chips technology for miniaturization and integration of separation techniques into monitoring systems: Capillary electrophoresis on a chip, J. Chromatog. A. 593 (1992) 253-258.

[5] A. Aota, K. Mawatari, T. Kitamori, Parallel multiphase microflows: fundamental physics, stabilization methods and applications, Lab Chip. 9 (2009) 2470-2476.

[6] L. Li, R.F. Ismagilov, Protein crystallization using microfluidic technologies based on valves, droplets, and slipchip, Annu. Rev. Biophys. 39 (2010) 139-158.

[7] G. Liu, C. Shen, Z. Yang, X. Cai, H. Zhang, A disposable piezoelectric micropump with high performance for closed-loop insulin therapy system, Sens. Actuators A. 163 (2010) 291-296.

[8] J.W. Chung, K. Lee, C. Neikirk, C.M. Nelson, R.D. Priestley, Photoresponsive coumarin-stabilized polymeric nanoparticles as a detectable drug carrier, Small. 8 (2012) 1693-1700.

[9] B.H. Weigl, R.L. Bardell, C.R. Cabrera, Lab-on-a-chip for drug development, Adv. Drug Deliver. Rev. 55 (2003) 349-377.

[10] L. Kang, B.G. Chung, R. Langer, A. Khademhosseini, Microfluidics for drug discovery and development: From target selection to product lifecycle management, Drug Discover.Today. 13 (2008) 1-13.

[11] S.Y. Teh, R. Lin, L.H. Hung, A.P. Lee, Droplet microfluidics, Lab Chip. 8 (2008) 198-220.

[12] C.N. Baroud, F. Gallaire, R. Dangla, Dynamics of microfluidic droplets, Lab Chip. 10 (2010) 2032-2045.

[13] R. Seemann, M. Brinkmann, T. Pfohl, S. Herminghaus, Droplet based microfluidics, Rep. Prog. Phys. 75 (2012) 016601.

[14] G.T. Vladisavljević, I. Kobayashi, M. Nakajima, Production of uniform droplets using membrane, microchannel and microfluidic emulsification devices, Microfluid. Nanofluid. 13 (2012) 151-178.

[15] J. Atencia, D.J. Beebe, Controlled microfluidic interfaces, Nature. 437 (2005) 648-655.

[16] I. Kobayashi, K. Uemura, M. Nakajima, Controlled generation of monodisperse discoid droplets using microchannel arrays, Langmuir. 22 (2006) 10893-10897.

[17] V. Barbier, H. Willaime, P. Tabeling, F. Jousse, Producing droplets in parallel microfluidic systems, Phys. Rev. E. 74 (2006) 046306.

[18] C. Holtze, Large-scale droplet production in microfluidic devices—an industrial perspective, J. Phys. D: Appl. Phys. 46 (2013) 114008.

[19] W. Li, E.W.K. Young, M. Seo, Z. Nie, P. Garstecki, C.A. Simmons, E. Kumacheva, Simultaneous generation of droplets with different dimensions in parallel integrated microfluidic droplet generators, Soft Matter. 4 (2008) 258-262.

[20] T. Nisisako, T. Torii, Microfluidic large-scale integration on a chip for mass production of monodisperse droplets and particles, Lab Chip. 8 (2008) 287-293.

[21] K. van Dijke, G. Veldhuis, K. Schroen, R. Boom, Parallelized edge-based droplet generation (EDGE) devices, Lab Chip. 9 (2009) 2824-2830.

[22] I. Kobayashi, Y. Wada, K. Uemura, M. Nakajima, Microchannel emulsification for mass production of uniform fine droplets: integration of microchannel arrays on a chip, Microfluid. Nanofluid. 8 (2010) 255-262.

[23] I. Kobayashi, A. Neves Marcos, Y. Wada, K. Uemura, M. Nakajima, Large microchannel emulsification device for mass producing uniformly sized droplets on a liter per hour scale, Green Process. Sci. 1 (2012) 353.

[24] S. Sugiura, M. Nakajima, S. Iwamoto, M. Seki, Interfacial tension driven monodispersed droplet formation from microfabricated channel array, Langmuir 17 (2001) 5562-5566.

[25] M.B. Romanowsky, A.R. Abate, A. Rotem, C. Holtze, D.A. Weitz, High throughput production of single core double emulsions in a parallelized microfluidic device, Lab Chip. 12 (2012) 802-807.

[26] L. Shui, J.C.T. Eijkel, A. van den Berg, Multiphase flow in microfluidic systems – Control and applications of droplets and interfaces, Adv. Colloid Interface Sci. 133 (2007) 35-49.

[27] F.S. Majedi, M.M. Hasani-Sadrabadi, S.H. Emami, M. Taghipoor, E. Dashtimoghadam, A. Bertsch, H. Moaddel, P. Renaud, Microfluidic synthesis of chitosan-based nanoparticles for fuel cell applications, Chem. Commun. 48 (2012) 7744-7746.

[28] A.M. Streets, Y. Huang, Chip in a lab: Microfluidics for next generation life science research, Biomicrofluidics. 7 (2013) 011302-011323.

[29] C.-X. Zhao, L. He, S.Z. Qiao, A.P.J. Middelberg, Nanoparticle synthesis in microreactors, Chem. Eng. Sci. 66 (2011) 1463-1479.

[30] J. Melin, S.R. Quake, Microfluidic large-scale integration: The evolution of design rules for biological automation, Annu. Rev. Biophys. Biomol. Struct. 36 (2007) 213-231.

[31] S. Kim, H.J. Kim, N.L. Jeon, Biological applications of microfluidic gradient devices, Integr. Biol. 2 (2010) 584-603.

[32] C. Zhang, J. Xu, W. Ma, W. Zheng, PCR microfluidic devices for DNA amplification, Biotechnol. Adv. 24 (2006) 243-284.

[33] A.M. Skelley, J.R. Scherer, A.D. Aubrey, W.H. Grover, R.H.C. Ivester, P. Ehrenfreund, F.J. Grunthaner, J.L. Bada, R.A. Mathies, Development and evaluation of a microdevice for amino acid biomarker detection and analysis on Mars, Proc. Natl. Acad. Sci. U S A. 102 (2005) 1041-1046.

[34] A.M. Taylor, N.L. Jeon, Micro-scale and microfluidic devices for neurobiology, Curr. Opin. Neurobiol. 20 (2010) 640-647.

[35] W. Gu, X. Zhu, N. Futai, B.S. Cho, S. Takayama, Computerized microfluidic cell culture using elastomeric channels and Braille displays, Proc. Natl. Acad. Sci. U S A. 101 (2004) 15861-15866.

[36] J. Wang, G. Sui, V.P. Mocharla, R.J. Lin, M.E. Phelps, H.C. Kolb, H.-R. Tseng, Integrated microfluidics for parallel screening of an in situ click chemistry library, Angew. Chem. Int. Ed. Engl. 45 (2006) 5276-5281.

[37] D. Huh, G.A. Hamilton, D.E. Ingber, From 3D cell culture to organs-on-chips, Trends Cell Biol. 21 (2011) 745-754.

[38] V. Lecault, A.K. White, A. Singhal, C.L. Hansen, Microfluidic single cell analysis: from promise to practice, Curr Opin Chem Biol. 16 (2012) 381-390.

[39] L. Gervais, N. de Rooij, E. Delamarche, Microfluidic chips for point-of-care immunodiagnostics, Adv. Mat. 23 (2011) H151-H176.

[40] W.G. Lee, Y.-G. Kim, B.G. Chung, U. Demirci, A. Khademhosseini, Nano/Microfluidics for diagnosis of infectious diseases in developing countries, Adv. Drug Deliver. Rev. 62 (2010) 449-457.

[41] S. Neethirajan, I. Kobayashi, M. Nakajima, D. Wu, S. Nandagopal, F. Lin, Microfluidics for food, agriculture and biosystems industries, Lab Chip. 11 (2011) 1574-1586.

[42] J. Leng, J.B. Salmon, Microfluidic crystallization, Lab Chip. 9 (2009) 24-34.

[43] T. Kawakatsu, Y. Kikuchi, M. Nakajima, Regular-sized cell creation in microchannel emulsification by visual microprocessing method, J. Am. Oil Chem. Soc. 74 (1997) 317-321.

[44] I. Kobayashi, M. Nakajima, K. Chun, Y. Kikuchi, H. Fujita, Silicon array of elongated through-holes for monodisperse emulsion droplets, AIChE J. 48 (2002) 1639-1644.

[45] T. Nisisako, T. Torii, T. Higuchi, Novel microreactors for functional polymer beads, Chem. Eng. J. 101 (2004) 23-29.

[46] J.A. Plaza, M.J. Lopez, A. Moreno, M. Duch, C. Cané, Definition of high aspect ratio glass columns, Sens. Actuators A. 105 (2003) 305-310.

[47] C.H. Lin, G.B. Lee, Y.H. Lin, G.L. Chang, A fast prototyping process for fabrication of microfluidic systems on soda-lime glass, J. Micromech. Microeng. 11 (2001) 726.

[48] S. Okushima, T. Nisisako, T. Torii, T. Higuchi, Controlled production of monodisperse double emulsions by two-step droplet breakup in microfluidic devices, Langmuir. 20 (2004) 9905-9908.

[49] T. Kim, S. Kwon, Design, fabrication and testing of a catalytic microreactor for hydrogen production, J. Micromech. Microeng. 16 (2006) 1760.

[50] T. Nisisako, T. Ando, T. Hatsuzawa, High-volume production of single and compound emulsions in a microfluidic parallelization arrangement coupled with coaxial annular world-to-chip interfaces, Lab Chip. 12 (2012) 3426-3435.

[51] S. Kuiper, C.J.M. van Rijn, W. Nijdam, M.C. Elwenspoek, Development and applications of very high flux microfiltration membranes, J. Membr. Sci. 150 (1998) 1-8.

[52] R. Jena, C.Y. Yue, Y.C. Lam, Micro fabrication of cyclic olefin copolymer (COC) based microfluidic devices, Microsyst. Technol. 18 (2012) 159-166.

[53] P. Nunes, P. Ohlsson, O. Ordeig, J. Kutter, Cyclic olefin polymers: emerging materials for lab-on-a-chip applications, Microfluid. Nanofluid. 9 (2010) 145-161.

[54] Z. Nie, S. Xu, M. Seo, P.C. Lewis, E. Kumacheva, Polymer particles with various shapes and morphologies produced in continuous microfluidic reactors, J. Am. Chem. Soc. 127 (2005) 8058-8063.

[55] T. Thorsen, R.W. Roberts, F.H. Arnold, S.R. Quake, Dynamic pattern formation in a vesicle-generating microfluidic device, Phys. Rev. Lett. 86 (2001) 4163-4166.

[56] T. Eusner, M. Hale, D.E. Hardt, Process robustness of hot embossing microfluidic devices, J. Manuf. Sci. Eng. 132 (2010) 030920-030928.

[57] H. Liu, M. Nakajima, T. Nishi, T. Kimura, Effect of channel structure on preparation of a water-in-oil emulsion by polymer microchannels, Eur. J. Lipid Sci. Technol. 107 (2005) 481-487.

[58] T. Nisisako, T. Torii, T. Higuchi, Droplet formation in a microchannel network, Lab Chip. 2 (2002) 24-26.

[59] C.H. Yeh, P.W. Lin, Y.C. Lin, Chitosan microfiber fabrication using a microfluidic chip and its application to cell cultures, Microfluid. Nanofluid. 8 (2010) 115-121.

[60] Y. Morimoto, W.H. Tan, Y. Tsuda, S. Takeuchi, Monodisperse semi-permeable microcapsules for continuous observation of cells, Lab Chip. 9 (2009) 2217-2223.

[61] K. Kim, J.B. Lee, High aspect ratio tapered hollow metallic microneedle arrays with microfluidic interconnector, Microsyst. Technol. 13 (2007) 231-235.

[62] J. Tong, M. Nakajima, H. Nabetani, Y. Kikuchi, Y. Maruta, Production of Oil-in-Water Microspheres Using a Stainless Steel Microchannel, J. Colloid Interface Sci. 237 (2001) 239-248.

[63] A. Luque, F.A. Perdigones, J. Esteve, J. Montserrat, A.M. Ganan-Calvo, J.M. Quero, Silicon microdevice for emulsion productionusing three-dimensional flow focusing, J. Microelectromech. Syst. 16 (2007) 1201-1208.

[64] T. Kawakatsu, Y. Kikuchi, M. Nakajima, Regular-sized cell creation in microchannel emulsification by visual microprocessing method, Journal of the American Oil Chemists' Society. 74 (1997) 317-321.

[65] T. Kawakatsu, G. Tragardh, C. Tragardh, M. Nakajima, N. Oda, T. Yonemoto, The effect of the hydrophobicity of microchannels and components in water and oil phases on droplet formation in microchannel water-in-oil emulsification, Colloids Surf. A. 179 (2001) 29-37.

[66] I. Kobayashi, Y. Murayama, T. Kuroiwa, K. Uemura, M. Nakajima, Production of monodisperse water-in-oil emulsions consisting of highly uniform droplets using asymmetric straight-through microchannel arrays, Microfluid. Nanofluid. 7 (2009) 107-119.

[67] F. Laermer, A. Urban, Through-Silicon Vias Using Bosch DRIE Process Technology, in: J.N. Burghartz (Ed.), Springer, New York, 2011, pp. 81-92.

[68] S. Sugiura, T. Oda, Y. Izumida, Y. Aoyagi, M. Satake, A. Ochiai, N. Ohkohchi, M. Nakajima, Size control of calcium alginate beads containing living cells using micro-nozzle array, Biomaterials. 26 (2005) 3327-3331.

[69] Y. Xia, G.M. Whitesides, Soft Lithography, Annu. Rev. Mater. Sci. 28 (1998) 153-184.

[70] M.E. Wilson, N. Kota, Y. Kim, Y. Wang, D.B. Stolz, P.R. LeDuc, O.B. Ozdoganlar, Fabrication of circular microfluidic channels by combining mechanical micromilling and soft lithography, Lab Chip. 11 (2011) 1550-1555.

[71] M. Abdelgawad, C. Wu, W.Y. Chien, W.R. Geddie, M.A.S. Jewett, Y. Sun, A fast and simple method to fabricate circular microchannels in polydimethylsiloxane (PDMS), Lab Chip. 11 (2011) 545-551.

[72] D.S. Zhao, B. Roy, M.T. McCormick, W.G. Kuhr, S.A. Brazill, Rapid fabrication of a poly(dimethylsiloxane) microfluidic capillary gel electrophoresis system utilizing high precision machining, Lab Chip. 3 (2003) 93-99.

[73] E. Kumacheva, P. Garstecki, Microfluidic synthesis of polymer particles with non-conventional shapes, in: E. Kumacheva, P. Garstecki (Eds.) Microfluidic Reactors for Polymer Particles, John Wiley & Sons, Chichester, UK, 2011, pp. 192-214.

[74] S. Takeuchi, P. Garstecki, D.B. Weibel, G.M. Whitesides, An axisymmetric flow-focusing microfluidic device, Adv. Mater. 17 (2005) 1067-1072.

[75] S. Takayama, E. Ostuni, X. Qian, J.C. McDonald, X. Jiang, P. LeDuc, M.H. Wu, D.E. Ingber, G.M. Whitesides, Topographical micropatterning of poly(dimethylsiloxane) using laminar flows of liquids in capillaries, Adv. Mater. 13 (2001) 570-574.

[76] J.R. Anderson, D.T. Chiu, R.J. Jackman, O. Cherniavskaya, J.C. McDonald, H. Wu, S.H. Whitesides, G.M. Whitesides, Fabrication of topologically complex three-dimensional microfluidic systems in PDMS by rapid prototyping, Anal. Chem. 72 (2000) 3158-3164.

[77] H. Hillborg, N. Tomczak, A. Olàh, H. Schönherr, G.J. Vancso, Nanoscale hydrophobic recovery: A chemical force microscopy study of UV/Ozone-treated cross-linked poly(dimethylsiloxane), Langmuir. 20 (2003) 785-794.

[78] A.R. Abate, D. Lee, T. Do, C. Holtze, D.A. Weitz, Glass coating for PDMS microfluidic channels by sol-gel methods, Lab Chip. 8 (2008) 516-518.

[79] W.-A.C. Bauer, M. Fischlechner, C. Abell, W.T.S. Huck, Hydrophilic PDMS microchannels for high-throughput formation of oil-in-water microdroplets and water-in-oil-in-water double emulsions, Lab Chip. 10 (2010) 1814-1819.

[80] W. Li, Z. Nie, H. Zhang, C. Paquet, M. Seo, P. Garstecki, E. Kumacheva, Screening of the effect of surface energy of microchannels on microfluidic emulsification, Langmuir. 23 (2007) 8010-8014.

[81] J. Zhou, A.V. Ellis, N.H. Voelcker, Recent developments in PDMS surface modification for microfluidic devices, Electrophoresis. 31 (2010) 2-16.

[82] A.S. Utada, L.Y. Chu, A. Fernandez Nieves, D.R. Link, C. Holtze, D.A. Weitz, Dripping, jetting, drops, and wetting: The magic of microfluidics, MRS Bulletin. 32 (2007) 702-708.

[83] M. Bu, T. Melvin, G.J. Ensell, J.S. Wilkinson, A.G.R. Evans, A new masking technology for deep glass etching and its microfluidic application, Sens. Actuatators A. 115 (2004) 476-482.

[84] X. Li, T. Abe, M. Esashi, Deep reactive ion etching of pyrex glass using SF6 plasma, Sens. Actuators A. 87 (2001) 139-145.

[85] A. Sayah, P.A. Thivolle, V.K. Parashar, M.A.M. Gijs, Fabrication of microfluidic mixers with varying topography in glass using the powder blasting process, J. Micromech. Microeng. 19 (2009) 085024.

[86] D. Hwang, T. Choi, C. Grigoropoulos, Appl. Phys. A: Mater. Sci. Process. 79 (2004) 605-612., Liquid-assisted femtosecond laser drilling of straight and three-dimensional microchannels in glass, Appl. Phys. A. 79 (2004) 605-612.

[87] C. Malek, R. Laurent, B. Jean-Jacques, B. Pascal, Deep microstructuring in glass for microfluidic applications, Microsyst. Technol. 13 (2007) 447-453.

[88] Q. Chen, Q. Chen, G. Maccioni, Fabrication of microfluidics structures on different glasses by simplified imprinting technique, Curr. Appl. Phys. 13 (2013) 256-261.

[89] A. Utada, E. Lorenceau, D. Link, P. Kaplan, H.W. Stone, DA Monodisperse double emulsions generated from a microcapillary device, Science. 308 (2005) 537-541.

[90] R.K. Shah, H.C. Shum, A.C. Rowat, D. Lee, J.J. Agresti, A.S. Utada, L.-Y. Chu, J.-W. Kim, A. Fernandez-Nieves, C.J. Martinez, D.A. Weitz, Designer emulsions using microfluidics, Mater. Today. 11 (2008) 18-27.

[91] H. Hotomi, Inkjet printing head and inkjet printing head manufacturing method, in: US (Ed.), 2001.

[92] C.H. Lin, L. Jiang, Y.H. Chai, H. Xiao, S.J. Chen, H.L. Tsai, Fabrication of microlens arrays in photosensitive glass by femtosecond laser direct writing, Appl. Phys. A. 97 (2009) 751-757.

[93] Y.C. Kim, J.H. Park, M.R. Prausnitz, Microneedles for drug and vaccine delivery, Adv. Drug Deliver. Rev. 64 (2012) 1547-1568.

[94] B. Jiang, Y. Liu, C. Chu, Q. Qiu, Research on microchannel of PMMA microfluidic chip under various injection molding parameters, Adv. Mater. Res. 87-88 (2010) 381-386.

[95] J.H. Xu, S.W. Li, J. Tan, Y.J. Wang, G.S. Luo, Preparation of highly monodisperse droplet in a T-junction microfluidic device, AIChE J. 52 (2006) 3005-3010.

[96] I.R.G. Ogilvie, V.J. Sieben, C.F.A. Floquet, R. Zmijan, M.C. Mowlem, H. Morgan, Reduction of surface roughness for optical quality microfluidic devices in PMMA and COC, J. Micromech. Microeng. 20 (2010) 065016.

[97] D. Carugo, L. Capretto, E. Nehru, M. Mansour, N. Smyth, N. Bressloff, X. Zhang, A microfluidic-based arteriolar network model for biophysical and bioanalytical investigations, Curr. Anal. Chem. 9 (2013) 47-59.

[98] I. Kobayashi, S. Hirose, T. Katoh, Y. Zhang, K. Uemura, M. Nakajima, High-aspect-ratio through-hole array microfabricated in a PMMA plate for monodisperse emulsion production, Microsyst. Technol. 14 (2008) 1349-1357.

[99] O. Görke, P. Pfeifer, K. Schubert, Highly selective methanation by the use of a microchannel reactor, Catal. Today. 110 (2005) 132-139.

[100] H. Ge, G. Chen, Q. Yuan, H. Li, Gas phase catalytic partial oxidation of toluene in a microchannel reactor, Catal. Today. 110 (2005) 171-178.

[101] I. Kobayashi, Y. Wada, Y. Hori, M.A. Neves, K. Uemura, M. Nakajima, Microchannel emulsification using stainless-steel chips: Oil droplet generation characteristics, Chem. Eng. Technol. 35 (2012) 1865-1871.

[102] I. Kobayashi, Y. Wada, K. Uemura, M. Nakajima, Generation of uniform drops via through-hole arrays micromachined in stainless-steel plates, Microfluid. Nanofluid. 5 (2008) 677-687.

[103] G.T. Vladisavljević, W.J. Duncanson, H.C. Shum, D.A. Weitz, Emulsion templating of poly(lactic acid) particles: Droplet formation behavior, Langmuir. 28 (2012) 12948-12954.

[104] G.R. Yi, T. Thorsen, V.N. Manoharan, M.J. Hwang, S.J. Jeon, D.J. Pine, S.R. Quake, S.M. Yang, Generation of uniform colloidal assemblies in soft microfluidic devices, Adv. Mater. 15 (2003) 1300-1304.

[105] M. He, J.S. Edgar, G.D.M. Jeffries, R.M. Lorenz, J.P. Shelby, D.T. Chiu, Selective encapsulation of single cells and subcellular organelles into picoliter- and femtoliter-volume droplets, Anal. Chem. 77 (2005) 1539-1544.

[106] S. van der Graaf, M.L.J. Steegmans, R.G.M. van der Sman, C.G.P.H. Schroën, R.M. Boom, Droplet formation in a T-shaped microchannel junction: A model system for membrane emulsification, Colloids Surf. A. 266 (2005) 106-116.

[107] D. Dendukuri, K. Tsoi, T.A. Hatton, P.S. Doyle, Controlled synthesis of nonspherical microparticles using microfluidics, Langmuir. 21 (2005) 2113-2116.

[108] C.X. Zhao, A.P.J. Middelberg, Two-phase microfluidic flows, Chem. Eng. Sci. 66 (2011) 1394-1411.

[109] P. Garstecki, M.J. Fuerstman, H.A. Stone, G.M. Whitesides, Formation of droplets and bubbles in a microfluidic T-junction-scaling and mechanism of break-up, Lab Chip. 6 (2006) 437-446.

[110] L. Shui, F. Mugele, A. van den Berg, J.C.T. Eijkel, Geometry-controlled droplet generation in head-on microfluidic devices, Appl. Phys. Lett. 93 (2008) 153113-153113.

[111] K. Wang, Y.C. Lu, J.H. Xu, J. Tan, G.S. Luo, Generation of micromonodispersed droplets and bubbles in the capillary embedded T-junction microfluidic devices, AIChE J. 57 (2011) 299-306.

[112] K. Wang, Y.C. Lu, J.H. Xu, J. Tan, G.S. Luo, Liquid–liquid micro-dispersion in a double-pore T-shaped microfluidic device, Microfluid. Nanofluid. 6 (2009) 557-564.

[113] L. Shui, A. van den Berg, J.C.T. Eijkel, Capillary instability, squeezing, and shearing in head-on microfluidic devices, J. Appl. Phys. 106 (2009) 124305-124307.

[114] L. Shui, A. van den Berg, J.C.T. Eijkel, Interfacial tension controlled W/O and O/W 2-phase flows in microchannel, Lab Chip. 9 (2009) 795-801.

[115] J.H. Xu, S.W. Li, J. Tan, Y.J. Wang, G.S. Luo, Controllable preparation of monodisperse O/W and W/O wmulsions in the same microfluidic device, Langmuir. 22 (2006) 7943-7946.

[116] M. De Menech, P. Garstecki, F. Jousse, H.A. Stone, Transition from squeezing to dripping in a microfluidic T-shaped junction, J.Fluid Mech. 595 (2008) 141-161.

[117] P. Garstecki, A. Gañán-Calvo, G. Whitesides, Formation of bubbles and droplets in microfluidic systems, Bull. Polish Acad. Sci., Tech. Sci. 53 (2005) 361-372.

[118] J.H. Xu, S.W. Li, J. Tan, G.S. Luo, Correlations of droplet formation in T-junction microfluidic devices: from squeezing to dripping, Microfluid. Nanofluid. 5 (2008) 711-717.

[119] S.M.S. Murshed, S. Tan, N. Nguyen, T. Wong, L. Yobas, Microdroplet formation of water and nanofluids in heat-induced microfluidic T-junction, Microfluid. Nanofluid. 6 (2009) 253-259.

[120] B.C. Lin, Y.C. Su, On-demand liquid-in-liquid droplet metering and fusion utilizing pneumatically actuated membrane valves, J. Microelectromech. Syst. 18 (2008) 115005.

[121] W.S. Lee, S. Jambovane, D. Kim, J. Hong, Predictive model on micro droplet generation through mechanical cutting, Microfluid. Nanofluid. 7 (2009) 431-438.

[122] Y. Yamanishi, F. Lin, F. Arai, On-demand and Size-controlled Production of emulsion droplets by magnetically driven microtool, in: Robotics and Automation (ICRA), 2010 IEEE International Conference on, 2010, pp. 4094-4099.

[123] L. Rayleigh, On the instability of jets, Proc. London Math. Soc. 10 (1879) 4-13.

[124] Y.C. Tan, V. Cristini, A.P. Lee, Monodispersed microfluidic droplet generation by shear focusing microfluidic device, Sens. Actuators B. 114 (2006) 350-356.

[125] J. Tan, J.H. Xu, S.W. Li, G.S. Luo, Drop dispenser in a cross-junction microfluidic device: Scaling and mechanism of break-up, Chem. Eng. J. 136 (2008) 306-311.

[126] A.R. Abate, J. Thiele, D.A. Weitz, One-step formation of multiple emulsions in microfluidics, Lab Chip. 11 (2011) 253-258.

[127] M.L.J. Steegmans, K.G.P.H. Schroën, R.M. Boom, Characterization of emulsification at flat microchannel Y junctions, Langmuir. 25 (2009) 3396-3401.

[128] R. Ferrigno, A.D. Stroock, T.D. Clark, M. Mayer, G.M. Whitesides, Membraneless Vanadium Redox Fuel Cell Using Laminar Flow, J. Am. Chem. Soc. 124 (2002) 12930-12931.

[129] E. Kjeang, N. Djilali, D. Sinton, Microfluidic fuel cells: A review, J. Power Sources. 186 (2009) 353-369.

[130] B.H. Weigl, J. Kriebel, K.J. Mayes, T. Bui, P. Yager, Whole Blood Diagnostics in Standard Gravity and Microgravity by Use of Microfluidic Structures (T-Sensors), Microchim. Acta. 131 (1999) 75-83.

[131] T. Nisisako, S. Okushima, T. Torii, Controlled formulation of monodisperse double emulsions in a multiple-phase microfluidic system, Soft Matter. 1 (2005) 23-27.

[132] R.F. Shepherd, J.C. Conrad, S.K. Rhodes, D.R. Link, M. Marquez, D.A. Weitz, J.A. Lewis, Microfluidic assembly of homogeneous and janus colloid-filled hydrogel granules, Langmuir. 22 (2006) 8618-8622.

[133] P. Kenis, R. Ismagilov, G. Whitesides, Microfabrication inside capillaries using multiphase laminar flow patterning, Science. 285 (1999) 83-85.

[134] W. Jeong, J. Kim, S. Kim, S. Lee, G. Mensing, D.J. Beebe, Hydrodynamic microfabrication via "on the fly" photopolymerization of microscale fibers and tubes, Lab Chip. 4 (2004) 576-580.

[135] P.B. Umbanhowar, V. Prasad, D.A. Weitz, Monodisperse emulsion generation via drop break off in a coflowing stream, Langmuir. 16 (1999) 347-351.

[136] A.S. Utada, A. Fernandez-Nieves, H.A. Stone, D.A. Weitz, Dripping to jetting transitions in coflowing liquid streams, Phys. Rev. Lett. 99 (2007) 094502.

[137] G. Vladisavljević, H. Shum, D. Weitz, Control over the shell thickness of core/shell drops in three-phase glass capillary devices, Prog. Colloid Polym. Sci. 139 (2012) 115-118.

[138] R. Suryo, O.A. Basaran, Tip streaming from a liquid drop forming from a tube in a co-flowing outer fluid, Phys. Fluids. 18 (2006) 082102-082113.

[139] P. Lewis, R. Graham, Z. Nie, S. Xu, M. Seo, E. Kumacheva, Continuous synthesis of copolymer particles in microfluidic reactors, Macromol. 38 (2005) 4536-4538.

[140] Q. Xu, M. Nakajima, The generation of highly monodisperse droplets through the breakup of hydrodynamically focused microthread in a microfluidic device, Appl. Phys. Lett. 85 (2004) 3726-3728.

[141] S.L. Anna, N. Bontoux, H.A. Stone, Formation of dispersions using ``flow focusing'' in microchannels, Appl. Phys. Lett. 82 (2003) 364-366.

[142] T. Schneider, G.H. Chapman, U.O. Häfeli, Effects of chemical and physical parameters in the generation of microspheres by hydrodynamic flow focusing, Colloids Surf. B. 87 (2011) 361-368.

[143] H. Kim, D. Luo, D. Link, D.A. Weitz, M. Marquez, Z. Cheng, Controlled production of emulsion drops using an electric field in a flow-focusing microfluidic device, Appl. Phys. Lett. 91 (2007) 133106-133103.

[144] C.T. Chen, G.B. Lee, Formation of Microdroplets in Liquids Utilizing Active Pneumatic Choppers on a Microfluidic Chip, J. Microelectromech. Syst. 15 (2006) 1492-1498.

[145] C.H. Lee, S.K. Hsiung, G.B. Lee, A tunable microflow focusing device utilizing controllable moving walls and its applications for formation of micro-droplets in liquids, J. Micromech. Microeng. 17 (2007) 1121.

[146] S.L. Anna, H.C. Mayer, Microscale tipstreaming in a microfluidic flow focusing device, Phys. Fluids. 18 (2006).

[147] P. Garstecki, H.A. Stone, G.M. Whitesides, Mechanism for Flow-Rate Controlled Breakup in Confined Geometries: A Route to Monodisperse Emulsions, Phys. Rev. Lett. 94 (2005) 164501.

[148] C. Zhou, P. Yue, J.J. Feng, Formation of simple and compound drops in microfluidic devices, Phys. Fluids. 18 (2006) 092105-092114.

[149] W.-C. Jeong, J.-M. Lim, J.-H. Choi, J.-H. Kim, Y.-J. Lee, S.-H. Kim, G. Lee, J.-D. Kim, G.-R. Yi, S.-M. Yang, Controlled generation of submicron emulsion droplets via highly stable tip-streaming mode in microfluidic devices, Lab Chip. 12 (2012) 1446-1453.

[150] J.H. Xu, G.S. Luo, G.G. Chen, J.D. Wang, Experimental and theoretical approaches on droplet formation from a micrometer screen hole, J. Membr. Sci. 266 (2005) 121-131.

[151] S.J. Peng, R.A. Williams, Controlled production of emulsions using a crossflow membrane: Part I: droplet formation from a dingle pore, Chem. Eng. Res. Des. 76 (1998) 894-901.

[152] N.A. Wagdare, A.T.M. Marcelis, O.B. Ho, R.M. Boom, C.J.M. van Rijn, High throughput vegetable oil-in-water emulsification with a high porosity micro-engineered membrane, J. Membr. Sci. 347 (2010) 1-7.

[153] G.T. Vladisavljević, R.A. Williams, Recent developments in manufacturing emulsions and particulate products using membranes, Adv. Colloid Interface Sci. 113 (2005) 1-20.

[154] R.G. Holdich, M.M. Dragosavac, G.T. Vladisavljević, E. Piacentini, Continuous membrane emulsification with pulsed (oscillatory) flow, Ind. Eng. Chem. Res. 52 (2012) 507-515.

[155] G.T. Vladisavljević, R.A. Williams, Manufacture of large uniform droplets using rotating membrane emulsification, J. Colloid. Interface Sci. 299 (2006) 396-402.

[156] V. Schadler, E.J. Windhab, Continuous membrane emulsification by using a membrane system with controlled pore distance, Desalination. 189 (2006) 130-135.

[157] M.S. Manga, O.J. Cayre, R.A. Williams, S. Biggs, D.W. York, Production of solid-stabilised emulsions through rotational membrane emulsification: influence of particle adsorption kinetics, Soft Matter. 8 (2012) 1532-1538.

[158] J. Zhu, D. Barrow, Analysis of droplet size during crossflow membrane emulsification using stationary and vibrating micromachined silicon nitride membranes, J. Membr. Sci. 261 (2005) 136-144.

[159] R.G. Holdich, M.M. Dragosavac, G.T. Vladisavljević, S.R. Kosvintsev, Membrane mmulsification with oscillating and stationary membranes, Ind. Eng. Chem. Res. 49 (2010) 3810-3817.

[160] S. Sugiura, M. Nakajima, N. Kumazawa, S. Iwamoto, M. Seki, Characterization of spontaneous transformation-based droplet formation during microchannel emulsification, J. Phys. Chem. B. 106 (2002) 9405-9409.

[161] S. Sugiura, M. Nakajima, M. Seki, Prediction of droplet diameter for microchannel emulsification, Langmuir. 18 (2002) 3854-3859.

[162] I. Kobayashi, S. Mukataka, M. Nakajima, Novel asymmetric through-hole array microfabricated on a silicon plate for formulating monodisperse emulsions, Langmuir. 21 (2005) 7629-7632.

[163] I. Kobayashi, M. Nakajima, S. Mukataka, Preparation characteristics of oil-in-water emulsions using differently charged surfactants in straight-through microchannel emulsification, Colloids Surf. A. 229 (2003) 33-41.

[164] C. Cramer, P. Fischer, E.J. Windhab, Drop formation in a co-flowing ambient fluid, Chem. Eng. Sci. 59 (2004) 3045-3058.

[165] A.S. Utada, A. Fernandez-Nieves, J.M. Gordillo, D.A. Weitz, Absolute instability of a liquid jet in a coflowing stream, Phys. Rev. Lett. 100 (2008) 014502.

[166] M. Seo, C. Paquet, Z. Nie, S. Xu, E. Kumacheva, Microfluidic consecutive flow-focusing droplet generators, Soft Matter. 3 (2007) 986-992.

[167] L.Y. Chu, A.S. Utada, R.K. Shah, J.W. Kim, D.A. Weitz, Controllable Monodisperse Multiple Emulsions, Angew. Chem. 119 (2007) 9128-9132.

[168] S.H. Kim, J.W. Kim, J.C. Cho, D.A. Weitz, Double-emulsion drops with ultra-thin shells for capsule templates, Lab Chip. 11 (2011) 3162-3166.

[169] R. Chen, P.F. Dong, J.H. Xu, Y.D. Wang, G.S. Luo, Controllable microfluidic production of gas-in-oil-in-water emulsions for hollow microspheres with thin polymer shells, Lab Chip. 12 (2012) 3858-3860.

[170] J.W. Kim, A.S. Utada, A. Fernández-Nieves, Z. Hu, D.A. Weitz, Fabrication of monodisperse gel shells and functional microgels in microfluidic devices, Angew. Chem. Int. Ed. 46 (2007) 1819-1822.

[171] L. Liu, W. Wang, X.J. Ju, R. Xie, L.Y. Chu, Smart thermo-triggered squirting capsules for nanoparticle delivery, Soft Matter. 6 (2010) 3759-3763.

[172] T. Kanai, D. Lee, H.C. Shum, R.K. Shah, D.A. Weitz, Gel-Immobilized colloidal crystal shell with enhanced thermal sensitivity at photonic wavelengths, Adv. Mater. 22 (2010) 4998-5002.

[173] C. Ye, A. Chen, P. Colombo, C. Martinez, Ceramic microparticles and capsules via microfluidic processing of a preceramic polymer, J. R. Soc. Interface. 7 (2010) S461-S473.

[174] H.C. Shum, A. Bandyopadhyay, S. Bose, D.A. Weitz, Double emulsion droplets as microreactors for synthesis of mesoporous hydroxyapatite, Chem. Mater. 21 (2009) 5548-5555.

[175] H.C. Shum, D. Lee, I. Yoon, T. Kodger, D.A. Weitz, Double emulsion templated monodisperse phospholipid vesicles, Langmuir. 24 (2008) 7651-7653.

[176] E. Lorenceau, A.S. Utada, D.R. Link, G. Cristobal, M. Joanicot, D.A. Weitz, Generation of polymerosomes from double-emulsions, Langmuir. 21 (2005) 9183-9186.

[177] S.H. Kim, H.C. Shum, J.W. Kim, J.C. Cho, D.A. Weitz, Multiple polymersomes for programmed release of multiple components, J. Am. Chem. Soc. 133 (2011) 15165-15171.

[178] D. Lee, D.A. Weitz, Double emulsion-templated nanoparticle colloidosomes with selective permeability, Adv. Mater. 20 (2008) 3498-3503.

[179] H.C. Shum, A.R. Abate, D. Lee, A.R. Studart, B. Wang, C.-H. Chen, J. Thiele, R.K. Shah, A. Krummel, D.A. Weitz, Droplet microfluidics for fabrication of non-spherical particles, Macromol. Rapid Commun. . 31 (2010) 108-118.

[180] W. Wang, R. Xie, X.-J. Ju, T. Luo, L. Liu, D.A. Weitz, L.-Y. Chu, Controllable microfluidic production of multicomponent multiple emulsions, Lab Chip. 11 (2011) 1587-1592.

[181] A. Rotem, A.R. Abate, A.S. Utada, V. Van Steijn, D.A. Weitz, Drop formation in non-planar microfluidic devices, Lab Chip. 12 (2012) 4263-4268.

[182] A.R. Abate, D.A. Weitz, Faster multiple emulsification with drop splitting, Lab Chip. 11 (2011) 1911-1915.

[183] A.R. Abate, D.A. Weitz, High-order multiple emulsions formed in poly(dimethylsiloxane) microfluidics, Small. 5 (2009) 2030-2032.

[184] D. Saeki, S. Sugiura, T. Kanamori, S. Sato, S. Ichikawa, Formation of monodisperse calcium alginate microbeads by rupture of water-in-oil-in-water droplets with an ultra-thin oil phase layer, Lab Chip. 10 (2010) 2292-2295.

[185] D. Saeki, S. Sugiura, T. Kanamori, S. Sato, S. Ichikawa, Microfluidic preparation of water-in-oil-in-water emulsions with an ultra-thin oil phase layer, Lab Chip. 10 (2010) 357-362.

[186] B. Zheng, J.D. Tice, R.F. Ismagilov, Formation of droplets of alternating composition in microfluidic channels and applications to indexing of concentrations in droplet-based assays, Anal. Chem. 76 (2004) 4977-4982.

[187] R.R. Pompano, W. Liu, W. Du, R.F. Ismagilov, Microfluidics using spatially defined arrays of droplets in one, two, and three dimensions, Annu. Rev. Anal. Chem. 4 (2011) 59-81.

[188] B.J. Sun, H.C. Shum, C. Holtze, D.A. Weitz, Microfluidic Melt Emulsification for Encapsulation and Release of Actives, ACS Appl. Mater. Interface. 2 (2010) 3411-3416.

[189] J. Wan, A. Bick, M. Sullivan, H.A. Stone, Controllable microfluidic production of microbubbles in water-in-oil emulsions and the formation of porous microparticles, Adv. Mater. 20 (2008) 3314-3318.

[190] D.R. Link, S.L. Anna, D.A. Weitz, H.A. Stone, Geometrically mediated breakup of drops in microfluidic devices, Phys. Rev. Lett. 92 (2004) 054503.

[191] Z. Che, N.T. Nguyen, T.N. Wong, Hydrodynamically mediated breakup of droplets in microchannels, Appl. Phys. Lett. 98 (2011) 054102-054103.

[192] J.M. Köhler, T. Henkel, A. Grodrian, T. Kirner, M. Roth, K. Martin, J. Metze, Digital reaction technology by micro segmented flow—components, concepts and applications, Chem. Eng. J. 101 (2004) 201-216.

[193] K. Liu, H.J. Ding, J. Liu, Y. Chen, X.Z. Zhao, Shape-controlled production of biodegradable calcium alginate gel microparticles using a novel microfluidic device, Langmuir. 22 (2006) 9453-9457.

[194] M. Simon, A. Lee, Microfluidic droplet manipulations and their applications, in: P. Day, A. Manz, Y. Zhang (Eds.) Microdroplet Technology: Principles and Emerging Applications in Biology and Chemistry, Springer, New York, 2012, pp. 22-50.

[195] J.S. Hong, S.J. Shin, S.H. Lee, E. Wong, J. Cooper-White, Spherical and cylindrical microencapsulation of living cells using microfluidic devices, Korea-Aust. Rheol. J. 19 (2007) 157-164.

[196] G.F. Christopher, J. Bergstein, N.B. End, M. Poon, C. Nguyen, S.L. Anna, Coalescence and splitting of confined droplets at microfluidic junctions, Lab Chip. 9 (2009) 1102-1109.

[197] J. Hong, M. Choi, J.B. Edel, A.J. deMello, Passive self-synchronized two-droplet generation, Lab Chip. 10 (2010) 2702-2709.

[198] D.R. Link, E. Grasland-Mongrain, A. Duri, F. Sarrazin, Z. Cheng, G. Cristobal, M. Marquez, D.A. Weitz, Electric control of droplets in microfluidic devices, Angew. Chem. Int. Ed. 45 (2006) 2556-2560.

[199] L.H. Hung, K.M. Choi, W.Y. Tseng, Y.C. Tan, K.J. Shea, A.P. Lee, Alternating droplet generation and controlled dynamic droplet fusion in microfluidic device for CdS nanoparticle synthesis, Lab Chip. 6 (2006) 174-178.

[200] Y.C. Tan, Y. Ho, A. Lee, Droplet coalescence by geometrically mediated flow in microfluidic channels, Microfluid. Nanofluid. 3 (2007) 495-499.

[201] Y.C. Tan, J.S. Fisher, A.I. Lee, V. Cristini, A.P. Lee, Design of microfluidic channel geometries for the control of droplet volume, chemical concentration, and sorting, Lab Chip. 4 (2004) 292-298.

[202] X. Niu, S. Gulati, J.B. Edel, A.J. deMello, Pillar-induced droplet merging in microfluidic circuits, Lab Chip. 8 (2008) 1837-1841.

[203] M. Zagnoni, G. Le Lain, J.M. Cooper, Electrocoalescence mechanisms of microdroplets using localized electric fields in microfluidic channels, Langmuir. 26 (2010) 14443-14449.

[204] X. Niu, F. Gielen, A.J. deMello, J.B. Edel, Electro-coalescence of digitally controlled droplets, Anal. Chem. 81 (2009) 7321-7325.

[205] J.A. Schwartz, J.V. Vykoukal, P.R.C. Gascoyne, Droplet-based chemistry on a programmable micro-chip, Lab Chip. 4 (2004) 11-17.

[206] B. Xu, N.T. Nguyen, T.N. Wong, Temperature-induced droplet coalescence in microchannels, Biomicrofluidics. 6 (2012) 012811-012818.

[207] T.D. Luong, N.T. Nguyen, A. Sposito, Thermocoalescence of microdroplets in a microfluidic chamber, Appl. Phys. Lett. 100 (2012) 254105-254103.

[208] T. Taniguchi, T. Torii, T. Higuchi, Chemical reactions in microdroplets by electrostatic manipulation of droplets in liquid media, Lab Chip. 2 (2002) 19-23.

[209] L. Hung, A. Lee, Microfluidic devices for the synthesis of nanoparticles and biomaterials, J. Med. Biol. Eng. 27 (2007) 1-6.

[210] T. Illg, P. Löb, V. Hessel, Flow chemistry using milli- and microstructured reactors—From conventional to novel process windows, Bioorgan. Med. Chem. 18 (2010) 3707-3719.

[211] G. Luo, L. Du, Y. Wang, Y. Lu, J. Xu, Controllable preparation of particles with microfluidics, Particuology. 9 (2011) 545-558.

[212] P.S. Dittrich, A. Manz, Lab-on-a-chip: microfluidics in drug discovery, Nat Rev Drug Discov. 5 (2006) 210-218.

[213] L. Shui, J.C.T. Eijkel, A. van den Berg, Multiphase flow in microfluidic systems – Control and applications of droplets and interfaces, Adv. Colloid Interface Sci. 133 (2007) 35-49.

[214] A. Gunther, K.F. Jensen, Multiphase microfluidics: from flow characteristics to chemical and materials synthesis, Lab Chip. 6 (2006) 1487-1503.

[215] A. Ufer, M. Mendorf, A. Ghaini, D.W. Agar, Liquid/Liquid Slug Flow Capillary Microreactor, Chem. Eng. Technol. 34 (2011) 353-360.

[216] J. Yoshida, A. Nagaki, T. Iwasaki, S. Suga, Enhancement of Chemical Selectivity by Microreactors, Chem. Eng. Technol. 28 (2005) 259-266.

[217] A.B. Theberge, F. Courtois, Y. Schaerli, M. Fischlechner, C. Abell, F. Hollfelder, W.T.S. Huck, Microdroplets in Microfluidics: An Evolving Platform for Discoveries in Chemistry and Biology, Angew. Chem., Int. Ed. 49 (2010) 5846-5868.

[218] Y. Önal, M. Lucas, P. Claus, Application of a Capillary Microreactor for Selective Hydrogenation of α,β-Unsaturated Aldehydes in Aqueous Multiphase Catalysis, Chem. Eng. Technol. 28 (2005) 972-978.

[219] W. Ehrfeld, V. Hessel, H. Lowe, Microreactors: new technology for modern chemistry, Wiley, Chichester, 2000.

[220] J.B.M.F.G.L.U.S.A.W. K. Schubert, Microstructure devices for applications in thermal and chemical process engineering, Microscale Therm. Eng. 5 (2001) 17-39.

[221] O. Geschke, H. Klank, P. Telleman, Microsystem engineering of lab-on-a-chip devices, Wiley, Weinheim, 2008.

[222] N. Lion, J. Rossier, H. Girault, Microfluidic applications in biology: from technologies to systems biology, Wiley, Weinheim, 2006.

[223] E. Kjeang, R. Michel, D.A. Harrington, N. Djilali, D. Sinton, A Microfluidic Fuel Cell with Flow-Through Porous Electrodes, J. Am. Chem. Soc. 130 (2008) 4000-4006.

[224] H.A. Stone, A.D. Stroock, A. Ajdari, Engineering flows in small devices: Microfluidics Toward a Lab-on-a-Chip, Annu. Rev. Fluid Mech. 36 (2004) 381-411.

[225] P. Garstecki, M. J. Fuerstman, M.A. Fischbach, S.K. Sia, G.M. Whitesides, Mixing with bubbles: a practical technology for use with portable microfluidic devices, Lab Chip. 6 (2006) 207-212.

[226] T. Bayraktar, S.B. Pidugu, Characterization of liquid flows in microfluidic systems, Int. J. Heat Mass Transfer. 49 (2006) 815-824.

[227] M. Brivio, W. Verboom, D.N. Reinhoudt, Miniaturized continuous flow reaction vessels: influence on chemical reactions, Lab Chip. 6 (2006) 329-344.

[228] P. Garstecki, Formation of Droplets and Bubbles in Microfluidic Systems, in: S. Kakaç, B. Kosoy, D. Li, A. Pramuanjaroenkij (Eds.) Microfluidics Based Microsystems, Springer Netherlands, 2010, pp. 163-181.

[229] G. Hetsroni, A. Mosyak, E. Pogrebnyak, L.P. Yarin, Fluid flow in micro-channels, Int. J. Heat Mass Transfer. 48 (2005) 1982-1998.

[230] C.M. Ho, Y.C. Tai, Micro-electro-mechanical-systems (MEMS) and fluid flows, Annu. Rev. Fluid Mech. 30 (1998) 579-612.

[231] J.J. Hwang, F.G. Tseng, C. Pan, Ethanol–CO2 two-phase flow in diverging and converging microchannels, Int. J. Multiphase Flow. 31 (2005) 548-570.

[232] A. Serizawa, Z. Feng, Z. Kawara, Two-phase flow in microchannels, Exp. Thermal Fluid Sci. 26 (2002) 703-714.

[233] Y.P. Peles, L.P. Yarin, G. Hetsroni, Thermohydrodynamic characteristics of two-phase flow in a heated capillary, Int. J. Multiphase Flow. 26 (2000) 1063-1093.

[234] K.A. Heyries, M.G. Loughran, D. Hoffmann, A. Homsy, L.J. Blum, C.A. Marquette, Microfluidic biochip for chemiluminescent detection of allergen-specific antibodies, Biosens. Bioelectron. 23 (2008) 1812-1818.

[235] Y.T. Kim, K. Karthikeyan, S. Chirvi, D.P. Dave, Neuro-optical microfluidic platform to study injury and regeneration of single axons, Lab Chip. 9 (2009) 2576-2581.

[236] J.H. Xu, G.S. Luo, S.W. Li, G.G. Chen, Shear force induced monodisperse droplet formation in a microfluidic device by controlling wetting properties, Lab Chip. 6 (2006) 131-136.

[237] H. Maeda, J. Wu, T. Sawa, Y. Matsumura, K. Hori, Tumor vascular permeability and the EPR effect in macromolecular therapeutics: a review, J. Control Release. 65 (2000) 271-284.

[238] J. O'Shaughnessy, Liposomal Anthracyclines for Breast Cancer: Overview, Oncologist. 8 (2003) 1-2.

[239] A.K. Patri, I.J. Majoros, J.R. Baker Jr, Dendritic polymer macromolecular carriers for drug delivery, Curr. Opin. Chem. Biol. 6 (2002) 466-471.

[240] M.L. Immordino, F. Dosio, L. Cattel, Stealth liposomes: review of the basic science, rationale, and clinical applications, existing and potential, Int. J. Nanomedicine. 1 (2006) 297-315.

[241] R.A. Jain, The manufacturing techniques of various drug loaded biodegradable poly(lactide-co-glycolide) (PLGA) devices, Biomaterials. 21 (2000) 2475-2490.

[242] K.-S. Huang, T.-H. Lai, Y.-C. Lin, Manipulating the generation of Ca-alginate microspheres using microfluidic channels as a carrier of gold nanoparticles, Lab Chip. 6 (2006) 954-957.

[243] C.-H. Yeh, K.-R. Chen, Y.-C. Lin, Developing heatable microfluidic chip to generate gelatin emulsions and microcapsules, Microfluid. Nanofluid. (2013) 1-10.

[244] C.-H. Yang, K.-S. Huang, J.-Y. Chang, Manufacturing monodisperse chitosan microparticles containing ampicillin using a microchannel chip, Biomed Microdevices. 9 (2007) 253-259.

[245] D. Ogonczyk, M. Siek, P. Garstecki, Microfluidic formulation of pectin microbeads for encapsulation and controlled release of nanoparticles, Biomicrofluidics. 5 (2011) 013405-013412.

[246] Y.-J. Eun, A.S. Utada, M.F. Copeland, S. Takeuchi, D.B. Weibel, Encapsulating Bacteria in Agarose Microparticles Using Microfluidics for High-Throughput Cell Analysis and Isolation, ACS Chem Biol. 6 (2010) 260-266.

[247] H. Zhang, E. Tumarkin, R. Peerani, Z. Nie, R.M.A. Sullan, G.C. Walker, E. Kumacheva, Microfluidic Production of Biopolymer Microcapsules with Controlled Morphology, J. Am. Chem. Soc. 128 (2006) 12205-12210.

[248] W.-G. Koh, M. Pishko, Fabrication of cell-containing hydrogel microstructures inside microfluidic devices that can be used as cell-based biosensors, Anal. Bioanal. Chem. 385 (2006) 1389-1397.

[249] B.G. Chung, K.-H. Lee, A. Khademhosseini, S.-H. Lee, Microfluidic fabrication of microengineered hydrogels and their application in tissue engineering, Lab Chip. 12 (2012) 45-59.

[250] R. Langer, Editorial: Tissue Engineering: Perspectives, Challenges, and Future Directions Tissue Eng. 13 (2007) 1-2.

[251] A. Peters, D. Brey, J. Burdick, High-throughput and combinatorial technologies for tissue engineering applications, Tissue Eng Part B Rev. 15 (2009) 225-239.

[252] L. Capretto, S. Mazzitelli, C. Nastruzzi, Design, production and optimization of solid lipid microparticles (SLM) by a coaxial microfluidic device, J. Control Release. 160 (2012) 409-417.

[253] H. Zhang, E. Tumarkin, R.M.A. Sullan, G.C. Walker, E. Kumacheva, Exploring Microfluidic Routes to Microgels of Biological Polymers, Macromol. Rapid Commun. 28 (2007) 527-538.

[254] L. Capretto, S. Mazzitelli, C. Balestra, A. Tosi, C. Nastruzzi, Effect of the gelation process on the production of alginate microbeads by microfluidic chip technology, Lab Chip. 8 (2008) 617-621.

[255] C.H. Choi, J.H. Jung, Y.W. Rhee, D.P. Kim, S.E. Shim, C.S. Lee, Generation of monodisperse alginate microbeads and in situ encapsulation of cell in microfluidic device, Biomed. Microdev. 9 (2007) 855-862.

[256] K.-S. Huang, K. Lu, C.-S. Yeh, S.-R. Chung, C.-H. Lin, C.-H. Yang, Y.-S. Dong, Microfluidic controlling monodisperse microdroplet for 5-fluorouracil loaded genipin-gelatin microcapsules, J. Controlled Release. 137 (2009) 15-19.

[257] S. Ostrovidov, N. Annabi, A. Seidi, M. Ramalingam, F. Dehghani, H. Kaji, A. Khademhosseini, Controlled Release of Drugs from Gradient Hydrogels for High-Throughput Analysis of Cell–Drug Interactions, Anal. Chem. 84 (2011) 1302-1309.

[258] S. Xu, Z. Nie, M. Seo, P. Lewis, E. Kumacheva, H.A. Stone, P. Garstecki, D.B. Weibel, I. Gitlin, G.M. Whitesides, Generation of monodisperse particles by using microfluidics: control over size, shape, and composition, Angew. Chem. In.t Ed. Engl. 44 (2005) 724-728.

[259] A. Khademhosseini, R. Langer, Microengineered hydrogels for tissue engineering, Biomaterials. 28 (2007) 5087-5092.

[260] J. Yeh, Y. Ling, J.M. Karp, J. Gantz, A. Chandawarkar, G. Eng, J. Blumling Iii, R. Langer, A. Khademhosseini, Micromolding of shape-controlled, harvestable cell-laden hydrogels, Biomaterials. 27 (2006) 5391-5398.

[261] A. Jahn, S.M. Stavis, J.S. Hong, W.N. Vreeland, D.L. DeVoe, M. Gaitan, Microfluidic Mixing and the Formation of Nanoscale Lipid Vesicles, ACS Nano. 4 (2010) 2077-2087.

[262] J.J. Agresti, E. Antipov, A.R. Abate, K. Ahn, A.C. Rowat, J.-C. Baret, M. Marquez, A.M. Klibanov, A.D. Griffiths, D.A. Weitz, Ultrahigh-throughput screening in drop-based microfluidics for directed evolution, Proc. Natl. Acad. Sci. 107 (2010) 4004–4009.

[263] J.F. Edd, D. Di Carlo, K.J. Humphry, S. Koster, D. Irimia, D.A. Weitz, M. Toner, Controlled encapsulation of single-cells into monodisperse picolitre drops, Lab Chip. 8 (2008) 1262-1264.

[264] A.R. Abate, C.H. Chen, J.J. Agresti, D.A. Weitz, Beating Poisson encapsulation statistics using close-packed ordering, Lab Chip. 9 (2009) 2628-2631.

[265] M. Chabert, J.-L. Viovy, Microfluidic high-throughput encapsulation and hydrodynamic self-sorting of single cells, Proc. Natl. Acad. Sci. U S A. 105 (2008) 3191-3196.

[266] A. Lenshof, T. Laurell, Continuous separation of cells and particles in microfluidic systems, Chem. Soc. Rev. 39 (2010) 1203-1217.

[267] D. Di Carlo, Inertial microfluidics, Lab Chip. 9 (2009) 3038-3046.

[268] T.M. Tran, F. Lan, C.S. Thompson, A.R. Abate, From tubes to drops: droplet-based microfluidics for ultrahigh-throughput biology, J. Phys. D: Appl. Phys. 46 (2013) 114004.

[269] K. Avgoustakis, A. Beletsi, Z. Panagi, P. Klepetsanis, A.G. Karydas, D.S. Ithakissios, PLGA–mPEG nanoparticles of cisplatin: in vitro nanoparticle degradation, in vitro drug release and in vivo drug residence in blood properties, J. Control. Release. 79 (2002) 123-135.

[270] G. Fontana, M. Licciardi, S. Mansueto, D. Schillaci, G. Giammona, Amoxicillin-loaded polyethylcyanoacrylate nanoparticles: Influence of PEG coating on the particle size, drug release rate and phagocytic uptake, Biomaterials. 22 (2001) 2857-2865.

[271] J. Panyam, W.Z. Zhou, S. Prabha, S.K. Sahoo, V. Labhasetwar, Rapid endo-lysosomal escape of poly(dl-lactide-co-glycolide) nanoparticles: implications for drug and gene delivery, FASEB J. 16 (2002) 1217-1226.

[272] G.P. Carino, J.S. Jacob, E. Mathiowitz, Nanosphere based oral insulin delivery, J. Control. Release. 65 (2000) 261-269.

[273] M. van de Weert, W. Hennink, W. Jiskoot, Protein instability in Poly(Lactic-co-Glycolic Acid) microparticles, Pharm. Res. 17 (2000) 1159-1167.

[274] L. Ménétrier-Deremble, P. Tabeling, Droplet breakup in microfluidic junctions of arbitrary angles, Phys. Rev. E. 74 (2006) 035303.

[275] A.M. Leshansky, L.M. Pismen, Breakup of drops in a microfluidic T junction, Phys. Fluids. 21 (2009) 023303-023306.

[276] T. Cubaud, T.G. Mason, High-viscosity fluid threads in weakly diffusive microfluidic systems, New J. Phys. 11 (2009) 075029.

[277] Z. Che, N.-T. Nguyen, T.N. Wong, Hydrodynamically mediated breakup of droplets in microchannels, Appl. Phys. Lett. 98 (2011) 054102-054103.

[278] J. Pihl, J. Sinclair, E. Sahlin, M. Karlsson, F. Petterson, J. Olofsson, O. Orwar, Microfluidic gradient-generating device for pharmacological profiling, Anal. Chem. 77 (2005) 3897-3903.

[279] D. Irimia, Microfluidic technologies for temporal perturbations of chemotaxis, Annu. Rev. Biomed. Eng. 12 (2010) 259-284.

[280] J.Y. Park, S.-K. Kim, D.-H. Woo, E.-J. Lee, J.-H. Kim, S.-H. Lee, Differentiation of neural progenitor cells in a microfluidic chip-generated cytokine gradient, Stem Cells. 27 (2009) 2646-2654.

[281] B.G. Chung, L.A. Flanagan, S.W. Rhee, P.H. Schwartz, A.P. Lee, E.S. Monuki, N.L. Jeon, Human neural stem cell growth and differentiation in a gradient-generating microfluidic device, Lab Chip. 5 (2005) 401-406.

[282] L. Capretto, S. Mazzitelli, G. Colombo, R. Piva, L. Penolazzi, R. Vecchiatini, X. Zhang, C. Nastruzzi, Production of polymeric micelles by microfluidic technology for combined drug delivery: Application to osteogenic differentiation of human periodontal ligament mesenchymal stem cells (hPDLSCs), Int. J. Pharm. 440 (2013) 195-206.

[283] N.M. Belliveau, J. Huft, P.J.C. Lin, S. Chen, A.K.K. Leung, T.J. Leaver, A.W. Wild, J.B. Lee, R.J. Taylor, Y.K. Tam, C.L. Hansen, P.R. Cullis, Microfluidic Synthesis of Highly Potent Limit-size Lipid Nanoparticles for In Vivo Delivery of siRNA, Mol Ther Nucleic Acids. 1 (2012) e37.

[284] R. Karnik, F. Gu, P. Basto, C. Cannizzaro, L. Dean, W. Kyei-Manu, R. Langer, O.C. Farokhzad, Microfluidic Platform for Controlled Synthesis of Polymeric Nanoparticles, Nano. Lett. 8 (2008) 2906-2912.

[285] J. Sun, Y. Xianyu, M. Li, W. Liu, L. Zhang, D. Liu, C. Liu, G. Hu, X. Jiang, A microfluidic origami chip for synthesis of functionalized polymeric nanoparticles, Nanoscale. (2013).

[286] F.S. Majedi, M.M. Hasani-Sadrabadi, S.H. Emami, M. Taghipoor, E. Dashtimoghadam, A. Bertsch, H. Moaddel, P. Renaud, Microfluidic synthesis of chitosan-based nanoparticles for fuel cell applications, Chem. Commun. 48 (2012) 7744-7746.

[287] R. Hood, C. Shao, D. Omiatek, W. Vreeland, D. DeVoe, Microfluidic synthesis of PEG- and folate-conjugated liposomes for one-step formation of targeted stealth nanocarriers, Pharm. Res. 30 (2013) 1597-1607.

[288] M. de la Fuente, M. Raviña, P. Paolicelli, A. Sanchez, B. Seijo, M.J. Alonso, Chitosan-based nanostructures: A delivery platform for ocular therapeutics, Adv. Drug Deliv. Rev. 62 (2010) 100-117.

[289] F.S. Majedi, M.M. Hasani-Sadrabadi, S. Hojjati Emami, M.A. Shokrgozar, J.J. VanDersarl, E. Dashtimoghadam, A. Bertsch, P. Renaud, Microfluidic assisted self-assembly of chitosan based nanoparticles as drug delivery agents, Lab Chip. 13 (2013) 204-207.

[290] Y. Kikutani, M. Ueno, H. Hisamoto, M. Tokeshi, T. Kitamori, Continuous-flow chemical processing in three-dimensional microchannel network for on-chip integration of multiple reactions in a combinatorial mode, QSAR Comb. Sci. 24 (2005) 742-757.

[291] E. Garcia-Egido, V. Spikmans, S.Y.F. Wong, B.H. Warrington, Synthesis and analysis of combinatorial libraries performed in an automated micro reactor system, Lab Chip. 3 (2003) 73-76.

[292] A. Šalić, A. Tušek, B. Zelić, Application of microreactors in medicine and biomedicine, J. Appl. Biomed. 10 (2012) 137.

[293] Y. Hoyoung, K. Kisoo, L. Won Gu, Cell manipulation in microfluidics, Biofabrication. 5 (2013) 022001.

[294] X. Chen, D. Cui, C. Liu, H. Cai, Microfluidic biochip for blood cell lysis, Chinese J. Anal. Chem. 34 (2006) 1656-1660.

[295] H. Yin, D. Marshall, Microfluidics for single cell analysis, Curr. Opin. Biotechnol. 23 (2012) 110-119.

[296] K. Takahashi, A. Hattori, I. Suzuki, T. Ichiki, K. Yasuda, Non-destructive on-chip cell sorting system with real-time microscopic image processing, J. Nanobiotechnol. 2 (2004) 5.

[297] M. Gan, J. Su, J. Wang, H. Wu, L. Chen, A scalable microfluidic chip for bacterial suspension culture, Lab Chip. 11 (2011) 4087-4092.

[298] C.D. Chin, T. Laksanasopin, Y.K. Cheung, D. Steinmiller, V. Linder, H. Parsa, J. Wang, H. Moore, R. Rouse, G. Umviligihozo, E. Karita, L. Mwambarangwe, S.L. Braunstein, J. van de Wijgert, R. Sahabo, J.E. Justman, W. El-Sadr, S.K. Sia, Microfluidics-based diagnostics of infectious diseases in the developing world, Nat Med. 17 (2011) 1015-1019.

[299] L. Xu, H. Yu, M.S. Akhras, S.-J. Han, S. Osterfeld, R.L. White, N. Pourmand, S.X. Wang, Giant magnetoresistive biochip for DNA detection and HPV genotyping, Biosens. Bioelectron. 24 (2008) 99-103.

[300] S. Fuse, N. Tanabe, M. Yoshida, H. Yoshida, T. Doi, T. Takahashi, Continuous-flow synthesis of vitamin D3, Chem. Commun. 46 (2010) 8722-8724.

[301] C.H. Arnaud, A.M. Thayer, inside instrumentation, Chem. Eng. News Arch. 87 (2009) 31.

[302] A.J. Hughes, A.E. Herr, Quantitative enzyme activity determination with zeptomole sensitivity by microfluidic gradient-gel zymography, Anal. Chem. 82 (2010) 3803-3811.

[303] S. Matosevic, N. Szita, F. Baganz, Fundamentals and applications of immobilized microfluidic enzymatic reactors, J. Chem. Technol. Biotechnol. 86 (2011) 325-334.

[304] S. Kundu, A.S. Bhangale, W.E. Wallace, K.M. Flynn, C.M. Guttman, R.A. Gross, K.L. Beers, Continuous flow enzyme-catalyzed polymerization in a microreactor, J. Am. Chem. Soc. 133 (2011) 6006-6011.

[305] C. Tonhauser, A. Natalello, H. Löwe, H. Frey, Microflow technology in polymer synthesis, Macromolecules. 45 (2012) 9551-9570.

[306] F. Schonfeld, V. Hessel, C. Hofmann, An optimised split-and-recombine micro-mixer with uniform 'chaotic' mixing, Lab Chip. 4 (2004) 65-69.

[307] L. Zhendong, L. Yangcheng, W. Jiawei, L. Guangsheng, Mixing characterization and scaling-up analysis of asymmetrical T-shaped micromixer: Experiment and CFD simulation, Chem. Eng. J. 181–182 (2012) 597-606.

[308] N. Nam-Trung, W. Zhigang, Micromixers—a review, J. Micromech. Microeng. 15 (2005) R1.

[309] N. Anton, F. Bally, C.A. Serra, A. Ali, Y. Arntz, Y. Mely, M. Zhao, E. Marchioni, A. Jakhmola, T.F. Vandamme, A new microfluidic setup for precise control of the polymer nanoprecipitation process and lipophilic drug encapsulation, Soft Matter. 8 (2012) 10628-10635.

[310] G.S. Jeong, S. Chung, C.-B. Kim, S.-H. Lee, Applications of micromixing technology, Analyst. 135 (2010) 460-473.

[311] R. Schenk, V. Hessel, B. Werner, F. Schönfeld, C. Hofmann, M. Donnet, N. Jongen, Micromixers as tool for powder production, in: 15 th International Symposium on Industrial Crystallization European Federation of Chemical Engineering, Sorrento, Italy, 2002, pp. 909.

[312] A. Bertsch, S. Heimgartner, P. Cousseau, P. Renaud, Static micromixers based on large-scale industrial mixer geometry, Lab Chip. 1 (2001) 56-60.

[313] V. Kumar, M. Paraschivoiu, K.D.P. Nigam, Single-phase fluid flow and mixing in microchannels, Chem. Eng. Sci. 66 (2011) 1329-1373.

[314] L.Y. Yeo, H.-C. Chang, P.P.Y. Chan, J.R. Friend, Microfluidic devices for bioapplications, Small. 7 (2011) 12-48.

[315] C.D. Chin, V. Linder, S.K. Sia, Commercialization of microfluidic point-of-care diagnostic devices, Lab Chip. 12 (2012) 2118-2134.

[316] M.A. Cervinski, C.M. Lockwood, A.M. Ferguson, R.R. Odem, U.H. Stenman, H. Alfthan, D.G. Grenache, A.M. Gronowski, Qualitative point-of-care and over-the-counter urine hCG devices differentially detect the hCG variants of early pregnancy, Clin. Chim. Acta. 406 (2009) 81-85.

[317] L. Bissonnette, M.G. Bergeron, Infectious disease management through Point-of-Care personalized medicine molecular diagnostic technologies, J. Pers. Med. 2 (2012) 50-70.

[318] J. Wang, Electrochemical glucose biosensors, Chem. Rev. 108 (2007) 814-825.

[319] P.N. Nge, C.I. Rogers, A.T. Woolley, Advances in microfluidic materials, functions, integration, and applications, Chem. Rev. 113 (2013) 2550-2583.

[320] G.B. Salieb-Beugelaar, G. Simone, A. Arora, A. Philippi, A. Manz, Latest developments in microfluidic cell biology and analysis systems, Anal. Chem. 82 (2010) 4848-4864.

[321] E.W.K. Young, D.J. Beebe, Fundamentals of microfluidic cell culture in controlled microenvironments, Chem. Soc. Rev. 39 (2010) 1036-1048.

[322] E. Leclerc, Y. Sakai, T. Fujii, Microfluidic PDMS (Polydimethylsiloxane) bioreactor for large-scale culture of hepatocytes, Biotechnol. Prog. 20 (2004) 750-755.

[323] T.-C. Chao, A. Ros, Microfluidic single-cell analysis of intracellular compounds, J. Roy. Soc. Interface. 5 (2008) S139-S150.

[324] R.N. Zare, S. Kim, Microfluidic Platforms for Single-Cell Analysis, Annu. Rev. Biomed. Eng. 12 (2010) 187-201.

[325] J.F. Zhong, Y. Chen, J.S. Marcus, A. Scherer, S.R. Quake, C.R. Taylor, L.P. Weiner, A microfluidic processor for gene expression profiling of single human embryonic stem cells, Lab Chip. 8 (2008) 68-74.

[326] A.J. deMello, Control and detection of chemical reactions in microfluidic systems, Nature. 442 (2006) 394-402.

[327] N.M. Toriello, E.S. Douglas, N. Thaitrong, S.C. Hsiao, M.B. Francis, C.R. Bertozzi, R.A. Mathies, Integrated microfluidic bioprocessor for single-cell gene expression analysis, Proc. Nat. Acad. Sci. USA. (2008).

[328] F.T.G. van den Brink, E. Gool, J.-P. Frimat, J. Bomer, A. van den Berg, S. Le Gac, Parallel single-cell analysis microfluidic platform, ELECTROPHORESIS. 32 (2011) 3094-3100.

[329] L.M. Griep, F. Wolbers, B. Wagenaar, P.M. Braak, B.B. Weksler, I.A. Romero, P.O. Couraud, I. Vermes, A.D. Meer, A. Berg, BBB ON CHIP: microfluidic platform to mechanically and biochemically modulate blood-brain barrier function, Biomed. Microdevices. 15 (2013) 145-150.

[330] N.-D. Dinh, Y.-Y. Chiang, H. Hardelauf, J. Baumann, E. Jackson, S. Waide, J. Sisnaiske, J.-P. Frimat, C.v. Thriel, D. Janasek, J.-M. Peyrin, J. West, Microfluidic construction of minimalistic neuronal co-cultures, Lab Chip. 13 (2013) 1402-1412.

[331] J.-P. Frimat, J. Sisnaiske, S. Subbiah, H. Menne, P. Godoy, P. Lampen, M. Leist, J. Franzke, J.G. Hengstler, C. van Thriel, J. West, The network formation assay: a spatially standardized neurite outgrowth analytical display for neurotoxicity screening, Lab Chip. 10 (2010) 701-709.

[332] L. Kim, M.D. Vahey, H.-Y. Lee, J. Voldman, Microfluidic arrays for logarithmically perfused embryonic stem cell culture, Lab Chip. 6 (2006) 394-406.

[333] Y. Marcy, C. Ouverney, E.M. Bik, T. Lösekann, N. Ivanova, H.G. Martin, E. Szeto, D. Platt, P. Hugenholtz, D.A. Relman, S.R. Quake, Dissecting biological "dark matter" with single-cell genetic analysis of rare and uncultivated TM7 microbes from the human mouth, Proc. Natl. Acad. Sci. USA. 104 (2007) 11889-11894.

[334] Y. Marcy, T. Ishoey, R.S. Lasken, T.B. Stockwell, B.P. Walenz, A.L. Halpern, K.Y. Beeson, S.M.D. Goldberg, S.R. Quake, Nanoliter Reactors Improve Multiple Displacement Amplification of Genomes from Single Cells, PLoS Genet. 3 (2007) e155.

[335] X. Weng, H. Jiang, D. Li, Microfluidic DNA hybridization assays, Microfluid. Nanofluid. 11 (2011) 367-383.

[336] O.Y.F. Henry, C.K. O'Sullivan, Rapid DNA hybridization in microfluidics, TrAC, Trends Anal. Chem. 33 (2012) 9-22.

[337] C.C. Lee, T.M. Snyder, S.R. Quake, A microfluidic oligonucleotide synthesizer, Nucleic acid Res. 38 (2010) 2514-2521.

[338] B.S. Ferguson, S.F. Buchsbaum, J.S. Swensen, K. Hsieh, X. Lou, H.T. Soh, Integrated Microfluidic Electrochemical DNA Sensor, Anal. Chem. 81 (2009) 6503-6508.

[339] C. Li, X. Dong, J. Qin, B. Lin, Rapid nanoliter DNA hybridization based on reciprocating flow on a compact disk microfluidic device, Anal. Chim. Acta. 640 (2009) 93-99.

[340] P. Neuži, S. Giselbrecht, K. Länge, T.J. Huang, A. Manz, Revisiting lab-on-a-chip technology for drug discovery, Nat. Rev. Drug Discover. 11 (2012) 620-632.

[341] H. Zhou, Z. Ning, F. Wang, D. Seebun, D. Figeys, Proteomic reactors and their applications in biology, FEBS J. 278 (2011) 3796-3806.

[342] E.M. Miller, S.L.S. Freire, A.R. Wheeler, Proteomics in Microfluidic Devices, Springer, Heidelberg, Germany, 2008.

[343] L.G. Puckett, E. Dikici, S. Lai, M. Madou, L.G. Bachas, S. Daunert, Investigation into the Applicability of the Centrifugal Microfluidics Platform for the Development of Protein−Ligand Binding Assays Incorporating Enhanced Green Fluorescent Protein as a Fluorescent Reporter, Anal. Chem. 76 (2004) 7263-7268.

[344] R.E. Holcomb, J.R. Kraly, C.S. Henry, Electrode array detector for microchip capillary electrophoresis, Analyst. 134 (2009) 486-492.

[345] L. Shintu, R. Baudoin, V. Navratil, J.-M. Prot, C. Pontoizeau, M. Defernez, B.J. Blaise, C. Domange, A.R. Péry, P. Toulhoat, C. Legallais, C. Brochot, E. Leclerc, M.-E. Dumas, Metabolomics-on-a-Chip and Predictive Systems Toxicology in Microfluidic Bioartificial Organs, Anal. Chem. 84 (2012) 1840-1848.

[346] M.B. Esch, T.L. King, M.L. Shuler, The role of body-on-a-chip devices in drug and toxicity studies, Ann. Rev. Biomed. Eng. 13 (2011) 55-72.

[347] A. Sin, K.C. Chin, M.F. Jamil, Y. Kostov, G. Rao, M.L. Shuler, The design and fabrication of three-chamber microscale cell culture analog devices with integrated dissolved oxygen sensors, Biotechnol. Prog. 20 (2004) 338-345.

[348] L. Yobas, S. Martens, W.-L. Ong, N. Ranganathan, High-performance flow-focusing geometry for spontaneous generation of monodispersed droplets, Lab Chip. 6 (2006) 1073-1079.

[349] G. Vladisavljević, I. Kobayashi, M. Nakajima, Effect of dispersed phase viscosity on maximum droplet generation frequency in microchannel emulsification using asymmetric straight-through channels, Microfluid. Nanofluid. 10 (2011) 1199-1209.

[350] I. Kobayashi, S. Mukataka, M. Nakajima, Production of monodisperse oil-in-water emulsions using a large silicon straight-through microchannel plate, Ind. Eng. Chem. Res. 44 (2005) 5852-5856.

[351] S. Sugiura, M. Nakajima, M. Seki, Effect of channel structure on microchannel emulsification, Langmuir. 18 (2002) 5708-5712.

[352] S. Sugiura, M. Nakajima, J. Tong, H. Nabetani, M. Seki, Preparation of monodispersed solid lipid microspheres using a microchannel emulsification technique, J. Colloid. Interface. Sci 227 (2000) 95-103.

[353] K. Nakagawa, S. Iwamoto, M. Nakajima, A. Shono, K. Satoh, Microchannel emulsification using gelatin and surfactant-free coacervate microencapsulation, J. Colloid Interface Sci. 278 (2004) 198-205.

[354] S. Sugiura, M. Nakajima, H. Itou, M. Seki, Synthesis of polymeric microspheres with narrow size distributions employing microchannel emulsification, Macromol. Rapid Commun. . 22 (2001) 773-778.

[355] I. Kobayashi, Y. Wada, K. Uemura, M. Nakajima, Microchannel emulsification for mass production of uniform fine droplets: integration of microchannel arrays on a chip, Microfluidics and Nanofluidics. 8 (2010) 255-262.

[356] T. Kawakatsu, H. Komori, M. Nakajima, Y. Kikuchi, H. Komori, Y. Yonemoto, Production of monodispersed oli-in-water emulsion using crossflow-type silicon microchannel plate, Chem. Eng. J. 32 (1999) 241-244.

[357] T. Kawakatsu, G. Trägårdh, Y. Kikuchi, M. Nakajima, H. Komori, T. Yonemoto, Effect of microchannel structure on droplet size during crossflow microchannel emulsification, J. Surfact. Deterg. 3 (2000) 295-302.

[358] I. Kobayashi, S. Mukataka, M. Nakajima, Effect of slot aspect ratio on droplet formation from silicon straight-through microchannels, J. Colloid Interface Sci. 279 (2004) 277-280.

[359] K. Dijke, I. Kobayashi, K. Schroën, K. Uemura, M. Nakajima, R. Boom, Effect of viscosities of dispersed and continuous phases in microchannel oil-in-water emulsification, Microfluid. Nanofluid. 9 (2010) 77-85.

[360] I. Kobayashi, Y. Wada, K. Uemura, M. Nakajima, Effect of channel and operation parameters on emulsion production using oblong straight-through microchannels, Japan J. Food Eng. 10 (2009) 69-75.

[361] M.A. Neves, H.S. Ribeiro, K.B. Fujiu, I. Kobayashi, M. Nakajima, Formulation of controlled size PUFA-loaded oil-in-water emulsions by microchannel emulsification using β-carotene-rich palm oil, Ind. Eng. Chem. Res. 47 (2008) 6405-6411.

[362] G.T. Vladisavljević, I. Kobayashi, M. Nakajima, Generation of highly uniform droplets using asymmetric microchannels fabricated on a single crystal silicon plate: Effect of emulsifier and oil types, Powder Technol. 183 (2008) 37-45.

[363] I. Kobayashi, T. Takano, R. Maeda, Y. Wada, K. Uemura, M. Nakajima, Straight-through microchannel devices for generating monodisperse emulsion droplets several microns in size, Microfluid. Nanofluid. 4 (2008) 167-177.

[364] I. Kobayashi, G.T. Vladisavljević, K. Uemura, M. Nakajima, CFD analysis of microchannel emulsification: Droplet generation process and size effect of asymmetric straight flow-through microchannels, Chem. Eng. Sci. 66 (2011) 5556-5565.

[365] M. Hashimoto, P. Garstecki, G.M. Whitesides, Synthesis of composite emulsions and complex foams with the use of microfluidic flow-focusing devices, Small. 3 (2007) 1792-1802.

[366] M. Hashimoto, S.S. Shevkoplyas, B. Zasońska, T. Szymborski, P. Garstecki, G.M. Whitesides, Formation of bubbles and droplets in parallel, coupled flow-focusing geometries, Small. 4 (2008) 1795-1805.

[367] C.H. Yeh, Y.C. Chen, Y.C. Lin, Generation of droplets with different concentrations using gradient-microfluidic droplet generator, Microfluid. Nanofluid. 11 (2011) 245-253.

[368] A. Kawai, S. Matsumoto, H. Kiriya, T. Oikawa, K. Hara, T. Ohkawa, K. Katayama, K. Nishizawa, Development of microreactor for manufacturing gel particles without class selection of diameter, Tosoh Res. Technol. Rev. 47 (2003) 3-9.

[369] G. Tetradis Meris, D. Rossetti, C.n. Pulido de Torres, R. Cao, G. Lian, R. Janes, Novel parallel integration of microfluidic device network for emulsion formation, Ind. Eng. Chem. Res. 48 (2009) 8881-8889.

[370] S.M. Senn, D. Poulikakos, Tree network channels as fluid distributors constructing double-staircase polymer electrolyte fuel cells, J. Appl. Phys. 96 (2004) 842-852.

[371] W. Li, J. Greener, D. Voicu, E. Kumacheva, Multiple modular microfluidic (M3) reactors for the synthesis of polymer particles, Lab Chip. 9 (2009) 2715-2721.

[372] M.R. Kendall, D. Bardin, R. Shih, P.A. Dayton, A.P. Lee, Scaled-up production of monodisperse, dual layer microbubbles using multi-array microfluidic module for medical imaging and drug delivery, Bubble Sci. Eng. Technol. 4 (2012) 12-20.

[373] T.S.A. Heugebaert, B.I. Roman, A. De Blieck, C.V. Stevens, A safe production method for acetone cyanohydrin, Tetrahedron Lett. 51 (2010) 4189-4191.

[374] V. Hessel, S. Hardt, H. Löwe, Chemical Micro-process Engineering – Fundamentals, Modeling and Reactions, Wiley-VCH, Weinheim, 2004.

[375] S. Lomel, L. Falk, J.M. Commenge, J.L. Houzelot, K. Ramdani, The microreactor: A systematic and efficient tool for the transition from batch to continuous process?, Chem. Eng. Res. Des. 84 (2006) 363-369.

[376] T. Illg, P. Löb, V. Hessel, Flow chemistry using milli- and microstructured reactors—From conventional to novel process windows, Bioorg. Med. Chem. 18 (2010) 3707-3719.

[377] T. Razzaq, C.O. Kappe, Continuousflow organic synthesis under high-temperature/pressure conditions, Chem. Asian J. 5 (2010) 1274-1289.

[378] Y. Voloshin, R. Halder, A. Lawal, Kinetics of hydrogen peroxide synthesis by direct combination of H2 and O2 in a microreactor, Catal. Today. 125 (2007) 40-47.

[379] M.B. Fox, D.C. Esveld, R.M. Boom, Conceptual design of a mass parallelized PEF microreactor, Trends Food Sci. Technol. 18 (2007) 484-491.

[380] S.R. Deshmukh, A.L.Y. Tonkovich, K.T. Jarosch, L. Schrader, S.P. Fitzgerald, D.R. Kilanowski, J.J. Lerou, T.J. Mazanec, Scale-up of microchannel reactors for fischer−tropsch synthesis, Ind. Eng. Chem. Res. 49 (2010) 10883-10888.

[381] N. Kockmann, M. Gottsponer, D.M. Roberge, Scale-up concept of single-channel microreactors from process development to industrial production, Chem. Eng. J. 167 (2011) 718-726.

[382] D. Fuerth, A. Bazylak, Up-Scaled Microfluidic Fuel Cells With Porous Flow-Through Electrodes, J. Fluids Eng. 135 (2013) 021102.

[383] E. Kjeang, J. McKechnie, D. Sinton, N. Djilali, Planar and three-dimensional microfluidic fuel cell architectures based on graphite rod electrodes, J. Power Sources. 168 (2007) 379-390.

[384] J. El-Ali, P.K. Sorger, K.F. Jensen, Cells on chips, Nature. 442 (2006) 403-411.

[385] T. Thorsen, S.J. Maerkl, S.R. Quake, Microfluidic Large-Scale Integration, Science. 298 (2002) 580-584.

[386] J.W. Hong, V. Studer, G. Hang, W.F. Anderson, S.R. Quake, A nanoliter-scale nucleic acid processor with parallel architecture, Nat Biotech. 22 (2004) 435-439.

[387] R. Gómez-Sjöberg, A.A. Leyrat, D.M. Pirone, C.S. Chen, S.R. Quake, Versatile, Fully Automated, Microfluidic Cell Culture System, Anal. Chem. 79 (2007) 8557-8563.

[388] S. Tay, J.J. Hughey, T.K. Lee, T. Lipniacki, S.R. Quake, M.W. Covert, Single-cell NF-[kgr]B dynamics reveal digital activation and analogue information processing, Nature. 466 (2010) 267-271.

[389] C.B. Rohde, F. Zeng, R. Gonzalez-Rubio, M. Angel, M.F. Yanik, Microfluidic system for on-chip high-throughput whole-animal sorting and screening at subcellular resolution, Proc. Natl. Acad. Sci. USA. 104 (2007) 13891-13895.

[390] H. Ma, L. Jiang, W. Shi, J. Qin, B. Lin, A programmable microvalve-based microfluidic array for characterization of neurotoxin-induced responses of individual C. elegans, Biomicrofluidics. 3 (2009) 044114-044118.

[391] X.C.i. Solvas, F.M. Geier, A.M. Leroi, J.G. Bundy, J.B. Edel, A.J. deMello, High-throughput age synchronisation of Caenorhabditis elegans, Chem. Commun. 47 (2011) 9801-9803.

[392] K. Chung, M.M. Crane, H. Lu, Automated on-chip rapid microscopy, phenotyping and sorting of C. elegans, Nat Meth. 5 (2008) 637-643.

[393] M.M. Crane, J.N. Stirman, C.-Y. Ou, P.T. Kurshan, J.M. Rehg, K. Shen, H. Lu, Autonomous screening of C. elegans identifies genes implicated in synaptogenesis, Nat Meth. 9 (2012) 977-980.

[394] H.C. Fan, J. Wang, A. Potanina, S.R. Quake, Whole-genome molecular haplotyping of single cells, Nat Biotech. 29 (2011) 51-57.

[395] J. Wang, H.C. Fan, B. Behr, Stephen R. Quake, Genome-wide single-cell analysis of recombination activity and De Novo mutation rates in human sperm, Cell. 150 (2012) 402-412.

[396] D. Castel, A. Pitaval, M.-A. Debily, X. Gidrol, Cell microarrays in drug discovery, Drug Discover Today. 11 (2006) 616-622.

[397] X. Feng, W. JinHui, W. ShuQi, D. Naside Gozde, G. Umut Atakan, D. Utkan, Microengineering methods for cell-based microarrays and high-throughput drug-screening applications, Biofabrication. 3 (2011) 034101.

[398] M. Hashimoto, R. Tong, D.S. Kohane, Microdevices for Nanomedicine, Mol. Pharm. (2013) In Press.

[399] B.K. McKenna, J.G. Evans, M.C. Cheung, D.J. Ehrlich, A parallel microfluidic flow cytometer for high-content screening, Nat Meth. 8 (2011) 401-403.

[400] S.C. Chapin, D.C. Pregibon, P.S. Doyle, High-throughput flow alignment of barcoded hydrogel microparticles, Lab Chip. 9 (2009) 3100-3109.

[401] J.-H. Huang, J. Kim, N. Agrawal, A.P. Sudarsan, J.E. Maxim, A. Jayaraman, V.M. Ugaz, Rapid fabrication of bio-inspired 3D microfluidic vascular networks, Adv. Mat. 21 (2009) 3567-3571.

[402] C.L. Hansen, M.O.A. Sommer, S.R. Quake, Systematic investigation of protein phase behavior with a microfluidic formulator, Proc. Natl. Acad. Sci. USA. 101 (2004) 14431-14436.

[403] C.L. Hansen, E. Skordalakes, J.M. Berger, S.R. Quake, A robust and scalable microfluidic metering method that allows protein crystal growth by free interface diffusion, Proc. Natl. Acad. Sci. USA. 99 (2002) 16531-16536.

[404] Y.-F. Chen, L. Jiang, M. Mancuso, A. Jain, V. Oncescu, D. Erickson, Optofluidic opportunities in global health, food, water and energy, Nanoscale. 4 (2012) 4839-4857.

[405] T.-Y. Chang, C. Pardo-Martin, A. Allalou, C. Wahlby, M.F. Yanik, Fully automated cellular-resolution vertebrate screening platform with parallel animal processing, Lab Chip. 12 (2012) 711-716.

[406] K.R. Stevens, M.D. Ungrin, R.E. Schwartz, S. Ng, B. Carvalho, K.S. Christine, R.R. Chaturvedi, C.Y. Li, P.W. Zandstra, C.S. Chen, S.N. Bhatia, InVERT molding for scalable control of tissue microarchitecture, Nat Commun. 4 (2013) 1847.

[407] R. Pal, M. Yang, R. Lin, B.N. Johnson, N. Srivastava, S.Z. Razzacki, K.J. Chomistek, D.C. Heldsinger, R.M. Haque, V.M. Ugaz, P.K. Thwar, Z. Chen, K. Alfano, M.B. Yim, M. Krishnan, A.O. Fuller, R.G. Larson, D.T. Burke, M.A. Burns, An integrated microfluidic device for influenza and other genetic analyses, Lab Chip. 5 (2005) 1024-1032.

[408] V. Lecault, A.K. White, A. Singhal, C.L. Hansen, Microfluidic single cell analysis: from promise to practice, Curr. Opin. Chem. Biol. 16 (2012) 381-390.

Table 1. Materials and typical techniques used for fabrication of microfluidic channels for emulsification.

Materials	Fabrication methods	Inherent surface affinity	Reference
Surface-oxidized silicon	Anisotropic wet etching, chemical dry etching	Hydrophilic	Kawakatsu et al. [43]; Kobayashi et al. [44]
Quartz glass, Hoya SD-2 glass, Pyrex glass	Mechanical cutting	Hydrophilic	Nisisako et al. [45]; Plaza et al. [46]
Soda lime glass, Pyrex glass, photoetchable glass	Isotropic wet etching	Hydrophilic	Lin et al. [47]; Okushima et al. [48]; Kim and Kwon [49]
Fused silica glass	Chemical dry etching	Hydrophilic	Nisisako et al. [50]
Silicon nitride	Chemical dry etching followed by anisotropic wet etching	Hydrophilic	Kuiper et al. [51]
Poly(dimethylsiloxane) (PDMS)	Soft lithography	Hydrophobic	Whitesides [1]
cyclic olefin copolymer (COP)	Hot embossing, injection molding, nanoimprint lithography, laser ablation	Hydrophobic	Jena et al. [52]; Nunes et al. [53]
polyurethane	Soft lithography	Hydrophobic	Nie et al. [54], Thorsen et al. [55]
poly(methyl methacrylate) (PMMA)	Hot embossing lithography, injection molding, mechanical cutting, laser ablation, stereolithography	Hydrophobic	Eusner et al. [56]; Liu et al. [57]; Nisisako et al. [58]; Yeh et al. [59]; Morimoto et al. [60]
Nickel	LIGA process	Hydrophobic	Kim and Lee [61]
Stainless steel	Mechanical cutting	Hydrophilic	Tong et al. [62]

Table 2. Maximum drop generation frequency (per single channel and overall), maximum dispersed phase flow rate, emulsion type and droplet diameter obtained in each of the cited publications using various microfluidic devices.

Device and channel size	Max drop generation frequency	Max disp. phase flow rate	Emulsion	Droplet diameter	Reference
Single T-junction 6.5 × 35 μm	80 Hz	0.006 mL h^{-1}	W/O	10–40 μm	Thorsen et al. [55]
Flow focusing device, orifice diameter=47 μm	1.2×10^{4} Hz	0.096 mL h^{-1}	W/O	20–140 μm	Yobas et al. [348]
211,248 straight-through MCs, 6.6 × 26.7 μm	3.3 Hz/MC, overall (3−5) × 10^{5} Hz	20–30 mL h^{-1}	O/W	≈32 μm	Kobayashi et al. [350]
12,000 Grooved-type MCs, 2 × 10 μm	43 Hz/MC, overall 5.2 × 10^{5} Hz	1.5 mL h^{-1}	O/W	10–15 μm	Kobayashi et al. [22]

Figures

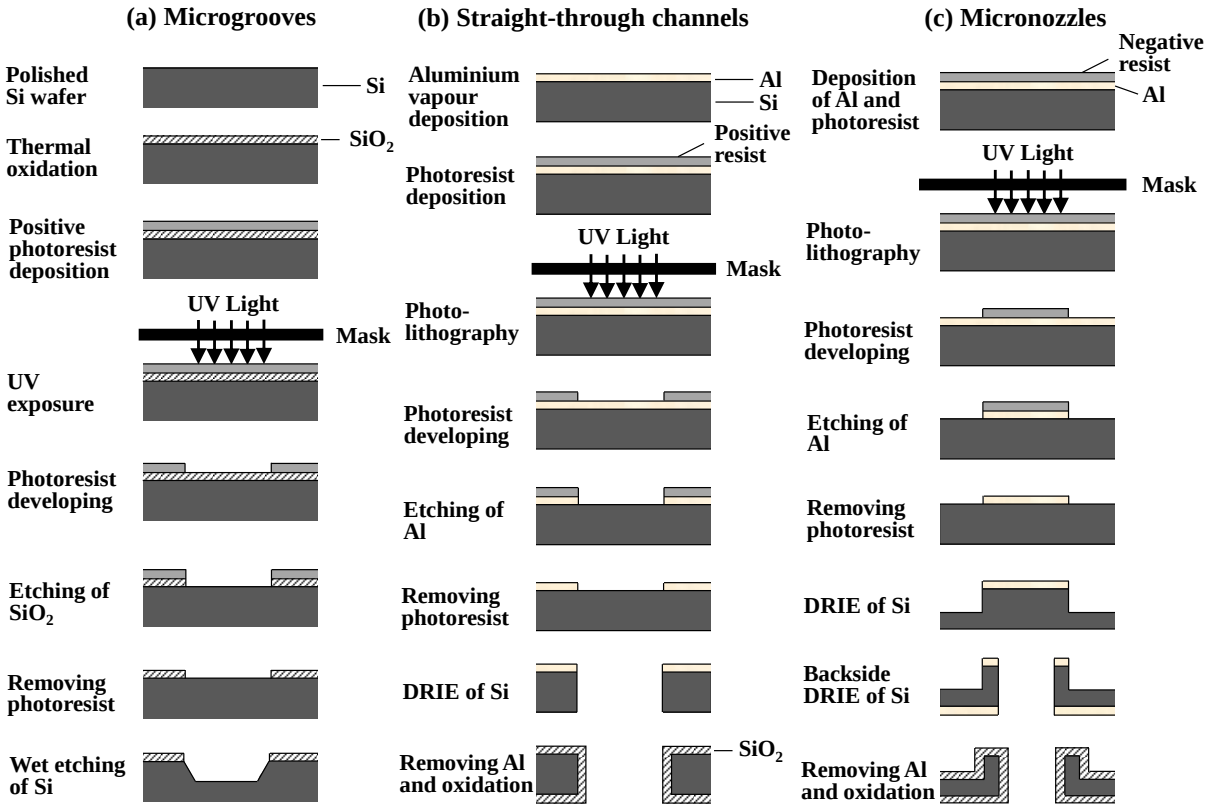

Figure 2.1.1. Fabrication of microchannels on single-crystal silicon wafers: (a) Fabrication of shallow microgrooves by photolithography and anisotropic wet etching adapted from [4]; (b) Fabrication of straight-through channels by photolithography and Deep Reactive ion Etching (DRIE) adapted from [44] (for clarity purpose, the thickness of the silicon substrate is unrealistically small compared to the thickness of deposited layers); (c) Fabrication of micronozzles by photolithography and two-step DRIE [63, 68].

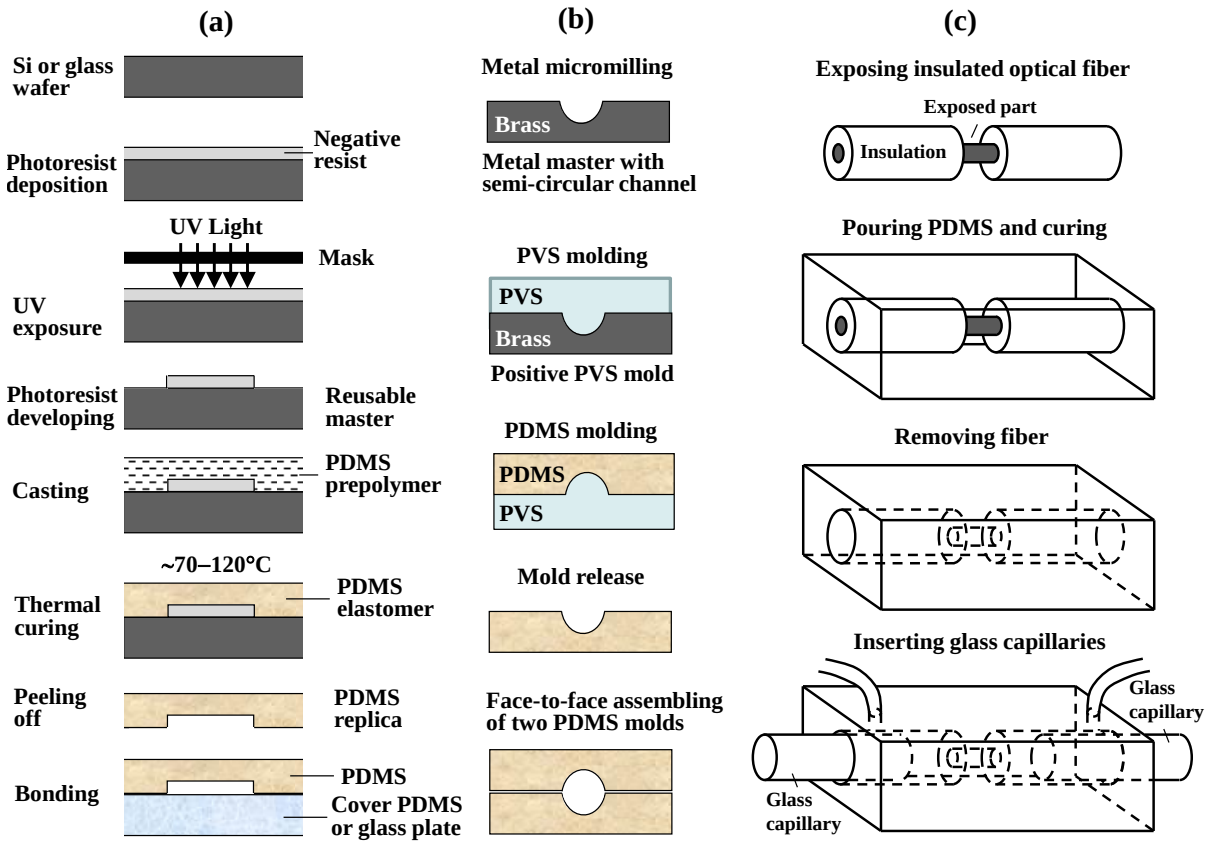

Figure 2.2.1. Fabrication of channel structures in PDMS by soft lithography: (a) rectangular channels obtained by conventional replica molding from a master consisted of photolithographically patterned negative photoresist on a silicon or glass wafer [69]; (b) circular channels obtained by attaching two semi-circular channels face-to-face. Semi-circular channels are fabricated by combining mechanical micromilling, PVS molding and photolithography [70] (c) 3D structure created by embedding a microfiber in a PDMS mold before curing [74].

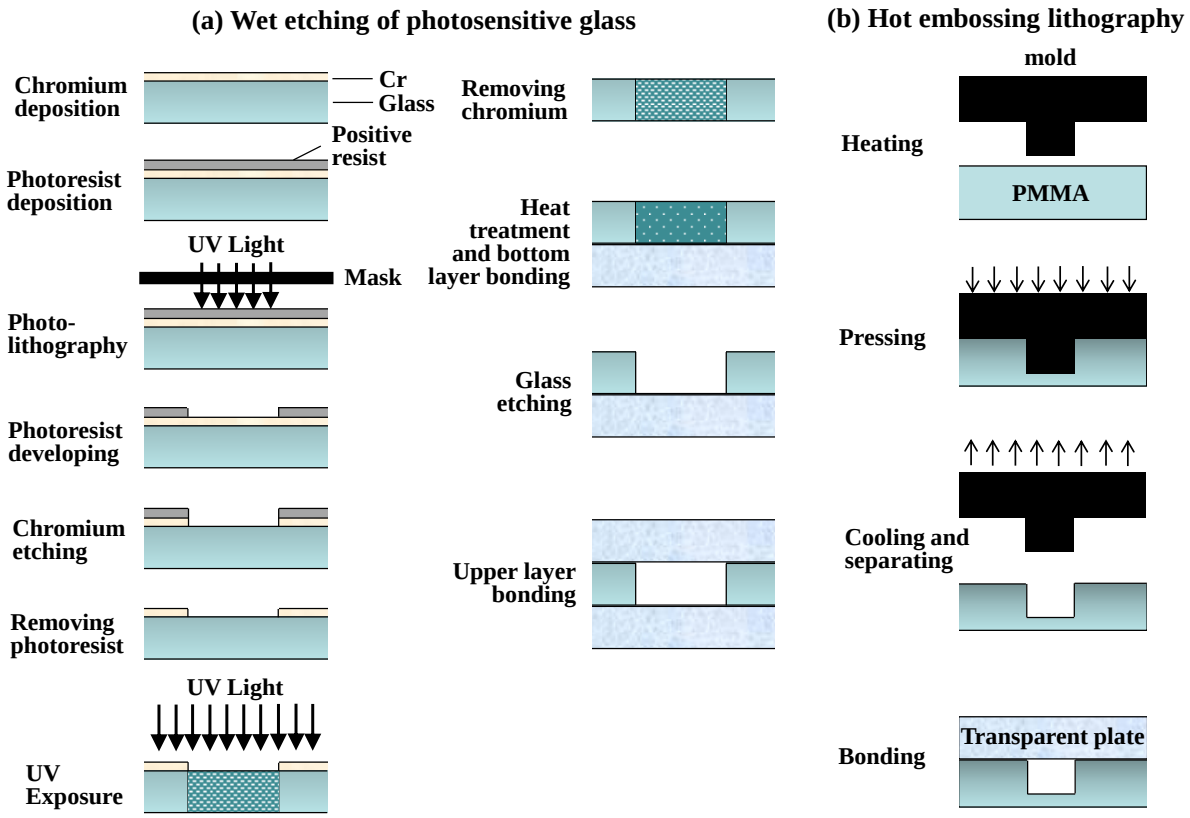

Figure 2.3.1. Fabrication of microfluidic channels in photosensitive glass and thermoplastics: (a) HF etching of photosensitive glass following UV exposure through chromium mask and heat treatment [49]; (b) Hot embossing lithography in poly(methyl methacrylate) (PMMA) [56].

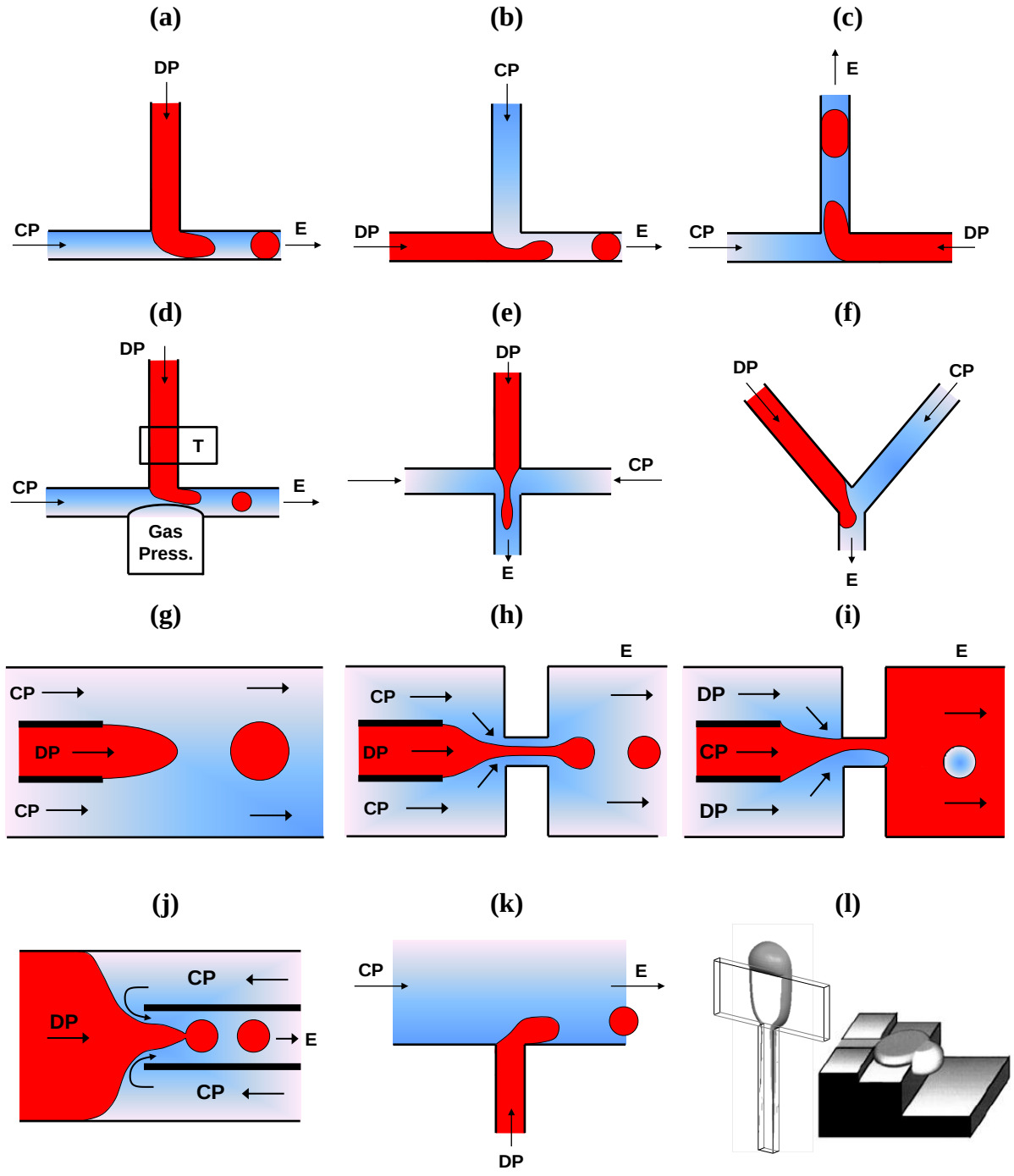

Figure 3.1.1. Microfluidic strategies for generation of single emulsions (DP – dispersed phase, CP – continuous phase, E – emulsion): (a) Standard T-junction [55]; (b) T-junction with injection of DP through the main channel [95]; (c) T-junction with head-on geometry; (d) Active T-junction with controllable moving wall structure [120] and integrated microheater [119]; (e) Cross junction [45]; (f) Y-junction [127]; (g) co-flow [135, 164, 165]; (h) Standard flow focusing device [141]; (i) Flow focusing device with CP supplied through the central channel [166]; (j) Flow focusing with counter-current flow [82]; (k) Cross flow

[150]; (i) Spontaneous droplet generation [133,134]. In all figures, DP does not wet the channel walls.

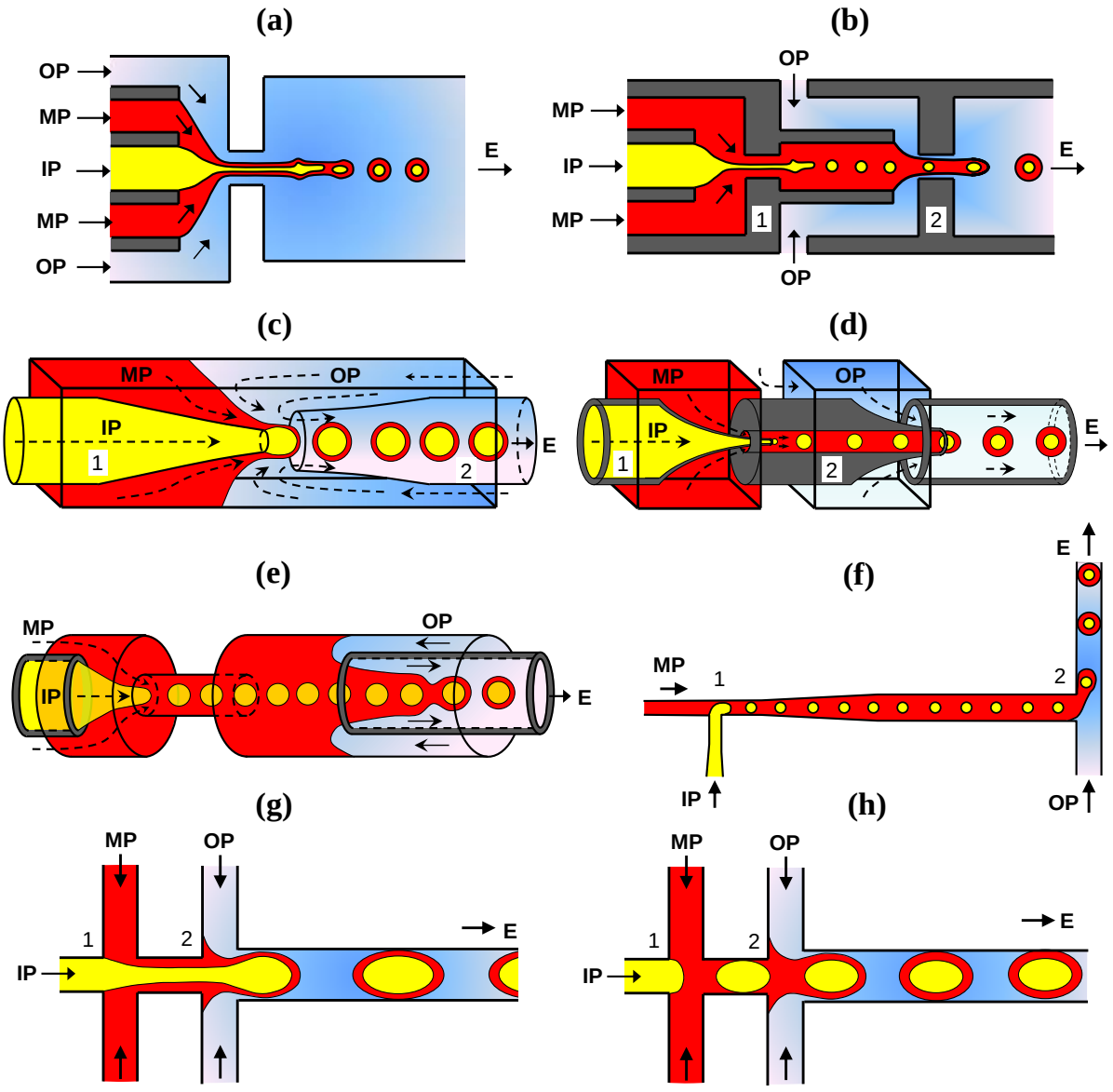

Figure 3.2.1. Microfluidic strategies for generation of core/shell droplets (IP – inner phase, MP – middle phase, OP – outer phase, E – emulsion): (a) Flow focusing in a planar device with co-flow: OP wets the orifice [54]; (b) Two planar sequential flow focusing drop generators: MP and OP wet orifices 1 and 2, resp. [166]; (c) Axisymmetric glass capillary device with combination of co-flow and flow focusing: MP and OP wet capillaries 1 and 2, resp. [89]; (d) Axisymmetric glass capillary device with two sequential co-flow drop generators: MP and OP wet capillaries 1 and 2, resp. [167]; (e) Axisymmetric PDMS device

with combination of co-flow and flow focusing: MP wets the orifice; (f) Two sequential T-junctions: MP and OP wets junctions 1 and 2, resp. [48, 131]; (g) Two sequential cross junctions with dripping instability present in T-junction 2: MP and OP wet T-junctions 1 and 2, resp. [126]; (h) Two sequential cross junctions with dripping instability present in both junctions: MP and OP wet T-junctions 1 and 2, resp. [126].

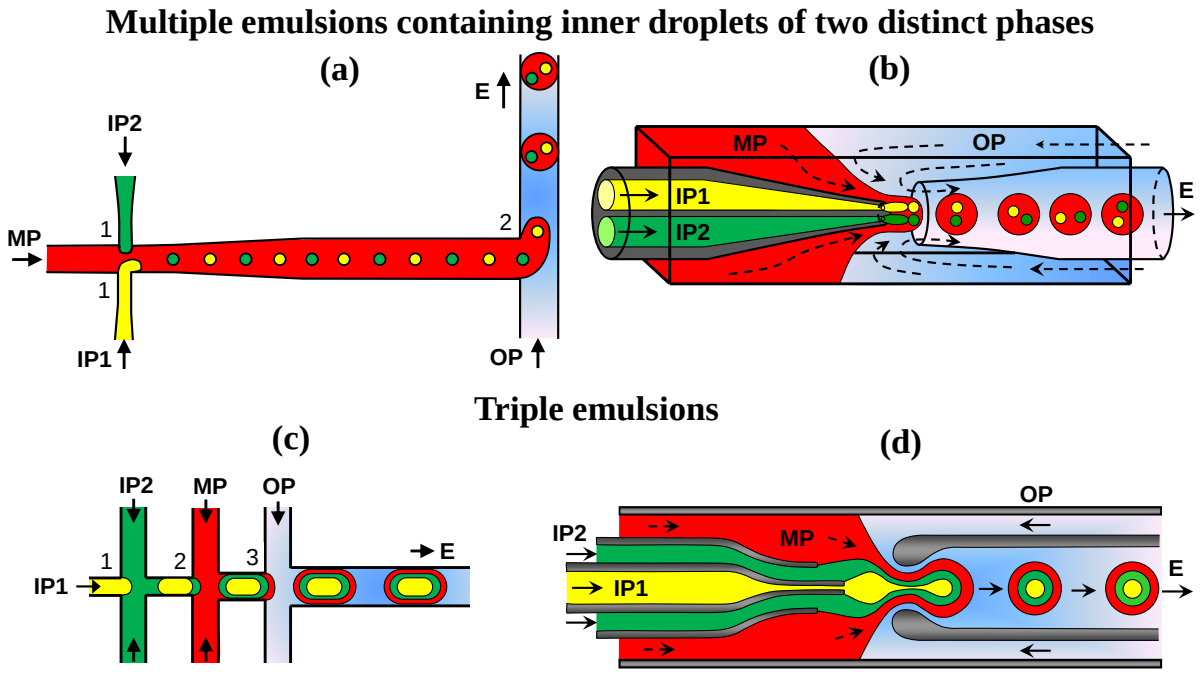

Figure 3.2.2. Microfluidic strategies for generation of higher-order multiple emulsions (IP1 – inner phase 1, IP2 – inner phase 2, MP – middle phase, OP – outer phase, E – emulsion): (a) Upstream cross junction and downstream T-junction connected in series: MP and OP wet T-junctions 1 and 2, resp. [48]; (b) Glass capillary device with a two-bore injection tube [188]; (c) Three sequential cross junctions: IP2, MP, and OP wet T-junctions 1, 2, and 3, resp. [183]; (d) Glass capillary device with two coaxial injection tubes [89].

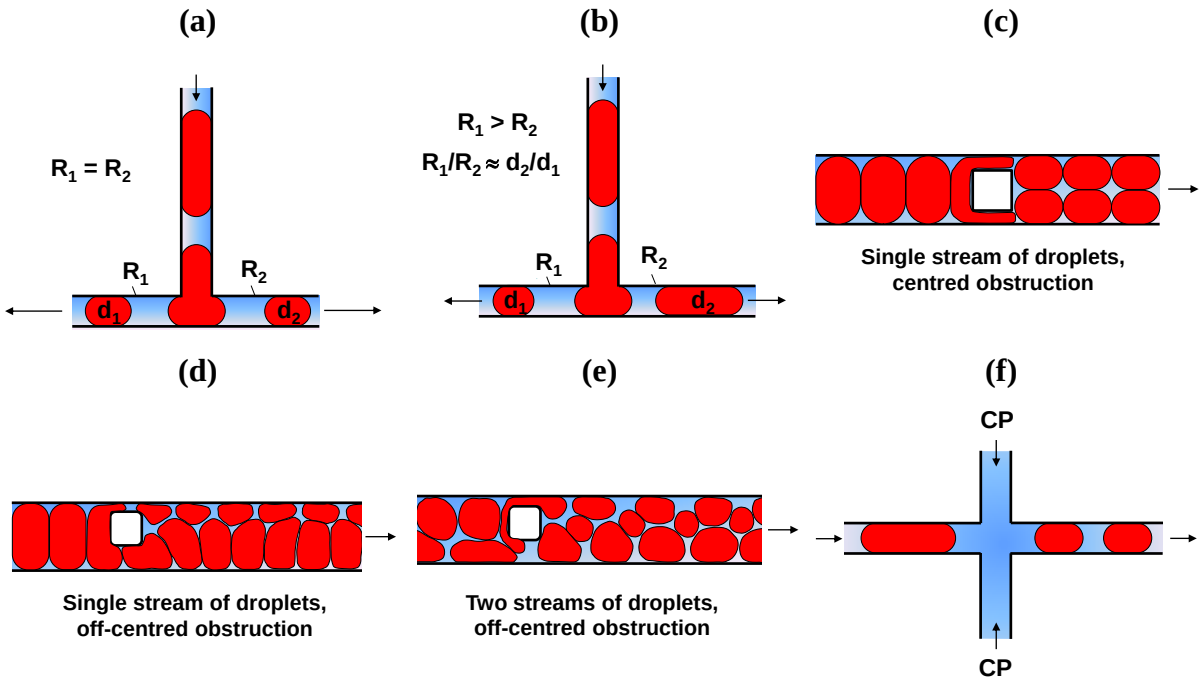

Figure 3.3.1. Droplet splitting in microfluidic channels (DP1 – dispersed phase 1, DP2 – dispersed phase 2, CP – continuous phase): (a) Symmetric droplet splitting in a T-junction. R_1 and R_2 are sidearm flow resistances [190]; (b) Asymmetric droplet splitting in a T-junction; (c) Flow of a single stream of droplets past centered obstruction [190]; (d) Flow of a single stream of droplets past off-centered obstruction [190]; (e) Flow of two parallel streams of droplets past off-centered obstruction [190]; (f) Droplet splitting in a flow focusing junction [191].

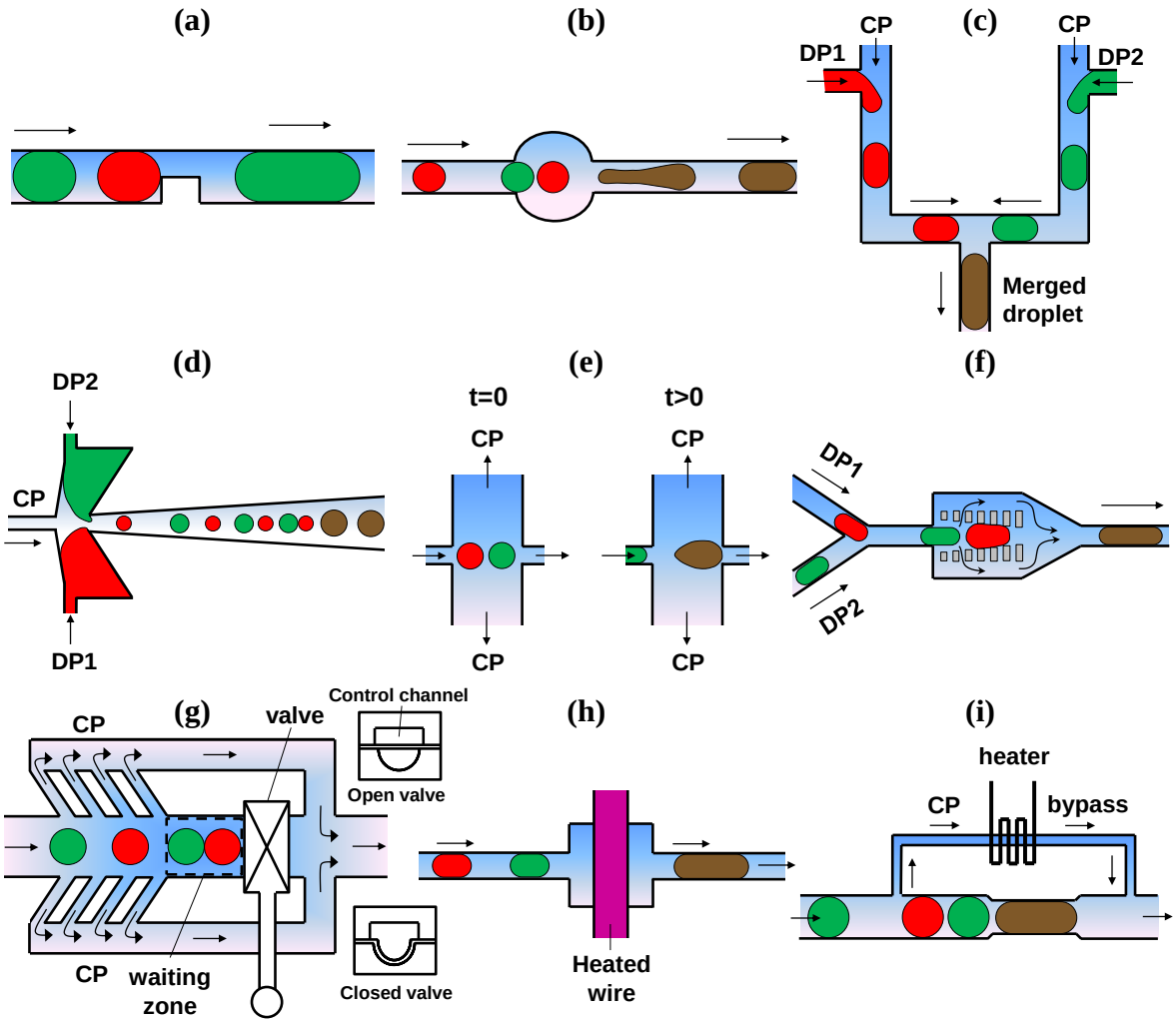

Figure 3.4.1. Strategies for droplet merging in microfluidic devices (DP1 – dispersed phase 1, DP2 – dispersed phase 2, CP – continuous phase): (a) Obstacle inserted in the channel [192]; (b) Circular expansion chamber [192, 193]; (c) T-junction [196]; (d) Tapered chamber with diverging walls [199, 209]; (e) Trifurcating junction [192, 200, 201]; (f) two sets of tapering pillars [202]; (g) pneumatically activated membrane valve; (h) expansion chamber with a heating wire [206, 207]; (i) Bypass line with a heating element [192].

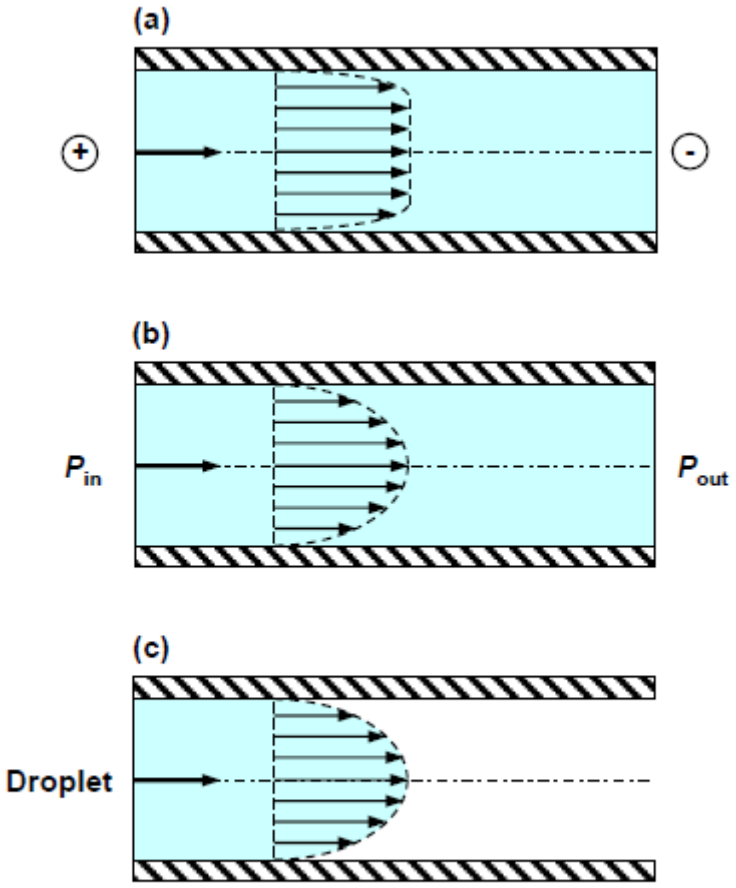

Figure 3.5.1. Types of driving forces that flow fluid in a microchannel. (a) electro-osmotic flow (b) pressure-driven flow and (c) capillary-driven flow

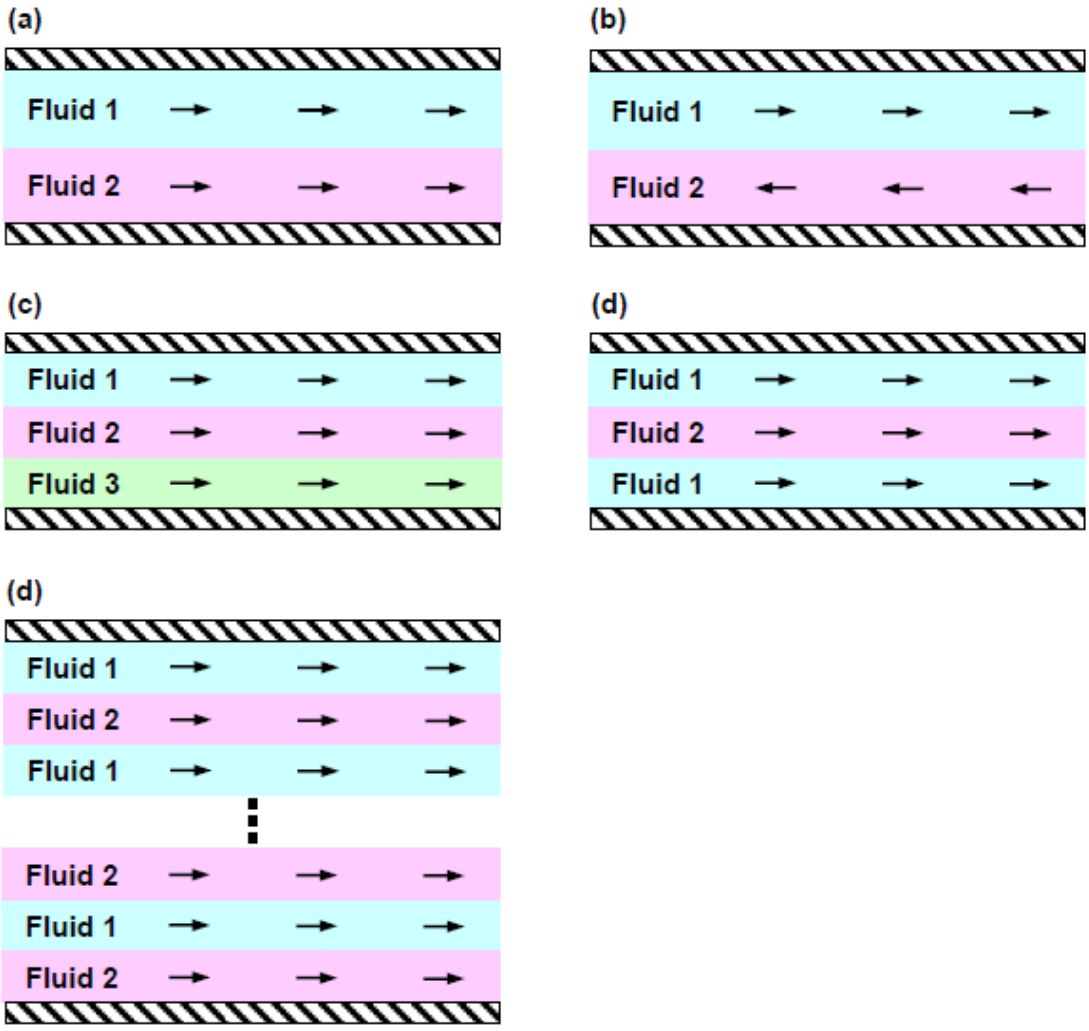

Figure 3.5.2. Typical types of parallel multiphase flows in a microchannel

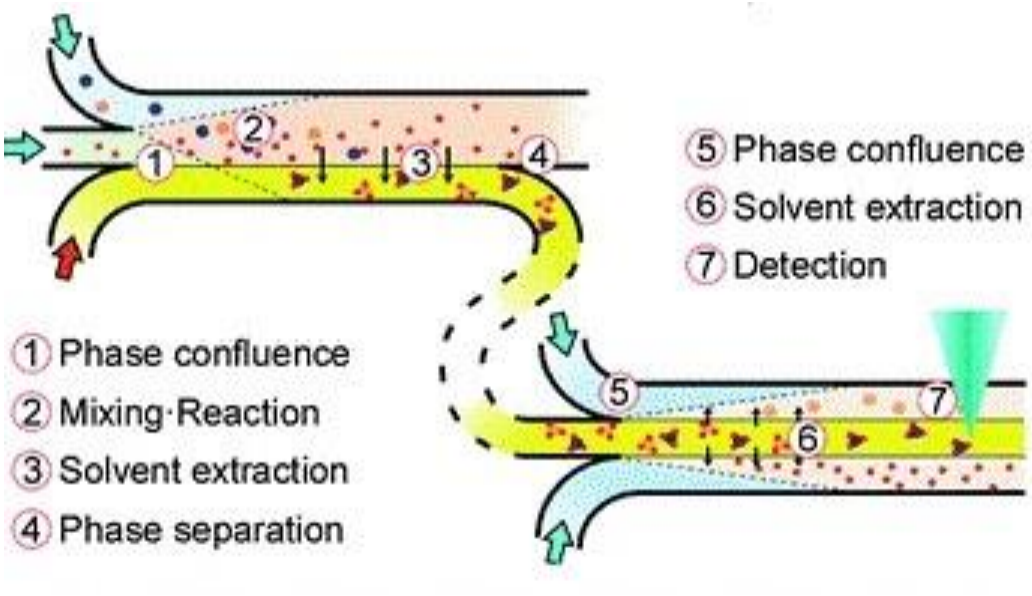

Figure 3.5.3. Typical combination of different reactions in continuous flow chemical processing involving multiphase parallel microflows. With permission [5].

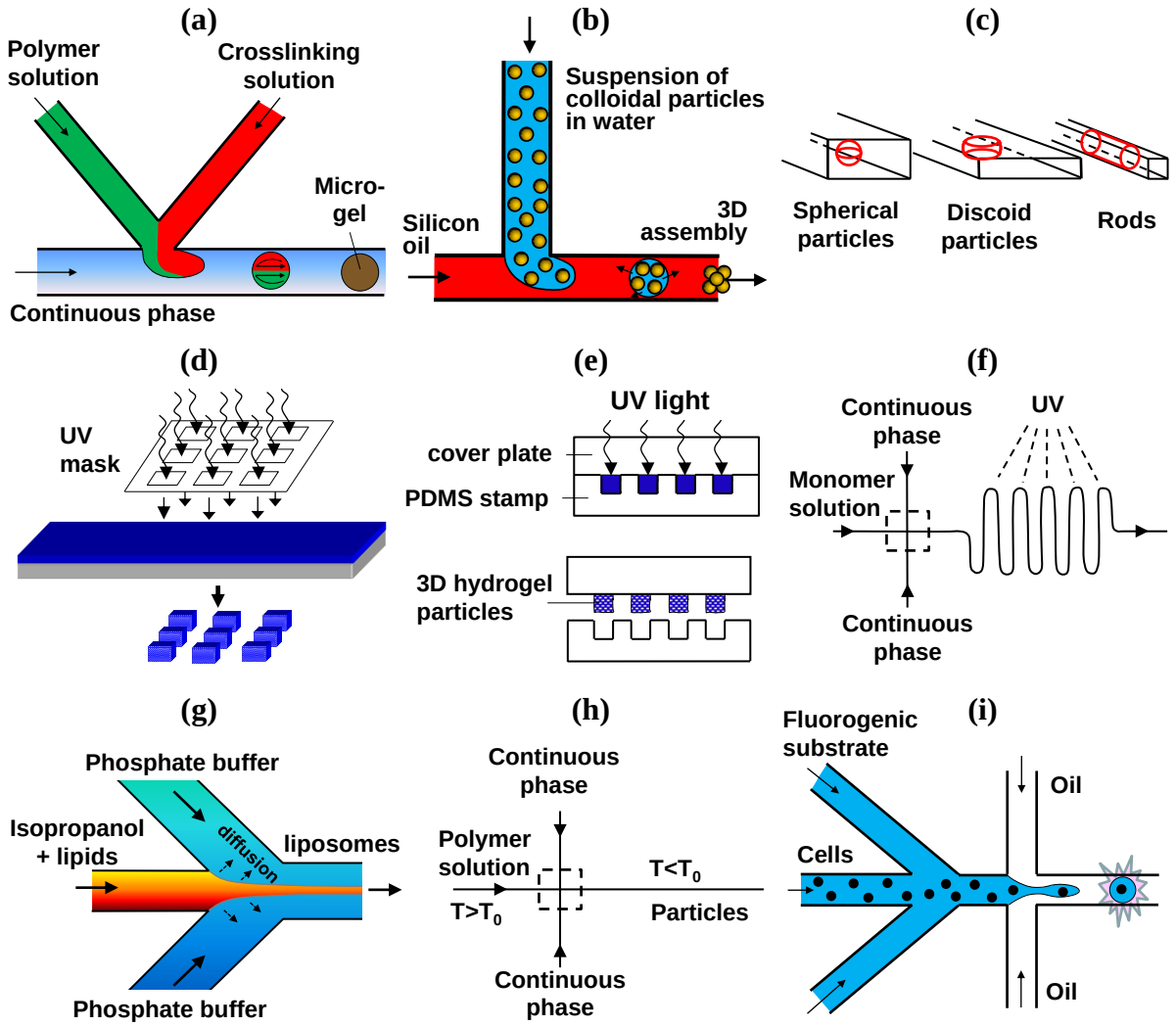

Figure 4.1.1 Microengineering methods for particle synthesis and high-throughput screening: (a) Rapid mixing of polymer and crosslinking solutions in T-junction [255]; (b) Emulsification/solvent evaporation [104]; (c) Emulsification in confined geometries [258]; (d) Photolithography [259]; (e) Micromolding [260]; (f) UV-induced polymerization [258]; (g) Nanoprecipitation as a result of mixing of two miscible solvents in laminar flow [261]; (h) Temperature-controlled emulsification/cooling below the phase transition temperature (T_0 – phase transition temperature) [258]; (i) Screening of cells by mixing a suspension of cells with a second aqueous stream containing a fluorogenic substrate in a flow focusing channel [262].

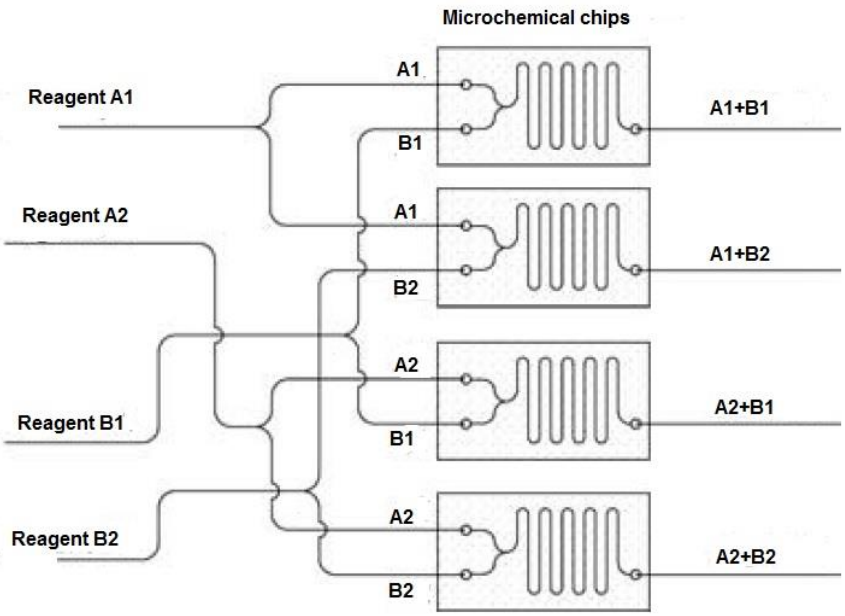

Figure 4.2. Parallel reaction system using microchemical chips for combinatorial synthesis adopted from [290].

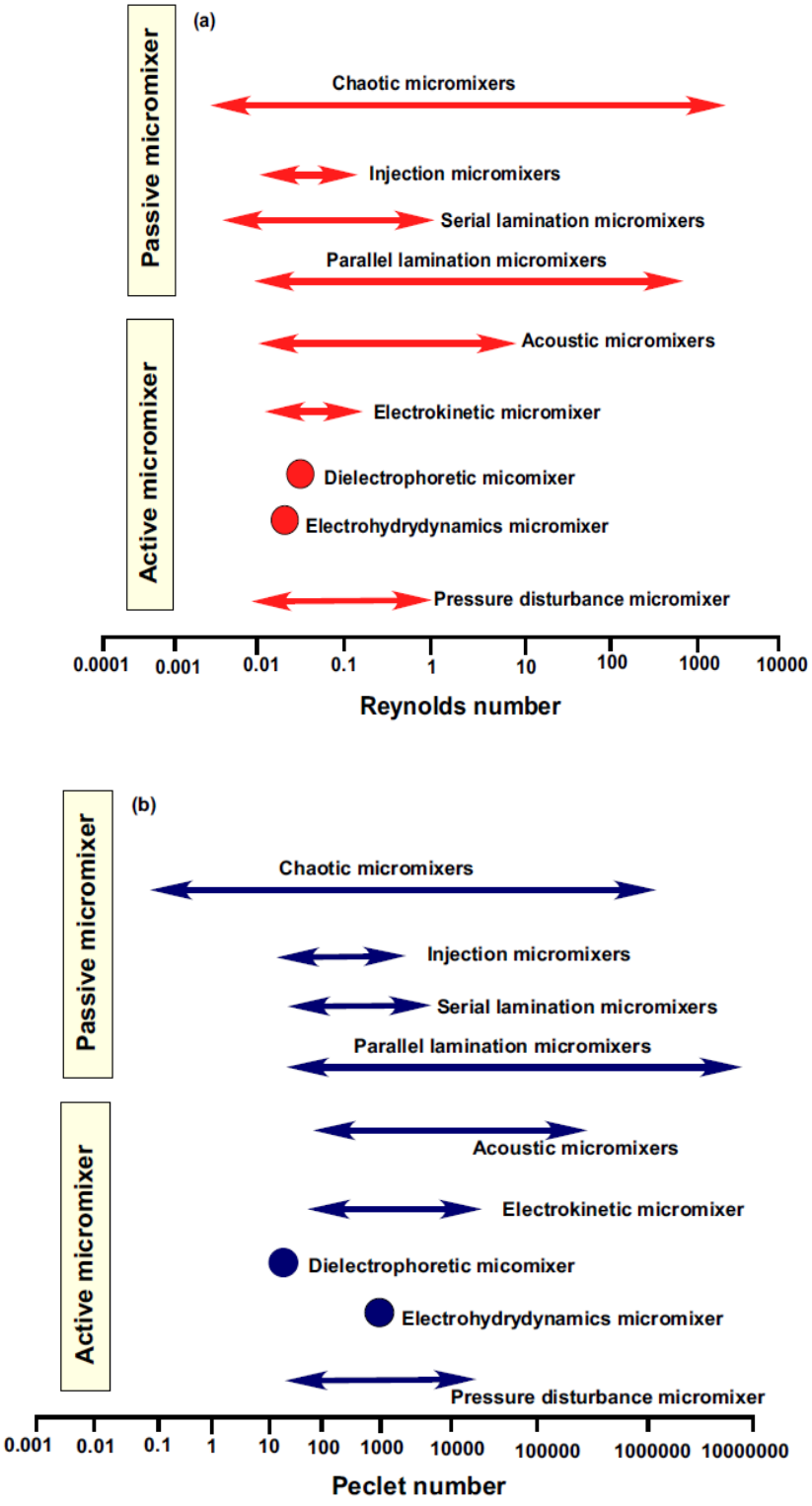

Figure 4.3. Operating ranges reported in the literature in active and passive micromixers in terms of (a) Reynolds and (b) Peclet numbers [313].

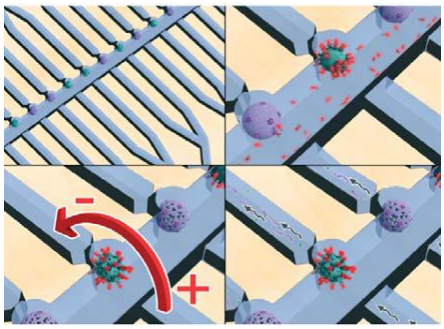

(a)

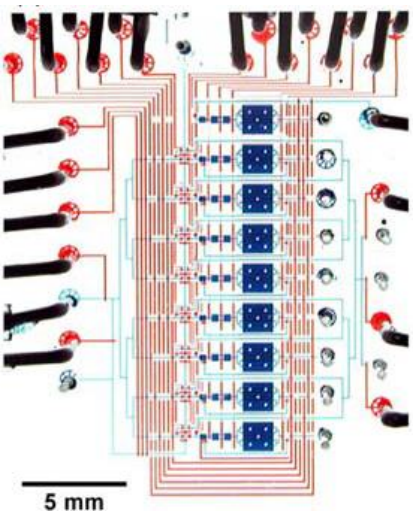

(b)

Figure 4.5. (a) Microfluidic platform for parallel single-cell analysis called PaSCAl that can easily be scale-up for analysis of thousands of cell in single embedded design (with permission from Van den Brink et al. [328]. **(c)** two-layered microfluidic device for trapping, lysing, and amplifying the genetic material of single cells (with permission [334]).

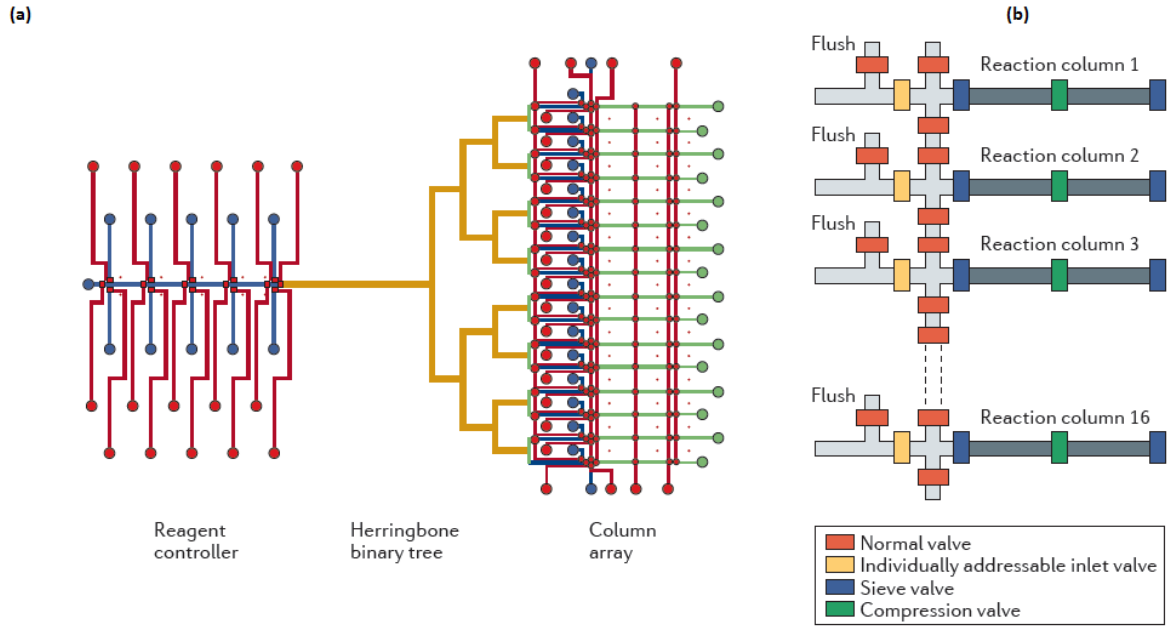

Figure 4.6. (a) Parallelized synthesis of oligonucleotides on a chip. (a) Schematic illustration of a 16-column microfluidic DNA synthesizer. The control lines (red), fluidic lines (blue), a herringbone mixer (yellow) and a square profiled binary tree and the reactor columns (green); (b) Schematic illustration of column array with valves for a controlled fluid inlet, fluid flow and washing of beads (with permission [337, 340]).

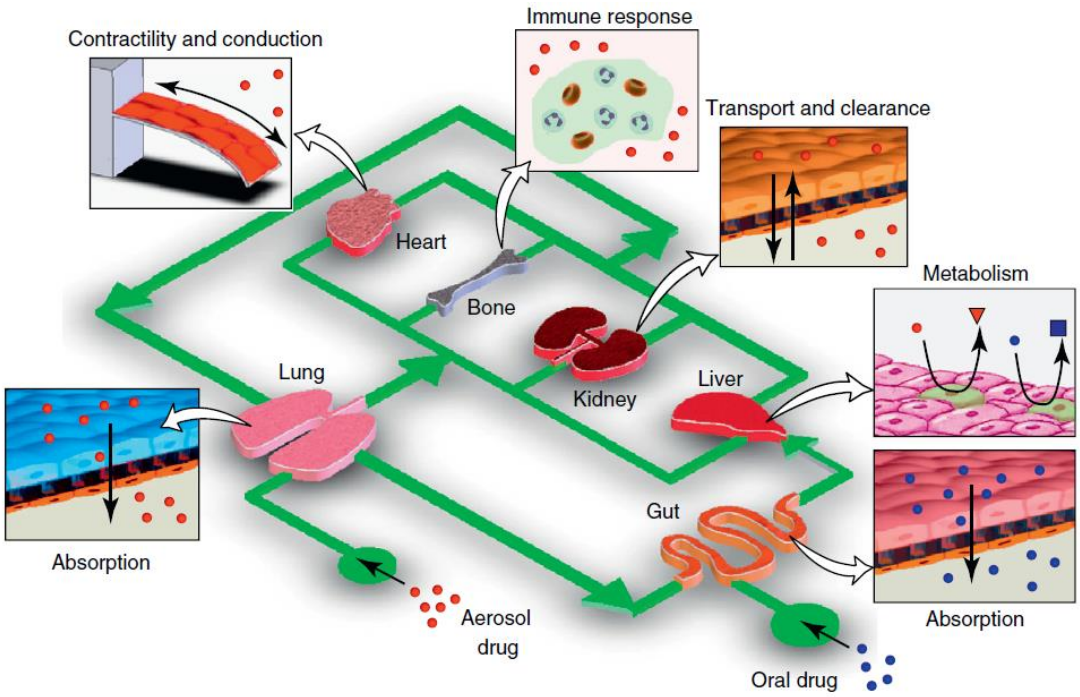

Figure 4.8. The human-on-a-chip concept. Biomimetic microsystems representing different organs can be integrated into a single microdevice and linked by a microfluidic circulatory system in a physiologically relevant manner to model a complex, dynamic process of drug absorption, distribution, metabolism and excretion, and to more reliably evaluate drug efficacy and toxicity. In this figure, an integrated system of microengineered organ mimics (lung, heart, gut, liver, kidney and bone) can be used to study the absorption of inhaled aerosol drugs (red) from the lung to microcirculation, as well as to measure their cardiotoxicity (e.g. changes in heart contractility or conduction), transport and clearance in the kidney, metabolism in the liver, and immune-cell contributions to these responses. Drug substances (blue) also can be introduced into the gut compartment to investigate interplay between orally administered drugs and molecular transporters and metabolizing enzymes expressed in the various organs. With permission [37]

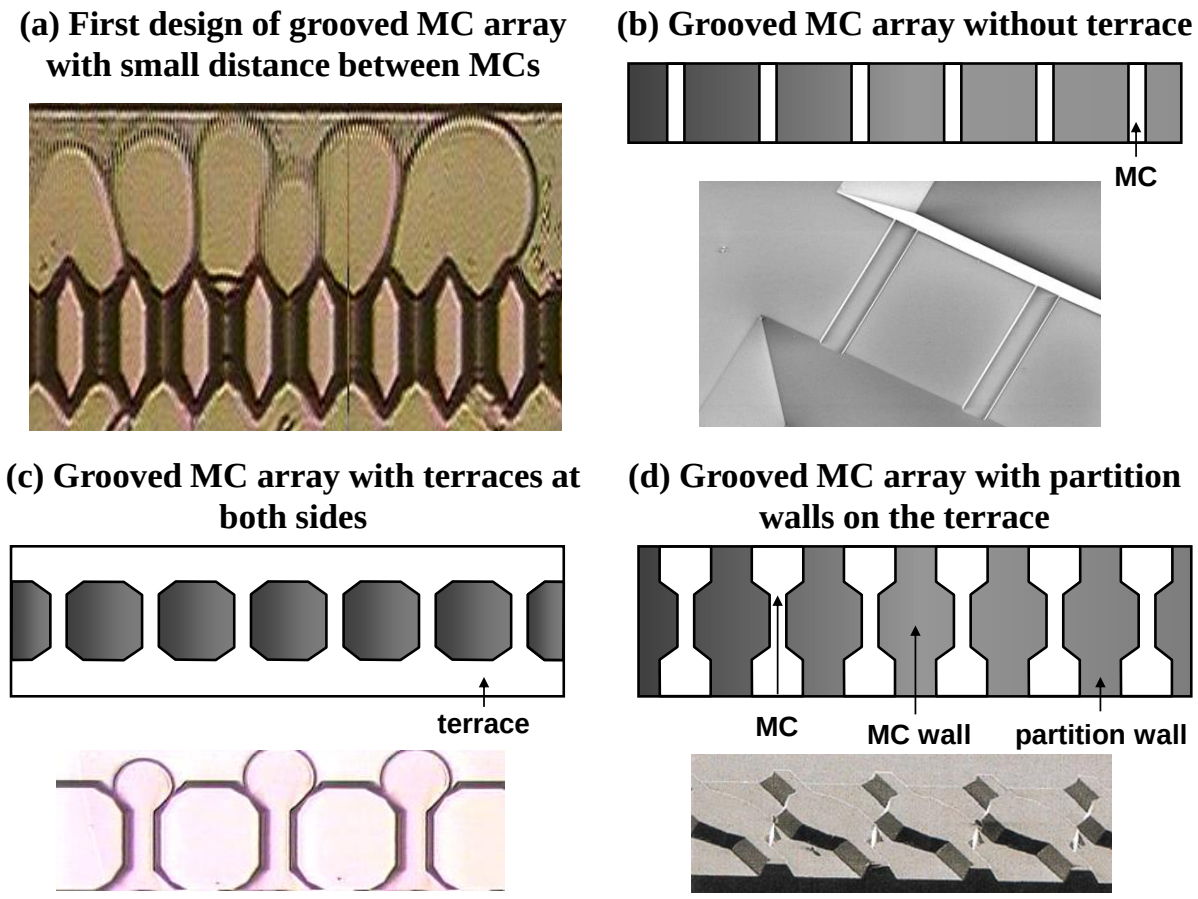

Figure 5.1.1. Different designs of grooved-type microchannel arrays for droplet generation.

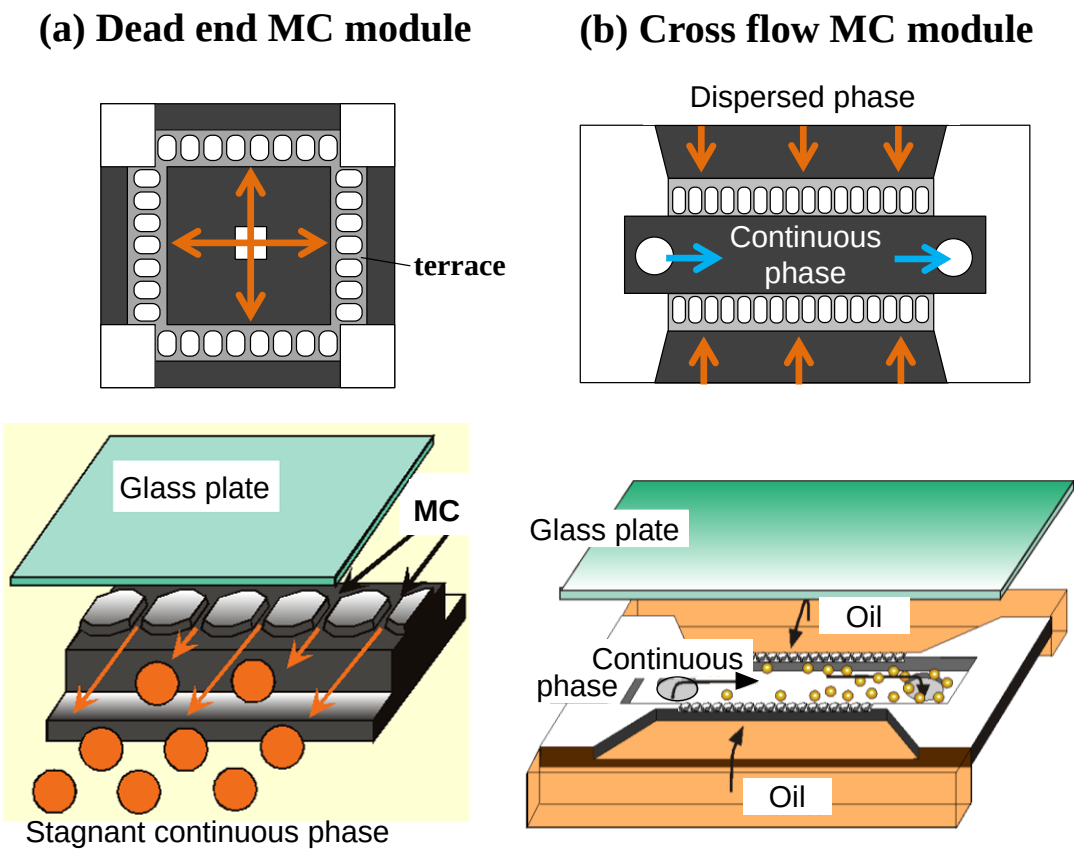

Figure 5.1.2. Grooved-type microchannel (MC) plates: (a) Dead-end plate with stagnant continuous phase [64]. (b) Cross-flow plate with recirculating continuous phase [356, 357].

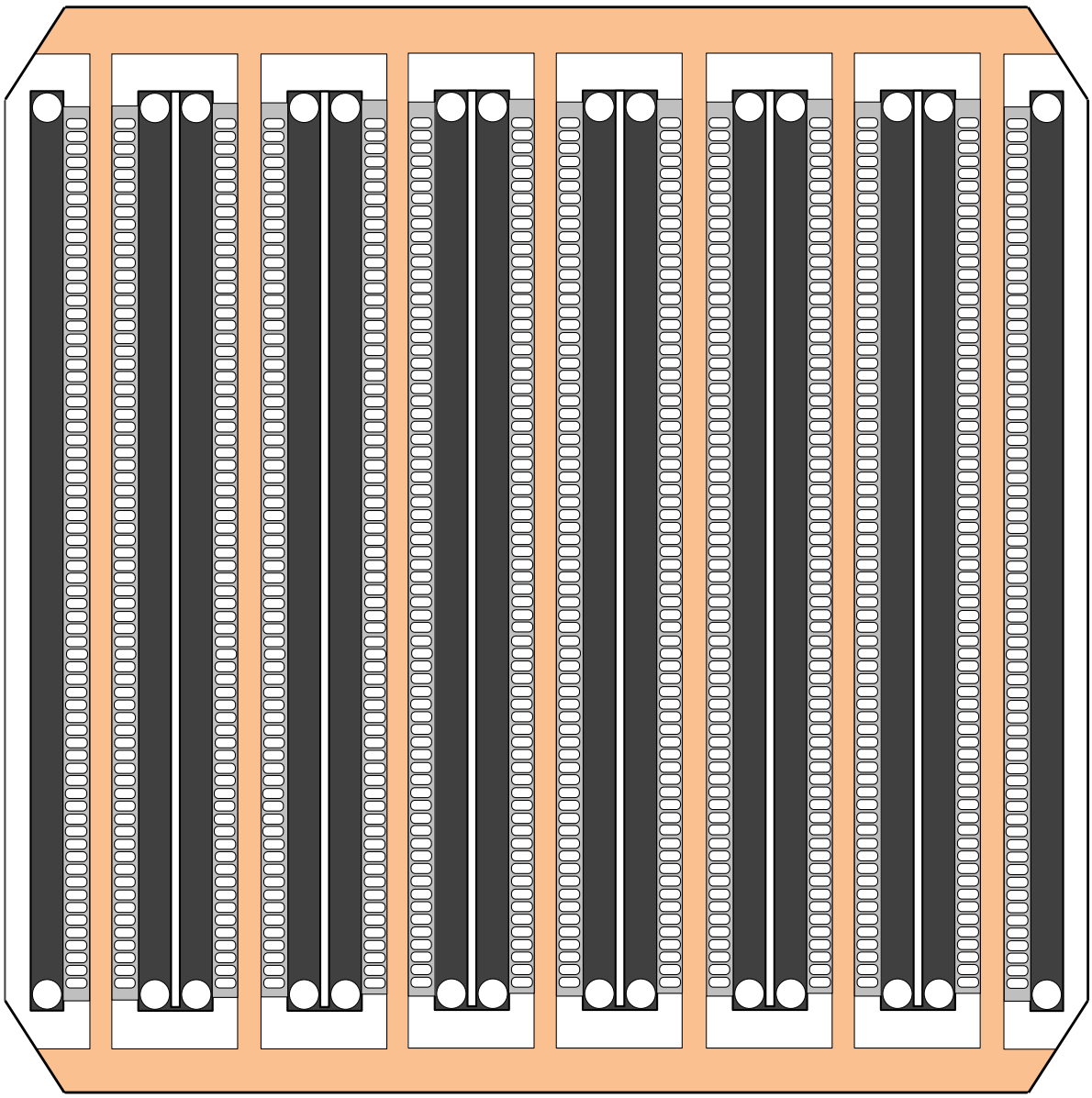

Figure 5.1.3. A large cross-flow single-crystal silicon plate (60×60 mm) with 14 parallel grooved-type MC arrays, each consisting of 850 MCs; not all MCs are shown in the figure for simplicity [22].

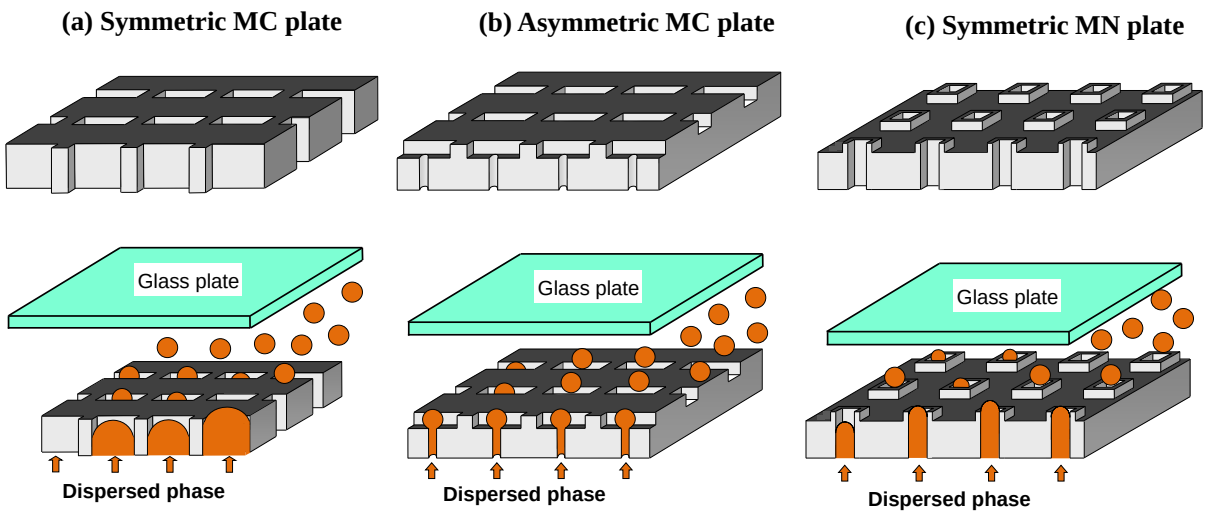

Figure 5.1.4. Straight-through MC array plates: (a) symmetric plate with microslots on both sides [44]; (b) Asymmetric plate with circular channels on the upstream side and slots on the downstream side [350]; (c) Symmetric plate with micronozzles (MNs) [68].

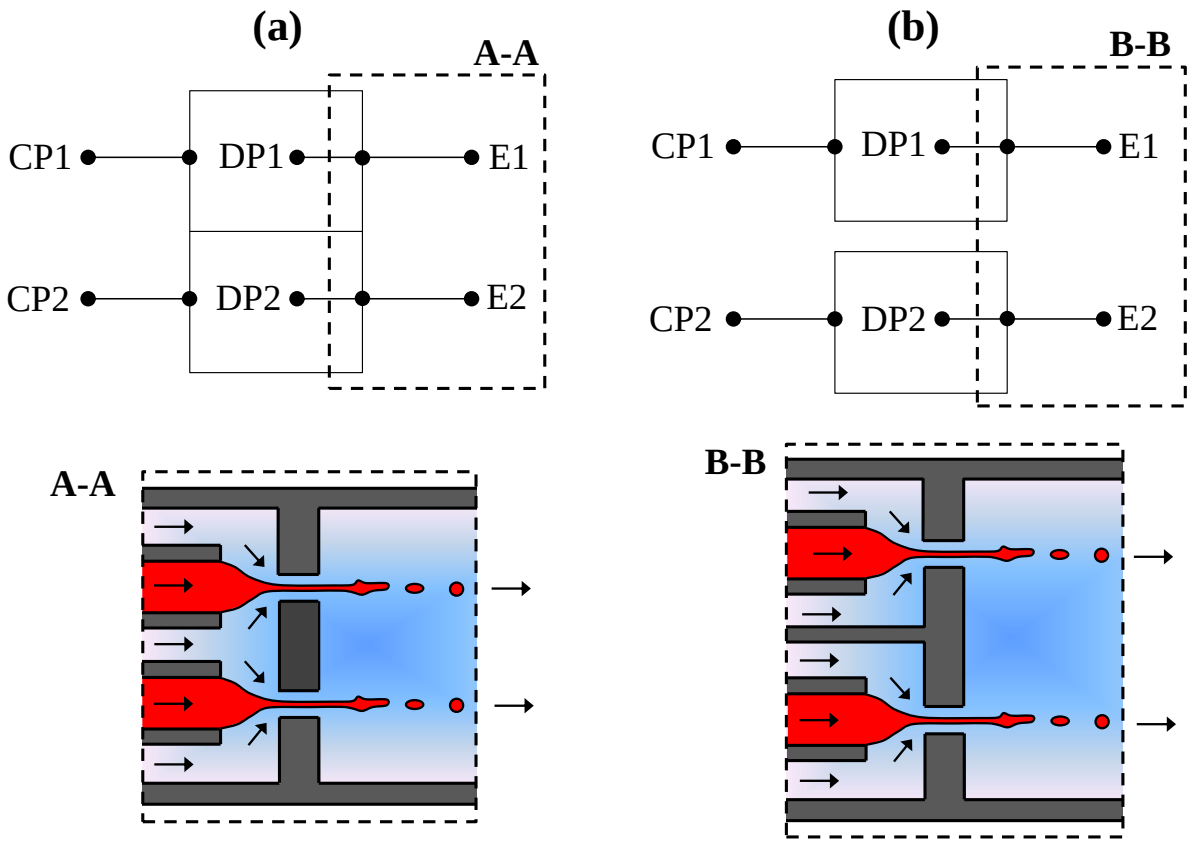

Figure 5.2.1. Integration of flow focusing droplet generators (FFDGs) on a single chip using a common outlet channel: (a) Two coupled FFDGs in which the inlets of continuous phase of the two adjacent generators are fused into one channel [366]; (b) Two parallel FFDGs supplied with two separate inlets of continuous phase [365]. The abbreviations CP, DP and E denote the inlets of continuous and dispersed phase and the outlet of emulsion droplets generated in a system, respectively. Two different inlets are provided for both the dispersed phase and continuous phase, which allows formation of droplets or bubbles of two distinct fluids and independent control of droplet size and drop generation rate in each generator.

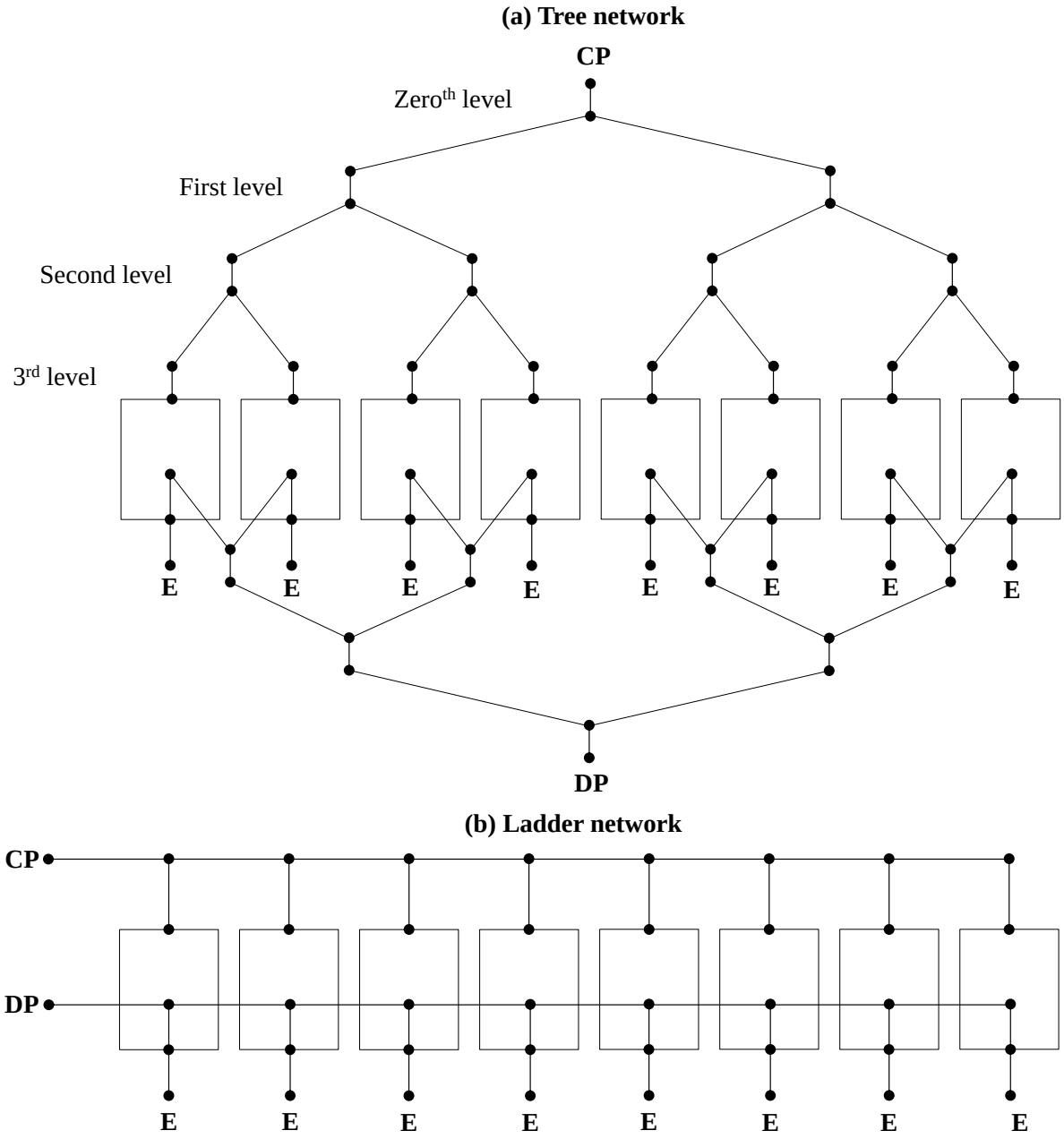

Figure 5.2.2. Common layouts of microfluidic channels for distribution of fluids from a single manifold into multiple parallel drop generation units. In each the device consists of 8 drop generation units (cross junctions). The abbreviations CP, DP and E denote the inlets of continuous and dispersed phase fluid and the outlet of emulsion product, respectively. (Adopted from [369]).

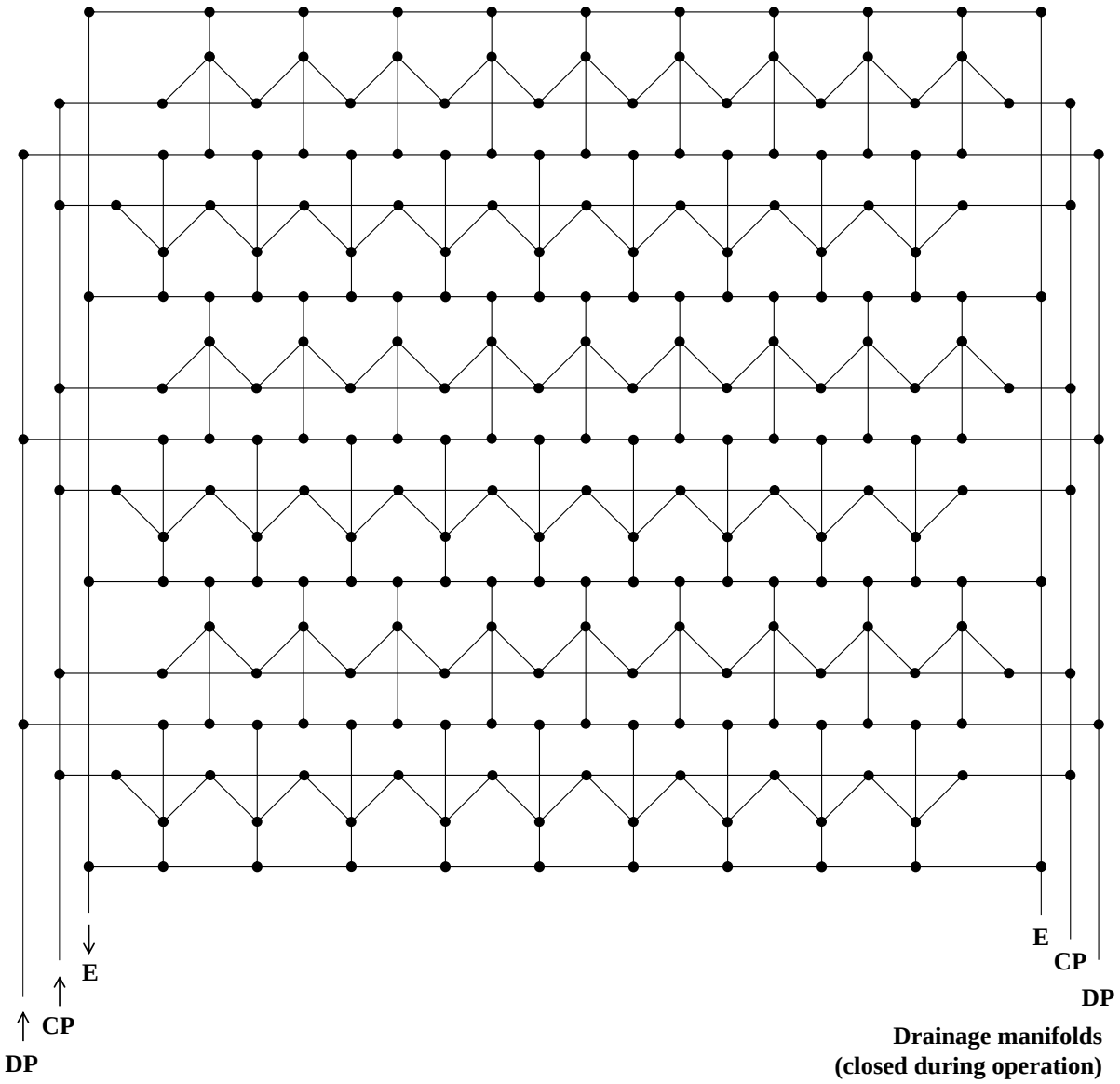

Figure 5.2.3. Integration of cross junctions in a single chip using ladder-type channel network. The chip is assembled from three microfluidic layers stacked on top of each other. The bottom layer comprises long vertical manifolds, the middle layer comprises horizontal long manifolds and the top layer comprises drop generation units with short inlet and outlet channels. The abbreviations CP, DP and E denote the inlets of continuous and dispersed phase fluid and the outlet of emulsion product, respectively [369].

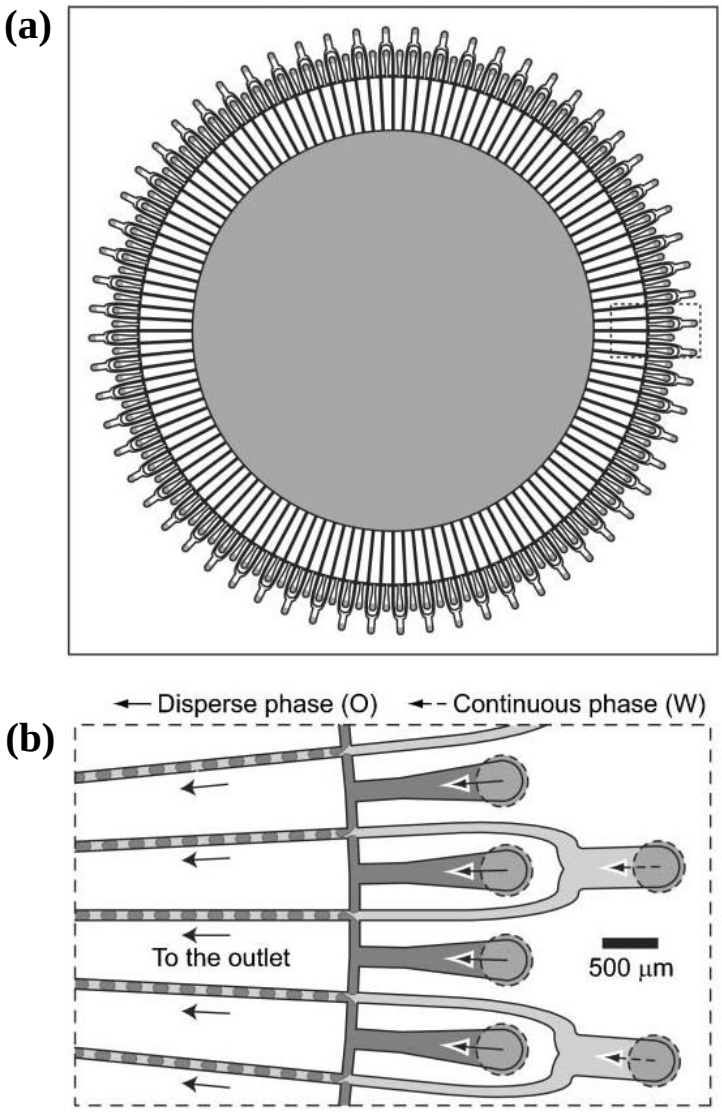

Figure 5.2.4. (a) Schematic of a glass 42 × 42 mm chip with 128 cross junctions radially arranged around an outlet hole with a diameter of 26 mm [20]; (b) Production of single emulsion in a magnified region on the chip surface shown by the dashed rectangle.

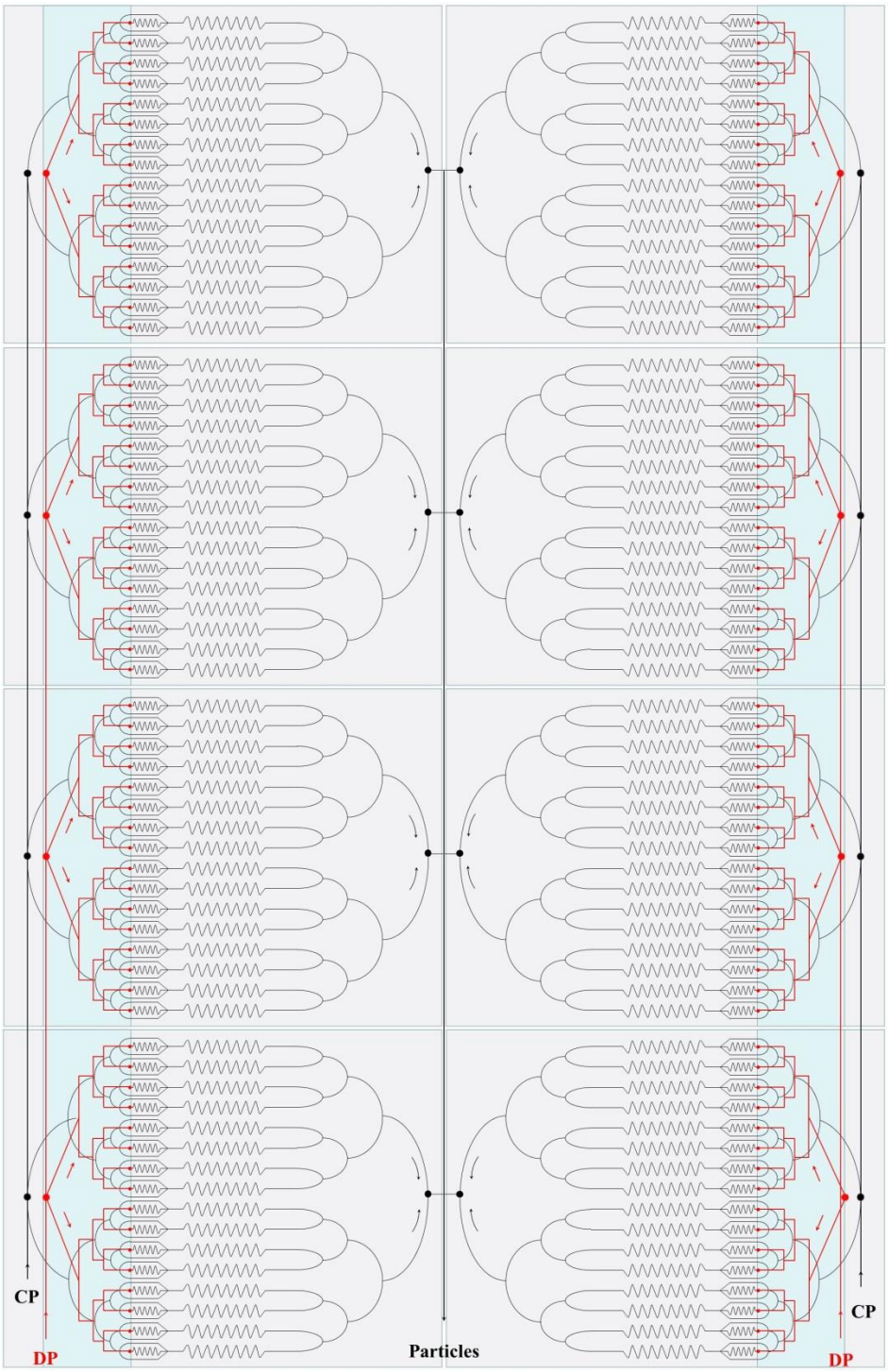

Figure 5.2.5. A schematic of a microfluidic system for synthesis of polymeric particles comprising eight modules with overall 128 flow focusing drop generation units (FFDGUs). Each module consists of 16 FFDGUs followed by 16 wavy channels for UV initiated droplet polymerisation. Manifolds for the injection of the dispersed phase (DP) are shown in red [371].

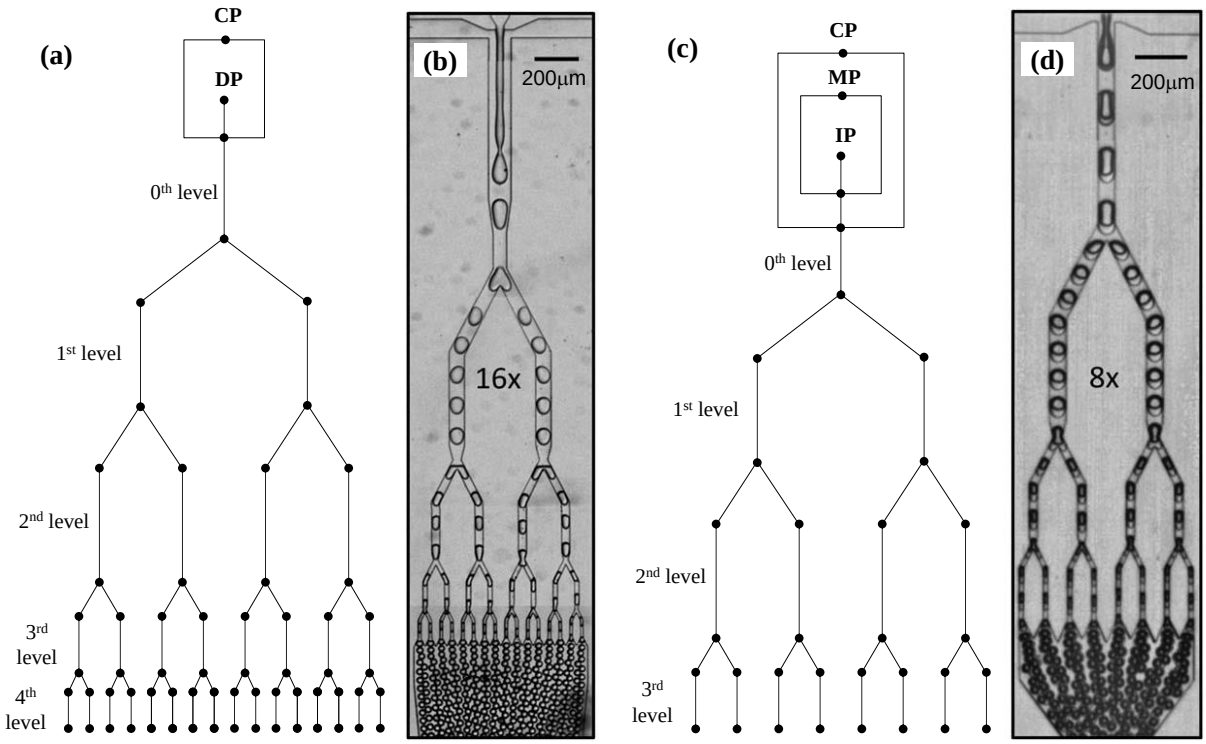

Figure 5.2.6. (a) A splitting array with 4 branching levels for production of single emulsions; (b) Production of W/O emulsion with a droplet diameter of 35 μm by splitting the primary droplets into 16 equal portions. The diameter of the original parent droplets was 88 μm [182]; (c) A splitting array with 3 branching levels for production of double emulsions; (d) Production of core/shell droplets by splitting original core/shell droplets into 8 equal portions [182]. The channel diameter at the m^{th} branching level is: $d_{cm} = d_{c0} / \sqrt{2^m}$, where d_{c0} is the channel diameter at the 0^{th} level. The droplet diameter at the m^{th} branching level is: $d_m = d_0 / \sqrt[3]{2^n}$, where d_0 is the droplet diameter at the 0^{th} level.

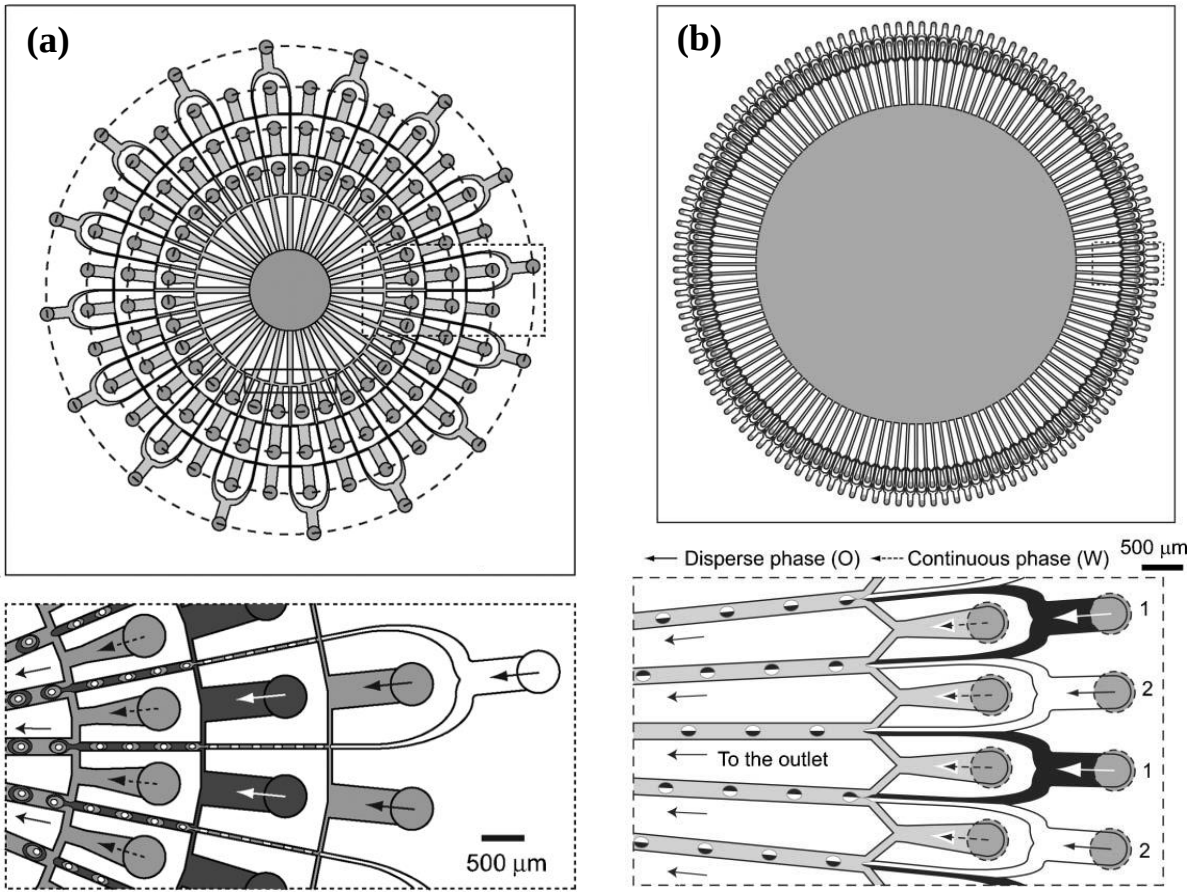

Figure 5.2.7. (a) Production of triple emulsions using 32 radially arranged droplet generators with 3 consecutive junctions. The inlets of the four liquid phases are placed on four concentric circles shown by the dashed lines [50]; (b) Production of bifacial (Janus) droplets using 128 radially arranged droplet generators. The dispersed phases were delivered from the outer inlets and the continuous phase was supplied through the inner inlets (dashed arrows). Labels 1 and 2 denote the inlets for each of the two distinct dispersed phases (black and white) [20].

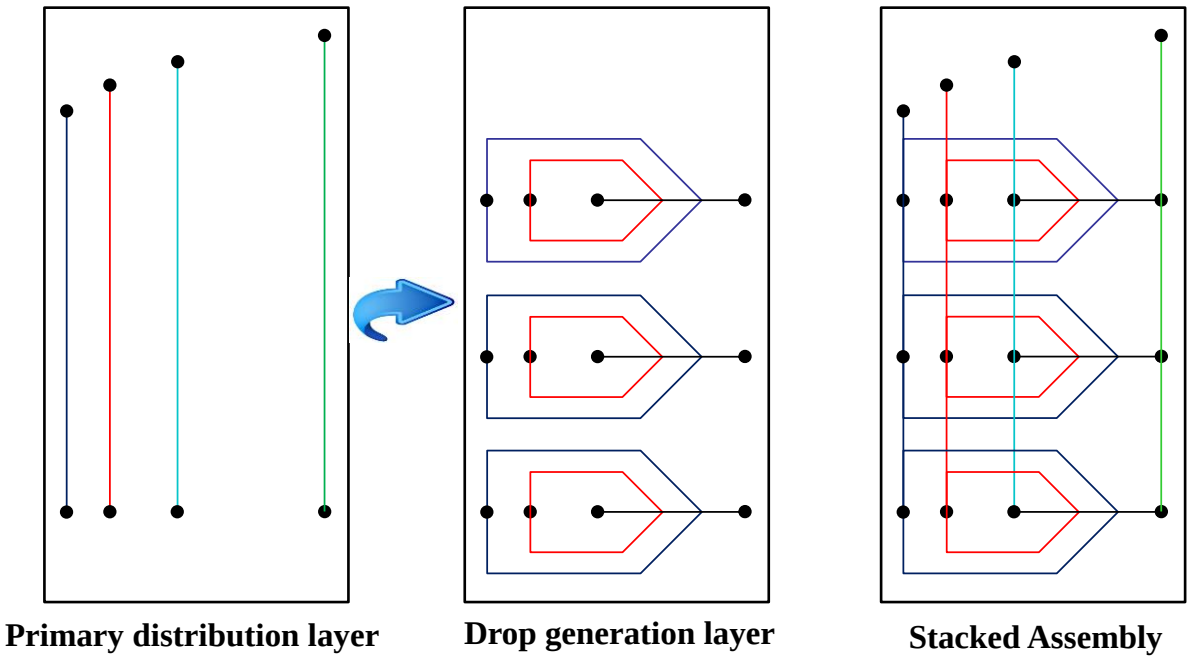

Figure 5.2.8. Formation of a microfluidic device consisting of 3 double emulsion drop generators. The primary distribution layer is placed above the drop generation layer. Channels marked light blue carry the core fluid, red the shell fluid, dark blue the continuous phase fluid, and green the double emulsion product [25].

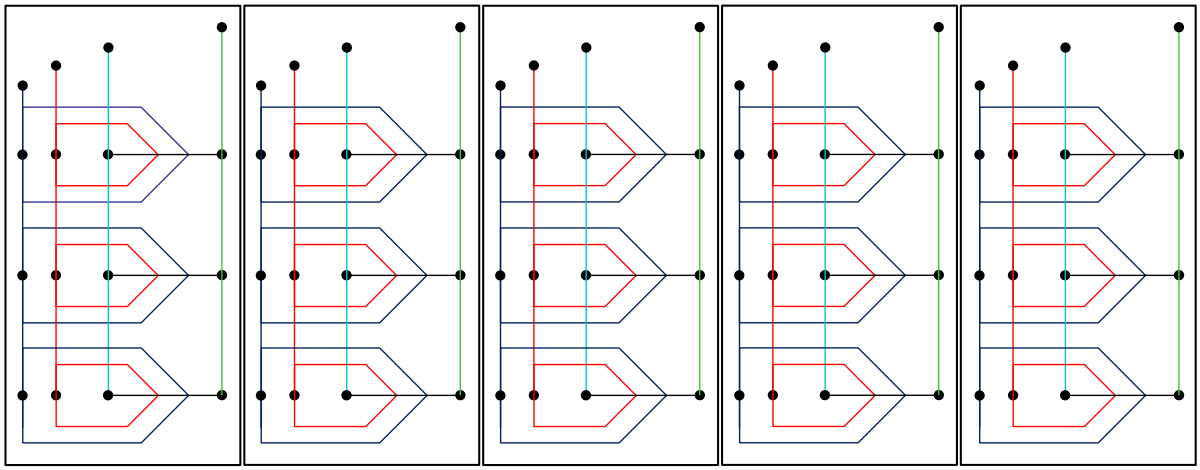

(a) Planar array of drop generation units, each with its own primary distribution layer

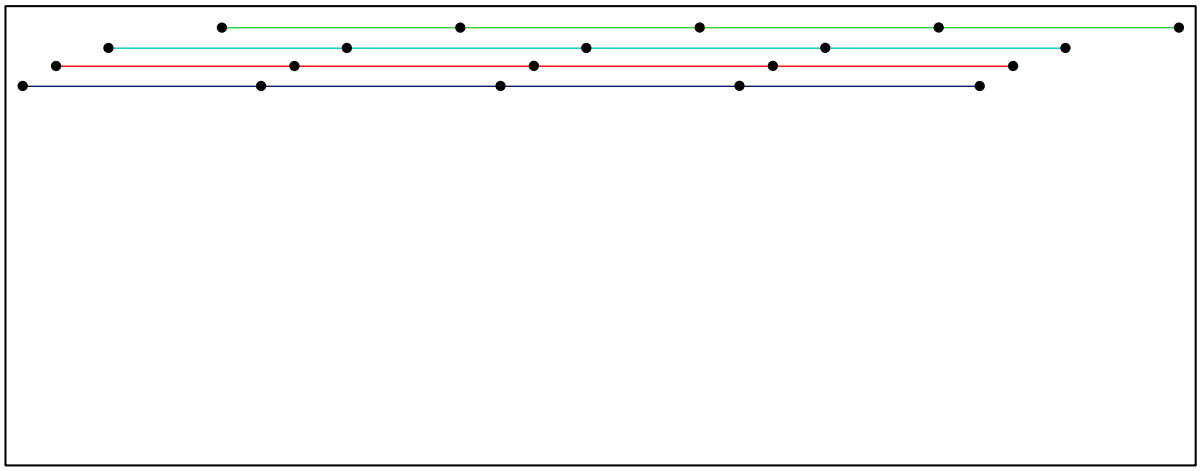

(b) Secondary distribution layer

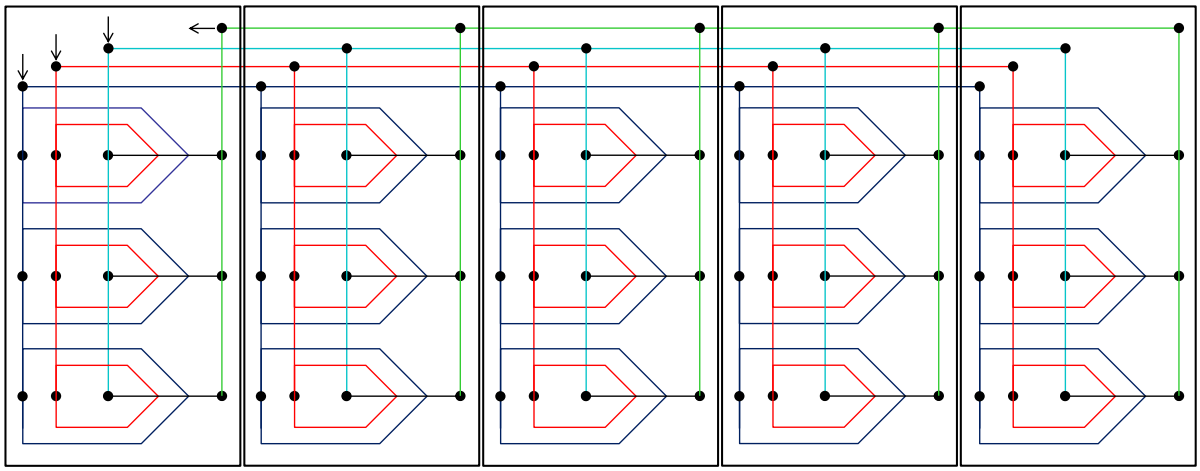

(c) A planar array of drop generation units joined by a 2D network of channels

Figure 5.2.9. Formation of a microfluidic device comprising 15 double emulsion drop generators arranged in 5 lines, each line containing 3 drop generators [25].

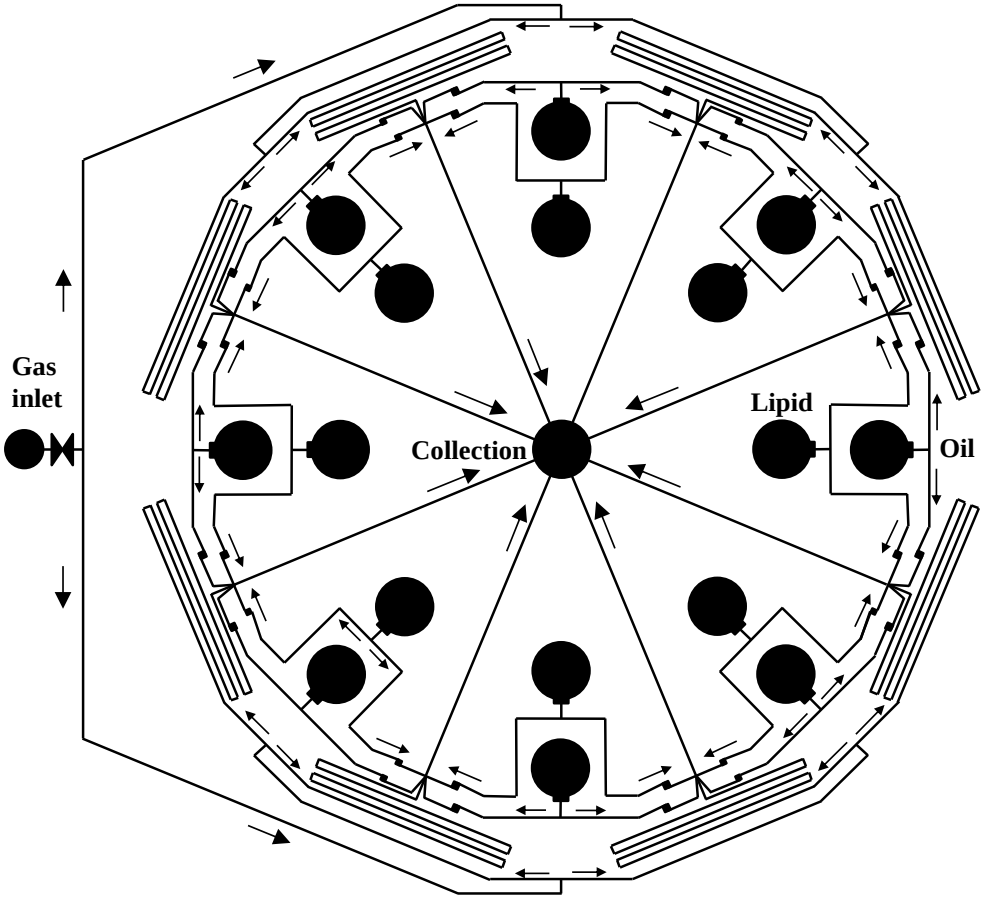

Figure 5.2.10. Schematic of a 33 mm PDMS module with 8 radial flow focusing drop generators for scaled-up production of dual layer microbubbles [372]

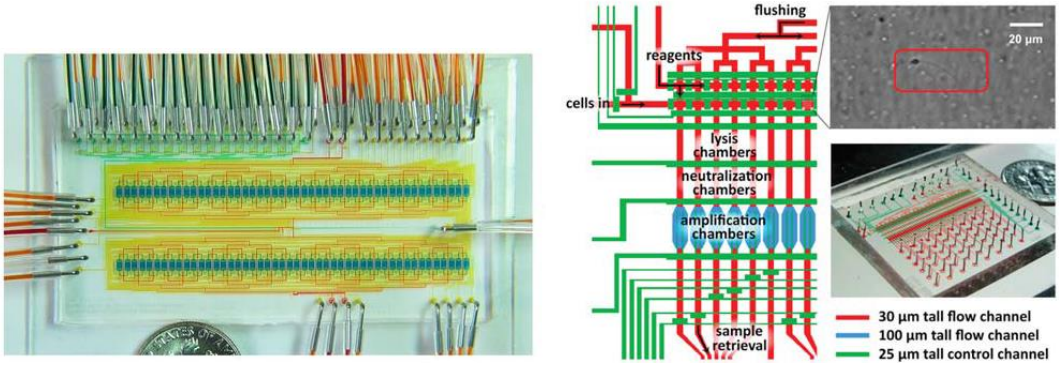

(a) **(b)**

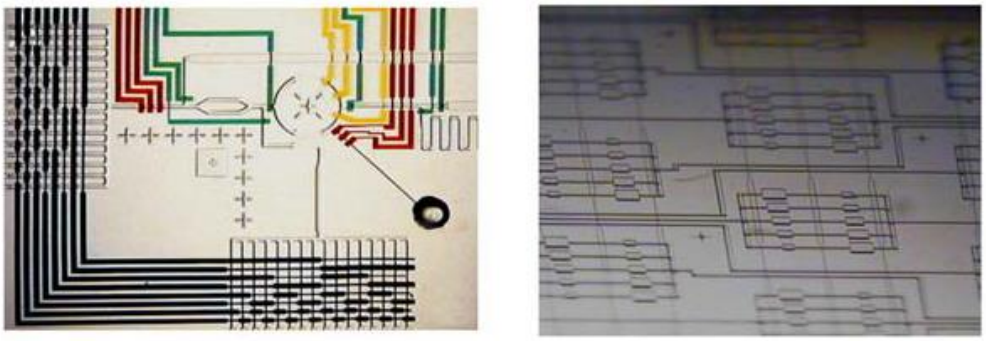

(c) **(d)**

Figure 5.4. (a) Parallelization in cell culture chip, with permission [387]; **(b)** Microfluidic device for single chromosome sequencing. Red and blue lines represent the flow channels and green are the control. Single cells are trapped in the cross-junction, lysed in the following chamber and then chromosomes are separated into the sequential channels, with permission [394]; **(c)** A microfluidic formulation device for high throughput solubility screening of proteins. The primary element is a mixing ring. Peristaltic pumps (in red) inject protein and precipitant into ring and yellow pumps mix the contents of the ring. Reprinted with permission from [402]; **(d)** A free interface diffusion based mixing array for protein crystal screening, with permission [403].